UNCOVERING THE ROLE OF HORMONES IN MAIZE BRACE ROOT DEVELOPMENT

by

Sarah Blizard

A thesis submitted to the Faculty of the University of Delaware in partial fulfillment of the requirements for the degree of Master of Science in Plant and Soil Sciences

Fall 2020

UNCOVERING THE ROLE OF HORMONES IN MAIZE BRACE ROOT DEVELOPMENT

by

Sarah Blizard

Approved: _____
Erin Sparks, Ph.D.
Professor in charge of thesis on behalf of the Advisory Committee

Approved: _____
Erik Ervin, Ph.D.
Chair of the Department of Plant and Soil Sciences

Approved: _____
Mark Rieger, Ph.D.
Dean of the College of Agriculture and Natural Resources

Approved: _____
Louis F. Rossi, Ph.D.
Vice Provost for Graduate and Professional Education and
Dean of the Graduate College

ACKNOWLEDGMENTS

I owe my advisor, Dr. Erin Sparks, a huge debt of gratitude for taking me on as a master's student in her lab, and for pushing me to become a better scientist. I would also like to thank other members of my lab for their help- Jon Reneau, Noah Ouslander, and Nathan Harlan. The microscopy portion of this project would not have been possible without the valuable assistance of Timothy Chaya. I would like to thank my committee members for their insight and advice. Finally, my husband, family, and friends have been constant sources of encouragement and support when I needed it the most.

TABLE OF CONTENTS

LIST OF TABLES

LIST OF FIGURES

ABSTRACT

Maize forms aboveground nodal roots, termed brace roots, that are proposed to function in water/nutrient uptake as well as lodging resistance. Despite their important functions, it remains unclear how these stem-borne brace roots are initiated. Auxin is a central regulator of plant development. My research tests the hypothesis that auxin is necessary and sufficient for brace root initiation. Using a combination of microscopy and transcriptomics, I have established the foundation for investigating if auxin is necessary for brace root initiation. I have further developed methods of local exogenous application of hormones to test if auxin is sufficient for brace root initiation. Together, these results have uncovered additional questions and provide the basis for a long-term investigation of the role of auxin in stem-borne root development.

Chapter 1

MAIZE NODAL ROOTS

*Adapted from Blizard & Sparks, 2020.

1.1 Plant root systems

Plant roots provide stability, water and nutrient uptake, and relationships with soil organisms. Root systems differ between the two major divisions of Angiosperms: eudicots and monocots. Eudicots have a tap root system, composed of a single embryonic primary root with post-embryonic lateral roots branching off. Monocots have a fibrous root system composed of embryonic primary root and seminal roots, post-embryonic nodal roots, and lateral roots branching from each of these root types. Each root type can have distinct anatomy, function, and developmental programs between species; thus, it is important to study roots based on their type and species.

1.1.1 Terminology

The terminology surrounding nodal roots can often be confusing. Nodal roots can be classified as adventitious roots, referring to any root that develops from non-root tissue. Adventitious roots can be formed as part of endogenous development, such as maize brace roots, or through wounding or stress (Steffens & Rasmussen, 2016). Roots can develop from stem tissue in both monocot and eudicot species and are

referred to as stem-borne roots. Stem-borne roots in monocots are also called nodal roots since they only form at nodes on the stem. Within maize, roots that form at nodes belowground are referred to as crown roots, while those that form aboveground are referred to as brace or prop roots. The first node that is formed from the embryo is referred to as the scutellar node, and roots that formed from this node are termed seminal roots. The next node that forms is also distinct and is termed the coleoptilar node. Roots that form from the coleoptilar node are under different genetic regulation compared to the rest of the crown root system (Hochholdinger & Feix 1998a; Woll et al., 2005). A glossary of terms is provided in Table 1.

Table 1. Glossary of Terms.

Term	Definition
Adventitious Roots	Broad term for any roots that are formed from non-root tissue including those produced during the course of normal development or those induced by wounding, stress, or flooding. These roots are found in both monocot and eudicot species.
Brace Roots	Also termed prop roots. Refers to the aboveground nodal roots of maize that were named for their proposed function in lodging resistance.
Coleoptilar Node	The first stem node located above the scutellar node that produces crown roots. Genetic evidence suggests that nodal roots from the coleoptilar node have distinct regulation compared to the rest of the crown roots.
Crown Roots	Nodal roots that form beginning at the coleoptilar node, usually emerging from five nodes in total, all located belowground.
Nodal Roots	Also termed axial roots. Refers to any root originating from the stem nodes of monocot plants.
Lateral Roots	Refers to roots that originate from other roots.

Scutellar Node	The embryonic stem node where the scutellum attaches above the radicle. Also, the point of formation for embryonic seminal roots.
Seminal Roots	Roots that develop from the scutellar node and are embryonic in origin.
Meristem	A region of actively dividing cells in plants.
Phytomer	A functional unit of a plant. In monocot stems, the phytomer consists of the node, internode and resulting organs (roots, branches, or leaves).
Primordia	Refers to the earliest developmental stage of an organ.
Vascular Plexus	Also termed anastomosis, nodal plexus, root vascular plexus, axial bundles, plexus strands, horizontal vascular bundles, anastomosing amphivasal fibro-vascular bundles. Refers to the network of interconnecting, web-like vascular strands that form at all nodes in grasses.

1.1.2 Maize root system

In maize plants, the nodal root system dominates for the majority of the plants' lifespan. The embryonic roots (primary and seminal) are vital to establishing the seedling in the early stages of development. However, the nodal root system will take over the majority of the functional capacity of the maize plant after vegetative leaf stage 6 (V6) (Hochholdinger et al., 2004). The maize root system will form approximately five nodes of crown roots belowground, and two or three nodes of brace roots aboveground (Hoppe et al., 1986). Higher nodes may contain brace root primordia that initiate but never emerge from the stem or penetrate the leaf sheath (Hoppe et al., 1986).

1.2 Nodal root development

As nodal roots are hierarchically classified as adventitious roots, the development of nodal roots will be discussed within the developmental framework defined for adventitious roots. The development of adventitious roots occurs in three stages: induction, initiation, and emergence (Bellini et al., 2014; de Klerk et al., 1999). During the induction phase, cells are proposed to de-differentiate from their terminal fate and gain a new cell fate as founder cells. The induction phase is not associated with any morphological alterations, and thus has been difficult to study in the context of adventitious root development (Bellini et al., 2014). In the initiation phase, the founder cells divide to form root primordia and define a root meristem, which can be morphologically distinguished. Lastly, during the emergence phase, the root primordium elongates and emerges from the stem.

For maize nodal roots, the tissue of origin that de-differentiates to establish the founder cells and initiate primordia remains a mystery. One clue comes from the observation that in some stem sections there is weaker staining for cellulose in the cell walls of cortex cells adjacent to the vascular plexus (Hoppe et al., 1986). The vascular plexus is composed of horizontal vascular bundles that are observed only at nodes, never in internodes, and nodal root primordia are always associated with this type of horizontal vasculature (Hoppe et al., 1986). Adventitious roots (whether induced by wounding/stress or through endogenous development) are always initiated from cells located adjacent to vascular tissues (Bellini et al., 2014; Lakehal & Bellini, 2019). Thus, it is likely that maize nodal roots originate from cortex cells adjacent to the vascular plexus. However, the vascular plexus forms at all nodes regardless of nodal root formation (Hoppe et al., 1986), suggesting that these structures are necessary but not sufficient for induction and initiation of nodal roots. Additional research is needed

to fully define the morphological and anatomical progression of nodal root initiation in maize.

The vascular plexus in monocots has been documented since the early 1900's, but the use of differing terminology has led to much confusion. As long ago as 1906, "anastomosing amphivasal fibro-vascular bundles" were observed in the family Cyperaceae (Plowman, 1906). There was considerable disagreement about what these bundles were or where they originated, discussed in detail by (Arber, 1930), who concludes that the "nodal plexus" does not originate from roots, buds, or leaves, but from meristematic activity in the ground tissue. Detailed descriptions and drawings of the nodal plexus reveal the complicated nature of this phenomenon (Evans, 1928; Sharman, 1942). Careful work tracing the path of these bundles revealed that a single vertical vascular bundle rarely passes through 2-3 nodes without branching at the node (Evans, 1928). At the internode, vascular bundles only run vertically, hence, exchange of water and nutrients can only occur at the node (Shane et al., 2000). There is great redundancy in the connections occurring at the node, which some speculate exist in order to get around blockages that occur in the vasculature, and to allow for exchange between the xylem and phloem (McCully & Mallett, 1993; Shane et al., 2000). Indeed, the node itself is an important site for mineral distribution to developing organs (Yamaji & Ma, 2014). A full understanding of the function of the vascular plexus and how it relates to nodal root development is necessary to define root initiation mechanisms.

As with other adventitious roots (Bellini et al., 2014), the earliest stage of nodal root development in maize that can reproducibly be identified is when a primordium already exists (Hoppe et al., 1986). For maize nodal roots, an immature

primordium is defined by the presence of root cap cells, a band of pro-vascular tissue that is continuous with the vascular plexus, and distinct flanking tissues (Hoppe et al., 1986). The primordium continues to expand and define the meristem before emerging from the stem. One notable difference between nodal root primordia forming belowground versus aboveground is the shape of the root cap. Belowground primordia have a conical root cap that is morphologically similar to that of the primary root, whereas aboveground primordia have a flattened root cap that extends further along the length of the root (Hoppe et al., 1986). The anatomy of the aboveground root cap becomes more similar to the belowground root cap after these roots penetrate the soil, suggesting that this root cap anatomy may be an adaptation for root survival in the air.

After emergence from the stem, nodal root width increases on sequentially higher nodes, and this increased width is associated with increased number of metaxylem elements (Hoppe et al., 1986; Stamp & Kiel, 1992). In addition, an anatomical change occurs in aboveground segments of brace roots relative to belowground segments of both brace and crown roots. Specifically, in the aboveground root segment, the outer epidermal cell layer is frequently dead, with only remnants of the cell wall remaining, and the underlying hypodermis and outer cortex cell layers show thickened cell walls compared to the belowground roots (Hoppe et al., 1986). These results support the role of the environment (aerial or subterranean) in shaping the development of nodal roots, however the mechanisms regulating these processes are poorly understood.

1.2.1 Molecular and Genetic Mechanisms of Nodal Root Development

The developmental programs controlling root initiation are unique to the root type (Hochholdinger et al., 2004), but post-initiation developmental pathways often

overlap (Birnbaum, 2016). Each root type expresses unique genes, and even between the same root type originating from different nodes the gene profiles are distinct (Stelpflug et al., 2016). The historical approach to identify molecular regulators of these developmental pathways is through forward genetics, however this approach has been limited for maize nodal roots due to the polygenic nature of root development, the inaccessibility of roots in the soil, the size and complexity of the root system, and the effect of the environment (Hochholdinger et al., 2004).

While only a handful of maize root mutants have been identified, they reveal interesting distinctions for the initiation and emergence cues of different root types. These mutants often affect specific root types leaving the rest of the root system untouched, supporting the idea of unique developmental programs (Hochholdinger et al., 2004). Six mutants show a reduction in one or more nodal root type: the *rtcs* (*rootless for crown and seminal roots*) mutant affects seminal and nodal root formation (Hetz et al., 1996); the *rt1* (*rootless1*) mutant reduces the number of crown roots and does not form brace roots (Jenkins, 1930); the *rum1* (*rootless with undetectable meristems1*) mutant does not form seminal roots or initiate lateral roots on the primary root and has limited crown root emergence at the coleoptilar node (Woll et al., 2005; Hetz et al., 1996); the *lrt1* (*lateral rootless1*) mutant does not initiate crown roots at the coleoptilar node, or lateral roots in the embryonic root system (Hochholdinger & Feix, 1998b; Hetz et al., 1996); the *zmccd8* (*carotenoid cleavage dioxygenase 8*) mutant shows delayed crown root emergence (Guan et al., 2012; Hetz et al., 1996); and the *zmrap2.7* mutant has a decreased number of nodes with brace roots (Li et al., 2019). Four mutants were identified through forward genetic screens (*rtcs*, *rt1*, *rum1*, and *lrt1*), and the other two (z*mccd8* and *zmrap2.7*)

were identified through reverse genetics. For the mutants identified through forward genetics only *rtcs* and *rum1* have been cloned, and both are associated with auxin signaling. In addition to these mutants, a maize transgenic line overexpressing *ARGOS8* has a delay in nodal root emergence (Shi et al., 2019).

In addition to the mutants that reduce nodal roots, there are a handful of lines that increase the number of roots in a node and/or the number of nodes that produce roots. Three lines have been identified that show an increase in nodal roots: *bige1* (*big embryo 1*) shows an increase in the number of roots for all root types reported (lateral, seminal, crown) and an increase in the number of nodes with roots (Suzuki et al., 2015); the dominant *Cg1* (*Corngrass1*) mutant of maize has increased number of nodes with roots (Chuck et al., 2007); a transgenic *ZmCCT* line has increased crown root numbers per node and an increased number of crown root nodes (Zhang et al., 2018). Each of these mutants were identified by screening for defects in other processes, and thus it remains unclear how these genes directly function to regulate nodal root development.

1.3 Auxin in Nodal Root Development

Auxin is a plant hormone well-known for its role in development, and specifically in maize lateral organ initiation (Gallavotti et al., 2008; Yu et al., 2015). Two of the maize nodal root mutants are auxin-related (Taramino et al., 2007; von Behrens et al., 2011) and the exogenous application of auxin increases the emergence of crown roots from the coleoptilar node (Nick, 1997). These results suggest that auxin also plays a central role in nodal root development. However, the mechanism of auxin regulation during nodal root initiation and emergence, and how auxin signaling can distinguish between different root types remains obscure.

Insight into the role of auxin during nodal root initiation comes from the *rtcs* mutant, which lacks all nodal root primordia as well as seminal roots at the embryonic scutellar node (Hetz et al., 1996). The *rtcs* mutant was cloned as a lateral organ boundary domain (LBD) protein that is auxin-inducible (Taramino et al., 2007). The LBD gene family members are known for defining the boundaries between lateral organs and for being involved in almost all aspects of plant development (Majer & Hochholdinger, 2011). The LBD motif of *rtcs* has high sequence conservation with the rice ortholog *Crown rootless1* (*Crl1*) suggesting that this motif is of particular importance for nodal root development (Inukai et al., 2005; Taramino et al., 2007).

The *rtcs* mutant suggests that auxin plays an early and important role in nodal root initiation. The *RTCS* transcript is expressed in emerging primordia and the protein continues to accumulate as the primordia develop (Taramino et al., 2007). *RTCS* is auxin-inducible and contains auxin-response elements within its promoter (Taramino et al., 2007). Furthermore, RTCS can bind to the LBD motif in the promoter of *ZmARF34* (*AUXIN RESPONSE FACTOR 34*), and ZmARF34 can reciprocally bind to the auxin-response elements in the *rtcs* promoter (Majer et al., 2012). *ZmARF34* was targeted in this analysis due to its homology to the *Arabidopsis thaliana* genes *AtARF7* and *AtARF19*, which are known to trigger lateral root initiation through reciprocal interactions with LBD genes (Okushima et al., 2007). Thus, it is possible and likely that RTCS has additional targets that are yet to be identified. *RTCS* has been duplicated in the maize genome and its paralog, RTCL (RTCS-LIKE), functions cooperatively with RTCS during root formation. However, unlike RTCS, RTCL is not involved in nodal root initiation, but instead controls the elongation of these roots (Xu et al., 2015).

Additional evidence suggests that auxin may also be involved in nodal root emergence. Specifically, the *rum1* mutant initiates crown root primordia at the coleoptilar node, but these primordia only emerge in 17% of mutant plants. This mutant also does not initiate lateral roots from primary and seminal roots, but the other nodal root types are formed normally (Woll et al., 2005). The *rum1* mutant encodes a nuclear-localized Aux/IAA (*ZmIAA10*) protein that is auxin-inducible (von Behrens et al., 2011). ZmARF34, which has a reciprocal binding interaction with RTCS, also functions downstream of RUM1 (von Behrens et al., 2011). Since the phenotypes of *rum1* and *rtcs* are dramatically different, uncovering the interplay of these three genes is an exciting area for future research. The *rum1* mutant highlights much of the unappreciated diversity in maize root type development by distinguishing the first coleoptilar node as distinct from the other crown root nodes and defining a unique regulation of lateral root development from embryonic roots and nodal roots. The *lrt1* mutant, which does not initiate crown roots at the coleoptilar node has not yet been cloned, but the mutant is insensitive to auxin, suggesting that this gene will also be related to auxin signaling (Hochholdinger & Feix, 1998b). Together, these results suggest that auxin is involved in the emergence of crown root primordia specifically from the coleoptilar node.

A reverse genetics approach was applied to understand the development specifically of the aboveground brace roots (Li et al., 2011). In this study, the transcriptome of maize nodes with brace roots and nodes without brace roots were compared (Li et al., 2011). Auxin-related genes were differentially regulated in this study (Li et al., 2011), but in the absence of anatomical information it is impossible to determine what stage of development (i.e. initiation or emergence) is being assessed.

Additional efforts to sequence small RNAs identified differential expression between nodes with brace roots, nodes without brace roots, and nodes with brace roots that were treated with auxin (Liu et al., 2013). There were a large number of differentially expressed miRNAs between the nodes with brace roots and nodes with auxin-treated brace roots, indicating a role for auxin in regulating miRNAs during brace root development. Further analysis of the target genes for these miRNAs showed auxin-related functions such as auxin-binding or auxin transport (Liu et al., 2013). While there seems to be preliminary evidence that auxin promotes brace root emergence, much work remains to determine what genes are involved in the process and differentiate between the various stages of development.

Together these data suggest an important role for auxin in nodal root initiation and emergence. However, the auxin-mediated signals involved in these processes remain an open area of investigation. Auxin may be regulated at the level of biosynthesis, transport, and/or transcription, but the regulation in the context of nodal root development is an open question.

1.3.1 Methods to visualize auxin

In order to visualize auxin in plant tissues, several reporter lines have been established. The most common reporter is a synthetic auxin promoter element called DR5, which has been fused to different reporter genes to visualize auxin transcriptional activity (Ulmasov et al., 1997; Chen et al., 2013; Friml et al., 2003; Gallavotti et al., 2008). In maize, the DR5::erRFP reporter line has been used to show that auxin maxima form at the site of organ initiation in inflorescences and roots (Gallavotti et al., 2008; Jansen et al., 2012; O'Connor et al., 2014). This reporter line

has also been used specifically to view the role of auxin in lateral root initiation from shoot-borne roots of maize (Yu et al., 2015).

A reporter line has also been generated to visualize the auxin efflux carrier gene PIN1 fused to a fluorescent protein (PIN1::PIN1-YFP). This line has been utilized to discover the localization of PIN proteins (Bainbridge et al., 2008; Benková et al., 2003; Carraro et al., 2006; Chettoor & Evans, 2015; Forestan et al., 2012; Forestan & Varotto, 2010, 2012; Gallavotti et al., 2008; Li et al., 2019; O'Connor et al., 2014; J.R. Wang et al., 2009; Xu et al., 2005; Yu et al., 2015), to visualize auxin dynamics after treatment with auxin or auxin inhibitor (Forestan et al., 2012) and to confirm the role of PIN in organ initiation (Benková et al., 2003; Bainbridge et al., 2008; Chettoor & Evans, 2015).

A more recent advance in visualizing auxin dynamics comes from the use of an Aux/IAA auxin interacting domain (DII) fused to the VENUS fluorescent protein (Brunoud et al., 2012). DII::VENUS degrades rapidly in the presence of auxin, while its mutated form, mDII::VENUS, does not degrade, allowing for the visualization of auxin distribution at cellular resolution in various tissues. This reporter line has also been modified for use in maize (Mir et al., 2017).

1.3.2 Exogenous application of auxin

Along with the natural forms of auxin, indole-3- acetic acid (IAA) and indole-3-butyric acid (IBA), there are several synthetic analogs, including 2,4-Dichlorophenoxyacetic acid (2,4-D) and 1-Naphthaleneacetic acid (NAA). Synthetic auxin inhibitors include 1-N-Naphthylphthalamic acid (NPA) and 2,3,5-triiodobenzoic acid (TIBA). The exogenous application of these hormones and inhibitors have been used in many ways to study the sufficiency of auxin during plant development. The

type of auxin or auxin inhibitor used can lead to different results based on their mode of action. For example, the widely used herbicide 2,4-D requires an influx carrier in order to be transported, whereas the naturally occurring auxin IAA in its non-ionized form can passively diffuse across the plasma membrane (Delbarre et al., 1996). In one study, there were differential developmental outcomes on maize root architecture in response to four types of auxins applied to maize seedlings grown in liquid MS medium (Martínez-de la Cruz et al., 2015). This outcome could be due to the ability of auxin to bind to carrier proteins and influence the root architecture.

Different methods for exogenous application of hormones to maize have been reported in the literature (summarized in Table 2). Early studies utilized a lanolin plug on maize coleoptiles to study fundamental plant responses such as phototropism or gravitropism (Baskin et al., 1985, 1986; Iino, 1995; Kaldenhoff & Iino, 1997). More recent studies rely on the addition of the hormone or inhibitor to the growth medium, or the addition of the solution to the watering or fertilizing regimen (Perez, 1987; Martínez-de la Cruz et al., 2015; Mir et al., 2017; Ponce et al., 2005; Gougler & Evans, 1981; Tian et al., 2008; Yue et al., 2015; Guo et al., 2005; Hetz et al., 1996; Jansen et al., 2012; Zhang et al., 2014; Alarcón et al., 2013; Justin & Armstrong, 1991; Kaldorf & Ludwig-Muller, 2000; Bronsema et al., 2001). Less commonly, foliar sprays on mature leaves, or scuffing of the cuticle have also been used (Kaya et al., 2013; Nick, 1997; Battal et al., 2008). There is difficulty in applying hormones to mature maize that is not supplied in the water/nutrient solution, because of the thick, waxy, cuticle that maize possesses. The development of new techniques to exogenously apply hormones to mature tissue will prove beneficial to the study of nodal root development in maize.

Table 2. A non-exhaustive summary of methods of exogenous application of auxin and auxin inhibitors to maize.

Hormone	Method	References
IAA (naturally occurring)	Added to growth medium	(Perez, 1987; Martínez-de la Cruz et al., 2015; Mir et al., 2017; Ponce et al., 2005)
	Added to nutrient solution	(Gougler & Evans, 1981; Tian et al., 2008; Yue et al., 2015)
	Scuffing	(Nick, 1997)
	Spray	(Kaya et al., 2013)
	Lanolin paste	(Baskin et al., 1985, 1986; Iino, 1995; Kaldenhoff & Iino, 1997)
NAA (synthetic)	Added to growth medium	(Guo et al., 2005; Hetz et al., 1996; Jansen et al., 2012; Martínez-de la Cruz et al., 2015; Zhang et al., 2014)
	Added to nutrient solution	(Alarcón et al., 2013; Gougler & Evans, 1981; Justin & Armstrong, 1991; Tian et al., 2008)
	Spray	(Battal et al., 2008)
IBA (synthetic)	Added to growth medium	(Kaldorf & Ludwig-Muller, 2000; Martínez-de la Cruz et al., 2015)

2,4-D (synthetic)	Added to growth medium	(Bronsema et al., 2001; Gougler & Evans, 1981; Perez, 1987; Martínez-de la Cruz et al., 2015))
	Added to nutrient solution	(Gougler & Evans, 1981)
	Lanolin paste	(Lur' & Setter, 1993)
NPA (inhibitor)	Added to growth medium	(Jansen et al., 2012; Ponce et al., 2005; Zhang et al., 2014)
	Scuffing	(Nick, 1997)
TIBA (inhibitor)	Added to growth medium	(Brons et al., 2001; Guo et al., 2005; Kerk & Feldman, 1994)

1.4 Other Hormones in Nodal Root Development

Ethylene is a gaseous plant hormone known to work cooperatively with auxin to induce adventitious root formation, primarily under flooding (reviewed in Steffens & Rasmussen, 2016). Indeed, ethylene promotes nodal root emergence in maize under flooded conditions (Drew et al., 1979). However, while much is known about auxin-ethylene interactions on root development in general (Alarcón et al., 2009, 2012, 2014; Chadwick & Burg, 1970; Muday et al., 2012; Stepanova et al., 2007; Stepanova & Alonso, 2019), how these interactions may regulate nodal root development remains largely unexplored.

From one study, the role of ethylene in nodal root development appears to be specific to the emergence stage under standard growth conditions. Specifically, the

exogenous application of the ethylene precursor ACC (1-aminocyclopropane1-carboxylic acid) to maize plants promotes brace root emergence (Shi et al., 2019). Reciprocally, a transgenic maize line that decreases ethylene signaling via ARGOS8 overexpression results in delayed nodal root emergence (Shi et al., 2019).

Together these results support a role for ethylene in regulating the emergence of nodal roots. However, the specific ethylene signaling mechanisms and potential interplay with auxin signaling remain to be defined. Additional forward and reverse genetic approaches will be critical to dissect the mechanism of ethylene signaling in nodal root development.

A third hormone that may be involved in nodal root development is strigolactone. Strigolactone is produced in plant roots and inhibits lateral shoot branch formation (reviewed in Waters et al., 2017). However, the function of strigolactone in adventitious root induction may depend on the classification of plants as either eudicot or monocot. In eudicots *Pisum sativum* (pea), *Arabidopsis thaliana*, and *Solanum lycopersicum* (tomato) the inhibition of strigolactone signaling promotes adventitious rooting (Kohlen et al., 2012; Rasmussen et al., 2012). However, in monocots *Oryza sativa* (rice) and maize, the inhibition of strigolactone delays adventitious rooting (Guan et al., 2012; Sun et al., 2015). Specifically for maize, a mutant defective in strigolactone biosynthesis, *zmccd8*, has increased lateral shoot branches, but a delay in nodal root outgrowth (Guan et al., 2012). These results suggest that strigolactones may play a different role in adventitious roots based on the classification as eudicot or monocot, however the function of strigolactones in maize nodal root development remains to be fully explored.

1.5 Other Signals in Nodal Root Development

In addition to the aforementioned hormone-related pathways for nodal root development, an AP2/ERF (APETALA2/ETHYLENE RESPONSIVE FACTOR) transcription factor, *ZmRAP2.7*, was identified as a regulator of brace root development from the reverse genetics transcriptome study described above (Li et al., 2011). *ZmRAP2.7* was identified as ten-times higher expressed in nodes with brace roots than nodes without brace roots (Li et al., 2019). A *zmrap2.7* mutant has significantly less stem-borne roots compared to wildtype, which is primarily attributed to one less whorl of brace roots, while the number of crown roots was similar to wildtype (Li et al., 2019). It is unclear whether the mutant is affected at the initiation stage or emergence stage, and future anatomical studies will help refine the role of *ZmRAP2.7* in nodal root development. Further support for the role of *ZmRAP2.7* in nodal root development comes from the elevated expression of *ZmRAP2.7* in nodes of the *Cg1* dominant mutant line (Li et al., 2019), which has a retention of juvenile traits (Chuck et al., 2007) including brace roots (Poethig, 2010).

The specific role of ZmRAP2.7 in nodal root development may be confounded by other phenotypic effects. Specifically, *zmrap2.7* also accelerates flowering time (Salvi et al., 2007), which has been linked to the number of nodes that produce roots. Quantitative trait loci (QTL) for nodal root number and the number of nodes with roots has a 46% overlap with QTL for flowering time in a maize-teosinte BC_2S_3 population (Zhang et al., 2018). The relationship between flowering time and nodal root traits was further defined by analysis of a transgenic line for a known flowering time gene, *ZmCCT*, which has late flowering and increased crown root number and increased number of crown root nodes (Zhang et al., 2018). Unfortunately, this study did not report the results of brace root traits in the transgenic *ZmCCT* line, thus

limiting the interpretation of the *ZmRAP2.7* study in the context of altered flowering time.

Lastly, the *bige1* mutant was identified in a screen for big embryos, but was also found to have increased nodal roots (Suzuki et al., 2015). The BIGE1 protein is a multidrug- and-toxin-extrusion (MATE) transporter localized to the *trans*-Golgi that may function in the CYP78A pathway (Suzuki et al., 2015). However, the exact signaling mechanism of *BIGE1* and its role in nodal root development is poorly understood.

1.6 Conclusion

There are many open questions regarding the mechanisms of nodal root development in maize. In this thesis, I hypothesize that auxin is necessary and sufficient for brace root initiation. I aim to test this hypothesis by quantification of reporter lines, transcriptomic analysis of nodes during brace root development, and exogenous application of hormones to the maize stem. These experiments provide a deeper understanding of the developmental mechanisms of maize brace roots, which works towards the goal of improving resistance to stress and climate change in this important cereal crop.

REFERENCES

Alarcón, M. V., Lloret, P. G., Iglesias, D. J., Talón, M., & Salguero, J. (2012). Comparison of Growth Responses to Auxin 1-Naphthaleneacetic Acid and the Ethylene Precursor 1-Aminocyclopropane-1-Carboxilic Acid in Maize Seedling Root. *Acta Biologica Cracoviensia. Series: Botanica*, *54*(1), 488.

Alarcón, M. V., Lloret, P. G., & Salguero, J. (2013). Auxin–ethylene interaction in transversal and longitudinal growth in maize primary root. *Botany*, *91*(10), 680–685.

Alarcón, M. V., Lloret, P. G., & Salguero, J. (2014). The Development of the Maize Root System: Role of Auxin and Ethylene. In A. Morte & A. Varma (Eds.), *Root Engineering: Basic and Applied Concepts* (pp. 75–103). Springer Berlin Heidelberg.

Alarcón, M. V., Lloret-Salamanca, A., Lloret, P. G., Iglesias, D. J., Talón, M., & Salguero, J. (2009). Effects of antagonists and inhibitors of ethylene biosynthesis on maize root elongation. *Plant Signaling & Behavior*, *4*(12), 1154–1156.

Anjam, M. S., Ludwig, Y., Hochholdinger, F., Miyaura, C., Inada, M., Siddique, S., & Grundler, F. M. W. (2016). An improved procedure for isolation of high-quality RNA from nematode-infected Arabidopsis roots through laser capture microdissection. *Plant Methods*, *12*, 25.

Arber, A. (1930). Studies in the Gramineae. IX. 1. The Nodal Plexus. 2. Amphivasal Bundles. *Annals of Botany*, *44*(175), 593–620.

Bainbridge, K., Guyomarc'h, S., Bayer, E., Swarup, R., Bennett, M., Mandel, T., & Kuhlemeier, C. (2008). Auxin influx carriers stabilize phyllotactic patterning. *Genes & Development*, *22*(6), 810–823.

Baskin, T. I., Briggs, W. R., & Iino, M. (1986). Can lateral redistribution of auxin account for phototropism of maize coleoptiles? *Plant Physiology*, *81*(1), 306–309.

Baskin, T. I., Iino, M., Green, P. B., & Briggs, W. R. (1985). High-resolution measurement of growth during first positive phototropism in maize. *Plant, Cell & Environment*, *8*(8), 595–603.

Battal, P., Erez, M. E., Turker, M., & Berber, I. (2008). Molecular and Physiological Changes in Maize (*Zea mays*) Induced by Exogenous NAA, ABA and MeJa during Cold Stress. *Annales Botanici Fennici*, *45*(3), 173–185.

Bellini, C., Pacurar, D. I., & Perrone, I. (2014). Adventitious roots and lateral roots: similarities and differences. *Annual Review of Plant Biology*, *65*, 639–666.

Benková, E., Michniewicz, M., Sauer, M., Teichmann, T., Seifertová, D., Jürgens, G., & Friml, J. (2003). Local, efflux-dependent auxin gradients as a common module for plant organ formation. *Cell*, *115*(5), 591–602.

Birnbaum, K. D. (2016). How many ways are there to make a root? *Current Opinion in Plant Biology*, *34*, 61–67.

Blizard, S. & Sparks, E.E. (2020). Maize Nodal Roots. *Annual Plant Reviews Online*, 3, 281-304.

Bosco, C. D., Dovzhenko, A., Liu, X., Woerner, N., Rensch, T., Eismann, M., Eimer, S., Hegermann, J., Paponov, I. A., Ruperti, B., Heberle-Bors, E., Touraev, A., Cohen, J. D., & Palme, K. (2012). The endoplasmic reticulum localized PIN8 is a pollen-specific auxin carrier involved in intracellular auxin homeostasis. *The Plant Journal: For Cell and Molecular Biology*, 71(5), 860–870.

Bronsema, F. B. F., van Oostveen, W. J. F., & van Lammeren, A. A. M. (2001). Influence of 2, 4-, TIBA and 3, 5- on the growth response of cultured maize embryos. *Plant Cell, Tissue and Organ Culture*, 65, 45–56.

Brunoud, G., Wells, D. M., Oliva, M., Larrieu, A., Mirabet, V., Burrow, A. H., Beeckman, T., Kepinski, S., Traas, J., Bennett, M. J., & Vernoux, T. (2012). A novel sensor to map auxin response and distribution at high spatio-temporal resolution. *Nature*, 482(7383), 103–106.

Carraro, N., Forestan, C., Canova, S., Traas, J., & Varotto, S. (2006). ZmPIN1a and ZmPIN1b encode two novel putative candidates for polar auxin transport and plant architecture determination of maize. *Plant Physiology*, 142(1), 254–264.

Chadwick, A. V., & Burg, S. P. (1970). Regulation of Root Growth by Auxin-Ethylene Interaction1. *Plant Physiology*, 45, 192–200.

Chen, Y., Hao, X., & Cao, J. (2014). Small auxin upregulated RNA (SAUR) gene family in maize: identification, evolution, and its phylogenetic comparison with Arabidopsis, rice, and sorghum. *Journal of Integrative Plant Biology*, *56*(2), 133–150.

Chen, Y., Yordanov, Y. S., Ma, C., Strauss, S., & Busov, V. B. (2013). DR5 as a reporter system to study auxin response in Populus. *Plant Cell Reports*, *32*(3), 453–463.

Chettoor, A. M., & Evans, M. M. S. (2015). Correlation between a loss of auxin signaling and a loss of proliferation in maize antipodal cells. *Frontiers in Plant Science*, *6*, 187.

Chuck, G., Cigan, A. M., Saeteurn, K., & Hake, S. (2007). The heterochronic maize mutant Corngrass1 results from overexpression of a tandem microRNA. *Nature Genetics*, *39*(4), 544–549.

de Klerk, G.J., van der Krieken, W., & de Jong, J. C. (1999). Review the formation of adventitious roots: New concepts, new possibilities. *In Vitro Cellular & Developmental Biology - Plant*, *35*(3), 189–199.

Delbarre, A., Muller, P., Imhoff, V., & Guern, J. (1996). Comparison of mechanisms controlling uptake and accumulation of 2,4-dichlorophenoxy acetic acid, naphthalene-1-acetic acid, and indole-3-acetic acid in suspension-cultured tobacco cells. *Planta*, *198*(4), 532–541.

Dembinsky, D., Woll, K., Saleem, M., Liu, Y., Fu, Y., Borsuk, L. A., Lamkemeyer, T., Fladerer, C., Madlung, J., Barbazuk, B., Nordheim, A., Nettleton, D., Schnable, P. S., & Hochholdinger, F. (2007). Transcriptomic and proteomic analyses of pericycle cells of the maize primary root. *Plant Physiology*, *145*(3), 575–588.

De Wolff, F. (1971). Techniques for the vegetative propagation of maize (Zea mays L.). *Euphytica/ Netherlands Journal of Plant Breeding*, *20*(4), 524–526.

Dhonukshe, P., Grigoriev, I., Fischer, R., Tominaga, M., Robinson, D. G., Hasek, J., Paciorek, T., Petrásek, J., Seifertová, D., Tejos, R., Meisel, L. A., Zazímalová, E., Gadella, T. W. J., Jr, Stierhof, Y.-D., Ueda, T., Oiwa, K., Akhmanova, A., Brock, R., Spang, A., & Friml, J. (2008). Auxin transport inhibitors impair vesicle motility and actin cytoskeleton dynamics in diverse eukaryotes. *Proceedings of the National Academy of Sciences of the United States of America*, *105*(11), 4489–4494.

Doebley, J., Stec, A., & Hubbard, L. (1997). The evolution of apical dominance in maize. *Nature*, *386*(6624), 485–488.

Drew, M. C., Jackson, M. B., & Giffard, S. (1979). Ethylene-promoted adventitious rooting and development of cortical air spaces (aerenchyma) in roots may be adaptive responses to flooding in Zea mays L. *Planta*, *147*(1), 83–88.

Du, Z., Zhou, X., Ling, Y., Zhang, Z., & Su, Z. (2010). agriGO: a GO analysis toolkit for the agricultural community. *Nucleic Acids Research*, *38*(Web Server issue), W64–W70.

Evans, A. T. (1928). Vascularization of the Node in Zea Mays. *Botanical Gazette* , *85*(1), 97–103.

Feraru, E., & Friml, J. (2008). PIN polar targeting. *Plant Physiology*, *147*(4), 1553–1559.

Forestan, C., Farinati, S., & Varotto, S. (2012). The Maize PIN Gene Family of Auxin Transporters. *Frontiers in Plant Science*, *3*, 16.

Forestan, C., & Varotto, S. (2010). PIN1 auxin efflux carriers localization studies in Zea mays [Review of *PIN1 auxin efflux carriers localization studies in Zea mays*]. *Plant Signaling & Behavior*, *5*(4), 436–439.

Forestan, C., & Varotto, S. (2012). The role of PIN auxin efflux carriers in polar auxin transport and accumulation and their effect on shaping maize development. *Molecular Plant*, *5*(4), 787–798.

Friml, J., Vieten, A., Sauer, M., Weijers, D., Schwarz, H., Hamann, T., Offringa, R., & Jürgens, G. (2003). Efflux-dependent auxin gradients establish the apical-basal axis of Arabidopsis. *Nature*, *426*(6963), 147–153.

Fukaki, H., Okushima, Y., & Tasaka, M. (2007). Auxin-mediated lateral root formation in higher plants. *International Review of Cytology*, *256*, 111–137.

Fukaki, H., & Tasaka, M. (2009). Hormone interactions during lateral root formation. *Plant Molecular Biology*, *69*(4), 437–449.

Gallavotti, A., Yang, Y., Schmidt, R. J., & Jackson, D. (2008). The Relationship between auxin transport and maize branching. *Plant Physiology*, *147*(4), 1913–1923.

Gao, L., Shen, G., Zhang, L., Qi, J., Zhang, C., Ma, C., Li, J., Wang, L., Malook, S. U., & Wu, J. (2019). An efficient system composed of maize protoplast transfection and HPLC-MS for studying the biosynthesis and regulation of maize benzoxazinoids. *Plant Methods*, *15*, 144.

Gerik, T. J., & Neely, C. L. (1987). Plant Density Effects on Main Culm and Tiller Development of Grain Sorghum 1. *Crop Science*, *27*(6), 1225–1230.

Gougler, J. A., & Evans, M. L. (1981). Adaptation of corn roots to exogenously applied auxin. *Physiologia Plantarum*, *51*(4), 394–398.

Guan, J. C., Koch, K. E., Suzuki, M., Wu, S., Latshaw, S., Petruff, T., Goulet, C., Klee, H. J., & McCarty, D. R. (2012). Diverse roles of strigolactone signaling in maize architecture and the uncoupling of a branching-specific subnetwork. *Plant Physiology*, *160*(3), 1303–1317.

Guilfoyle, T. J., & Hagen, G. (2007). Auxin response factors. *Current Opinion in Plant Biology*, *10*(5), 453–460.

Guo, Y., Chen, F., Zhang, F., & Mi, G. (2005). Auxin transport from shoot to root is involved in the response of lateral root growth to localized supply of nitrate in maize. *Plant Science: An International Journal of Experimental Plant Biology*, *169*(5), 894–900.

Hetz, W., Hochholdinger, F., Schwall, M., & Feix, G. (1996). Isolation and characterization of rtcs, a maize mutant deficient in the formation of nodal roots. *The Plant Journal: For Cell and Molecular Biology*, *10*(5), 845–857.

Hitch, P. A., & Sharman, B. C. (1971). The Vascular Pattern of Festucoid Grass Axes, with Particular Reference to Nodal Plexi. *Botanical Gazette* , *132*(1), 38–56.

Hochholdinger, F., & Feix, G. (1998a). Early post-embryonic root formation is specifically affected in the maize mutant lrt1. *The Plant Journal: For Cell and Molecular Biology*, *16*(2), 247–255.

Hochholdinger, F., & Feix, G. (1998b). Cyclin expression is completely suppressed at the site of crown root formation in the nodal region of the maize root mutant rtcs. *The Journal of Plant Physiology*, 153 (3-4), 425-429.

Hochholdinger, F., Woll, K., Sauer, M., & Dembinsky, D. (2004). Genetic dissection of root formation in maize (Zea mays) reveals root-type specific developmental programmes. *Annals of Botany*, *93*(4), 359–368.

Hoppe, D. C., McCully, M. E., & Wenzel, C. L. (1986). The nodal roots of Zea: their development in relation to structural features of the stem. *Canadian Journal of Botany*, 64, 2524-2537.

Iino, M. (1995). Gravitropism and Phototropism of Maize Coleoptiles: Evaluation of the Cholodny-Went Theory Through Effects of Auxin Application and Decapitation. *Plant & Cell Physiology*, *36*(2), 361–367.

Inukai, Y., Sakamoto, T., Ueguchi-Tanaka, M., Shibata, Y., Gomi, K., Umemura, I., Hasegawa, Y., Ashikari, M., Kitano, H., & Matsuoka, M. (2005). Crown rootless1, which is essential for crown root formation in rice, is a target of an AUXIN RESPONSE FACTOR in auxin signaling. *The Plant Cell*, *17*(5), 1387–1396.

Jansen, L., Roberts, I., De Rycke, R., & Beeckman, T. (2012). Phloem-associated auxin response maxima determine radial positioning of lateral roots in maize. *Philosophical Transactions of the Royal Society of London. Series B, Biological Sciences*, *367*(1595), 1525–1533.

Jenkins, M. T. (1930). Heritable Characters of MaizeXXXIV—Rootless. *The Journal of Heredity*, *21*(2), 79–80.

Jiang, K., Meng, Y. L., & Feldman, L. J. (2003). Quiescent center formation in maize roots is associated with an auxin-regulated oxidizing environment. *Development* , *130*(7), 1429–1438.

Justin, S. H. F. W., & Armstrong, W. (1991). A reassessment of the influence of NAA on aerenchyma formation in maize roots. *The New Phytologist*, *117*(4), 607–618.

Kaldenhoff, R., & Iino, M. (1997). Restoration of phototropic responsiveness in decapitated maize coleoptiles. *Plant Physiology*, *114*(4), 1267–1272.

Kaldorf, M., & Ludwig-Muller, J. (2000). AM fungi might affect the root morphology of maize by increasing indole-3-butyric acid biosynthesis. *Physiologia Plantarum*, *109*(1), 58–67.

Kaya, C., Ashraf, M., Dikilitas, M., & Tuna, A. L. (2013). Alleviation of salt stress-induced adverse effects on maize plants by exogenous application of indoleacetic acid (IAA) and inorganic nutrients - A field trial. *Australian Journal of Crop Science*, *7*(2), 249–254.

Kerk, N., & Feldman, L. (1994). The quiescent center in roots of maize: initiation, maintenance and role in organization of the root apical meristem. *Protoplasma*, *183*, 100–106.

Knauss, S., Rohrmeier, T., & Lehle, L. (2003). The auxin-induced maize gene ZmSAUR2 encodes a short-lived nuclear protein expressed in elongating tissues. *The Journal of Biological Chemistry*, *278*(26), 23936–23943.

Kohlen, W., Charnikhova, T., Lammers, M., Pollina, T., Tóth, P., Haider, I., Pozo, M. J., de Maagd, R. A., Ruyter-Spira, C., Bouwmeester, H. J., & López-Ráez, J. A. (2012). The tomato CAROTENOID CLEAVAGE DIOXYGENASE8 (SlCCD8) regulates rhizosphere signaling, plant architecture and affects reproductive development through strigolactone biosynthesis. *The New Phytologist*, *196*(2), 535–547.

Krause, G. H., & Weis, E. (1991). Chlorophyll Fluorescence and Photosynthesis: The Basics. *Annual Review of Plant Physiology and Plant Molecular Biology*, *42*(1), 313–349.

Kurihara, D., Mizuta, Y., Sato, Y., & Higashiyama, T. (2015). ClearSee: a rapid optical clearing reagent for whole-plant fluorescence imaging. *Development*, *142*(23), 4168–4179.

Kushwah, S., Jones, A. M., & Laxmi, A. (2011). Cytokinin interplay with ethylene, auxin, and glucose signaling controls Arabidopsis seedling root directional growth. *Plant Physiology*, *156*(4), 1851–1866.

Lakehal, A., & Bellini, C. (2019). Control of adventitious root formation: insights into synergistic and antagonistic hormonal interactions. *Physiologia Plantarum*, *165*(1), 90–100.

Li, J., Chen, F., Li, Y., Li, P., Wang, Y., Mi, G., & Yuan, L. (2019). ZmRAP2.7, an AP2 Transcription Factor, Is Involved in Maize Brace Roots Development. *Frontiers in Plant Science*, *10*, 820.

Liu, P., Yan, K., Lei, Y.X., Xu, R., Zhang, Y.M., Yang, G.D., Huang, J.G., Wu, C.A., & Zheng, C.C. (2013). Transcript profiling of microRNAs during the early development of the maize brace root via Solexa sequencing. *Genomics*, *101*(2), 149–156.

Liu, Y., Jiang, H. Y., Chen, W., Qian, Y., Ma, Q., Cheng, B., & Zhu, S. (2011). Genome-wide analysis of the auxin response factor (ARF) gene family in maize (Zea mays). *Plant Growth Regulation*, *63*, 225–234.

Li, Y.J., Fu, Y.R., Huang, J.G., Wu, C.A., & Zheng, C.C. (2011). Transcript profiling during the early development of the maize brace root via Solexa sequencing. *The FEBS Journal*, *278*(1), 156–166.

Li, Z., Li, P., & Zhang, J. (2019). Expression analysis of PIN-formed auxin efflux transporter genes in maize. *Plant Signaling & Behavior*, *14*(9), 1632689.

Perez, L., Aguilar, R., & Sanchez-de-Jimenez E. (1987). Effect of an exogenous auxin on maize tissues. Alteration of protein synthesis and phosphorylation. *Physiol. Plantarum*, *69*, 517–522.

Ludwig, Y., Zhang, Y., & Hochholdinger, F. (2013). The maize (Zea mays L.) AUXIN/INDOLE-3-ACETIC ACID gene family: phylogeny, synteny, and unique root-type and tissue-specific expression patterns during development. *PloS One*, *8*(11), e78859.

Lur', H.-S., & Setter, T. 1. (1993). Role of Auxin in Maize Endosperm Development. *Plant Physiology*, *103*, 273–280.

Majer, C., & Hochholdinger, F. (2011). Defining the boundaries: structure and function of LOB domain proteins. *Trends in Plant Science*, *16*(1), 47–52.

Majer, C., Xu, C., Berendzen, K. W., & Hochholdinger, F. (2012). Molecular interactions of ROOTLESS CONCERNING CROWN AND SEMINAL ROOTS, a LOB domain protein regulating shoot-borne root initiation in maize (Zea mays L.). *Philosophical Transactions of the Royal Society of London. Series B, Biological Sciences*, *367*(1595), 1542–1551.

Martínez-de la Cruz, E., García-Ramírez, E., Vázquez-Ramos, J. M., Reyes de la Cruz, H., & López-Bucio, J. (2015). Auxins differentially regulate root system architecture and cell cycle protein levels in maize seedlings. *Journal of Plant Physiology*, *176*, 147–156.

McCarty, D. R., Mark Settles, A., Suzuki, M., Tan, B. C., Latshaw, S., Porch, T., Robin, K., Baier, J., Avigne, W., Lai, J., Messing, J., Koch, K. E., & Curtis Hannah, L. (2005). Steady-state transposon mutagenesis in inbred maize: Maize steady-state transposon mutagenesis. *The Plant Journal: For Cell and Molecular Biology*, *44*(1), 52–61.

McCully, M. E., & Mallett, J. E. (1993). The Branch Roots of Zea. 3, Vascular Connections and Bridges for Nutrient Recycling. *Annals of Botany*, *71*(4), 327–341.

Mir, R., Aranda, L. Z., Biaocchi, T., Luo, A., Sylvester, A. W., & Rasmussen, C. G. (2017). A DII Domain-Based Auxin Reporter Uncovers Low Auxin Signaling during Telophase and Early G1. *Plant Physiology*, *173*(1), 863–871.

Muday, G. K., Rahman, A., & Binder, B. M. (2012). Auxin and ethylene: collaborators or competitors? *Trends in Plant Science*, *17*(4), 181–195.

Nakazono, M., Qiu, F., Borsuk, L. A., & Schnable, P. S. (2003). Laser-capture microdissection, a tool for the global analysis of gene expression in specific plant cell types: identification of genes expressed differentially in epidermal cells or vascular tissues of maize. *The Plant Cell*, *15*(3), 583–596.

Nick, P. (1997). Phototropic Stimulation can Shift the Gradient of Crown Root Emergence in Maize. *Journal of the German Botanical Society*, *110*(4), 291–297.

Nielsen, R. L. (2014). Determining corn leaf stages. *Corny News Network*. https://www.agry.purdue.edu/ext/corn/news/articles.04/VStageMethods-0515.pdf

O'Connor, D. L., Runions, A., Sluis, A., Bragg, J., Vogel, J. P., Prusinkiewicz, P., & Hake, S. (2014). A division in PIN-mediated auxin patterning during organ initiation in grasses. *PLoS Computational Biology*, *10*(1), e1003447.

Okada, K., Ueda, J., Komaki, M. K., Bell, C. J., & Shimura, Y. (1991). Requirement of the Auxin Polar Transport System in Early Stages of Arabidopsis Floral Bud Formation. *The Plant Cell*, *3*(7), 677–684.

Okushima, Y., Fukaki, H., Onoda, M., Theologis, A., & Tasaka, M. (2007). ARF7 and ARF19 regulate lateral root formation via direct activation of LBD/ASL genes in Arabidopsis. *The Plant Cell*, *19*(1), 118–130.

Ortiz-Ramírez, C., Arevalo, E. D., Xu, X., Jackson, D. P., & Birnbaum, K. D. (2018). An Efficient Cell Sorting Protocol for Maize Protoplasts. *Current Protocols in Plant Biology*, *3*(3), e20072.

Plowman, A. B. (1906). The Comparative Anatomy and Phylogeny of the Cyperaceae. *Annals of Botany*, *20*(77), 1–33.

Poethig, R. S. (2010). The past, present, and future of vegetative phase change. *Plant Physiology*, *154*(2), 541–544.

Ponce, G., Barlow, P. W., Feldman, L. J., & Cassab, G. I. (2005). Auxin and ethylene interactions control mitotic activity of the quiescent centre, root cap size, and pattern of cap cell differentiation in maize. *Plant, Cell & Environment*, *28*(6), 719–732.

Porfírio, S., Gomes da Silva, M. D. R., Peixe, A., Cabrita, M. J., & Azadi, P. (2016). Current analytical methods for plant auxin quantification--A review. *Analytica Chimica Acta*, *902*, 8–21.

Portwood, J. L., Woodhouse, M. R., Cannon, E. K., Gardiner, J. M., Harper, L. C., Schaeffer, M. L., Walsh, J. R., Sen, T. Z., Cho, K. T., Schott, D. A., Braun, B. L., Dietze, M., Dunfee, B., Elsik, C. G., Manchanda, N., Coe, E., Sachs, M., Stinard, P., Tolbert, J., … Andorf, C. M. (2019). MaizeGDB 2018: the maize multi-genome genetics and genomics database. *Nucleic Acids Research*, *47*(D1), D1146–D1154.

Rasmussen, A., Mason, M. G., De Cuyper, C., Brewer, P. B., Herold, S., Agusti, J., Geelen, D., Greb, T., Goormachtig, S., Beeckman, T., & Beveridge, C. A. (2012). Strigolactones suppress adventitious rooting in Arabidopsis and pea. *Plant Physiology*, *158*(4), 1976–1987.

Rhoades, M. W., Reinhart, B. J., Lim, L. P., Burge, C. B., Bartel, B., & Bartel, D. P. (2002). Prediction of plant microRNA targets. *Cell*, *110*(4), 513–520.

Rubery, P. H. (1990). Phytotropins: receptors and endogenous ligands. *Symposia of the Society for Experimental Biology.*, *44*, 119–146.

Salvi, S., Sponza, G., Morgante, M., Tomes, D., Niu, X., Fengler, K. A., Meeley, R., Ananiev, E. V., Svitashev, S., Bruggemann, E., Li, B., Hainey, C. F., Radovic, S., Zaina, G., Rafalski, J.-A., Tingey, S. V., Miao, G.-H., Phillips, R. L., & Tuberosa, R. (2007). Conserved noncoding genomic sequences associated with a flowering-time quantitative trait locus in maize. *Proceedings of the National Academy of Sciences of the United States of America*, *104*(27), 11376–11381.

Shane, M. W., Mc Cully, M. E., & Canny, M. J. (2000). The Vascular System of Maize Stems Revisited: Implications for Water Transport and Xylem Safety. *Annals of Botany*, *86*, 245–258.

Sharman, B. C. (1942). Developmental Anatomy of the Shoot of Zea mays L. *Annals of Botany*, *6*(22), 245–282.

Shi, J., Drummond, B. J., Habben, J. E., Brugire, N., Weers, B. P., Hakimi, S. M., Lafitte, H. R., Schussler, J. R., Mo, H., Beatty, M., Zastrow-Hayes, G., & O'Neill, D. (2019). Ectopic expression of ARGOS8 reveals a role for ethylene in root-lodging resistance in maize. *The Plant Journal: For Cell and Molecular Biology*, *97*(2), 378–390.

Spicer, R., & Groover, A. (2010). Evolution of development of vascular cambia and secondary growth. *The New Phytologist*, *186*(3), 577–592.

Stamp, P., & Kiel, C. (1992). Root Morphology of Maize and Its Relationship to Root Lodging. *Journal of Agronomy and Crop Science*, *168*(2), 113–118.

Steffens, B., & Rasmussen, A. (2016). The Physiology of Adventitious Roots. *Plant Physiology*, *170*(2), 603–617.

Stelpflug, S. C., Sekhon, R. S., Vaillancourt, B., Hirsch, C. N., Buell, C. R., de Leon, N., & Kaeppler, S. M. (2016). An Expanded Maize Gene Expression Atlas based on RNA Sequencing and its Use to Explore Root Development. *The Plant Genome*, *9*(1).

Stepanova, A. N., & Alonso, J. M. (2019). From Ethylene-Auxin Interactions to Auxin Biosynthesis and Signal Integration. *The Plant Cell*, *31*(7), 1393–1394.

Stepanova, A. N., Yun, J., Likhacheva, A. V., & Alonso, J. M. (2007). Multilevel interactions between ethylene and auxin in Arabidopsis roots. *The Plant Cell*, *19*(7), 2169–2185.

Sun H., Lang Z., Zhu L., & Huang D. (2013). Optimized condition for protoplast isolation from maize, wheat and rice leaves. *Chinese journal of biotechnology*, *29*(2), 224–234.

Sun, H., Tao, J., Hou, M., Huang, S., Chen, S., Liang, Z., Xie, T., Wei, Y., Xie, X., Yoneyama, K., Xu, G., & Zhang, Y. (2015). A strigolactone signal is required for adventitious root formation in rice. *Annals of Botany*, *115*(7), 1155–1162.

Suzuki, M., Sato, Y., Wu, S., Kang, B.-H., & McCarty, D. R. (2015). Conserved Functions of the MATE Transporter BIG EMBRYO1 in Regulation of Lateral Organ Size and Initiation Rate. *The Plant Cell*, *27*(8), 2288–2300.

Swarup, R., Parry, G., Graham, N., Allen, T., & Bennett, M. (2002). Auxin crosstalk: integration of signaling pathways to control plant development. *Plant Molecular Biology*, *49*(3-4), 411–426.

Taramino, G., Sauer, M., Stauffer, J. L., Jr, Multani, D., Niu, X., Sakai, H., & Hochholdinger, F. (2007). The maize (Zea mays L.) RTCS gene encodes a LOB domain protein that is a key regulator of embryonic seminal and post-embryonic shoot-borne root initiation: Map-based cloning of the maize RTCS gene. *The Plant Journal: For Cell and Molecular Biology*, *50*(4), 649–659.

Teale, W., & Palme, K. (2018). Naphthylphthalamic acid and the mechanism of polar auxin transport. *Journal of Experimental Botany*, *69*(2), 303–312.

The Maize Auxin Gene Catalog – *Auxin Regulatory and Expression Database for Maize*. (n.d.). Retrieved May 28, 2020, from https://maizeauxre.missouri.edu/home_gene_catalog_1/

Tian, Q., Chen, F., Liu, J., Zhang, F., & Mi, G. (2008). Inhibition of maize root growth by high nitrate supply is correlated with reduced IAA levels in roots. *Journal of Plant Physiology*, *165*(9), 942–951.

Tiwari, S. B., Wang, X. J., Hagen, G., & Guilfoyle, T. J. (2001). AUX/IAA proteins are active repressors, and their stability and activity are modulated by auxin. *The Plant Cell*, *13*(12), 2809–2822.

T.W. Donaldson, D.E. Bayer, and O.A. Leonard. (1973). Absorption of 2,4-Dichlorophenoxyacetic Acid and 3-(p-Chlorophenyl)-1,1-dimethylurea (Monuron) by Barley Roots. *Plant Physiology*, *52*, 638–645.

Ulmasov, T., Murfett, J., Hagen, G., & Guilfoyle', T. J. (1997). Aux/lAA Proteins Repress Expression of Reporter Genes Containing Natural and Highly Active Synthetic Auxin Response Elements. *The Plant Cell*, *9*, 1963–1971.

Ursache, R., Andersen, T. G., Marhavý, P., & Geldner, N. (2018). A protocol for combining fluorescent proteins with histological stains for diverse cell wall components. *The Plant Journal: For Cell and Molecular Biology*, *93*(2), 399–412.

von Behrens, I., Komatsu, M., Zhang, Y., Berendzen, K. W., Niu, X., Sakai, H., Taramino, G., & Hochholdinger, F. (2011). Rootless with undetectable meristem 1 encodes a monocot-specific AUX/IAA protein that controls embryonic seminal and post-embryonic lateral root initiation in maize. *The Plant Journal: For Cell and Molecular Biology*, *66*(2), 341–353.

Wang, J.R., Hu, H., Wang, G.H., Li, J., Chen, J.Y., & Wu, P. (2009). Expression of PIN genes in rice (Oryza sativa L.): tissue specificity and regulation by hormones. *Molecular Plant*, *2*(4), 823–831.

Wang, Y., Deng, D., Shi, Y., Miao, N., Bian, Y., & Yin, Z. (2012). Diversification, phylogeny, and evolution of auxin response factor (ARF) family: insights gained from analyzing maize ARF genes. *Molecular Biology Reports*, *39*(3), 2401–2415.

Waters, M. T., Gutjahr, C., Bennett, T., & Nelson, D. C. (2017). Strigolactone Signaling and Evolution. *Annual Review of Plant Biology*, *68*, 291–322.

Woll, K., Borsuk, L. A., Stransky, H., Nettleton, D., Schnable, P. S., & Hochholdinger, F. (2005). Isolation, characterization, and pericycle-specific transcriptome analyses of the novel maize lateral and seminal root initiation mutant rum1. *Plant Physiology*, *139*(3), 1255–1267.

Xing, H., Pudake, R. N., Guo, G., Xing, G., Hu, Z., Zhang, Y., Sun, Q., & Ni, Z. (2011). Genome-wide identification and expression profiling of auxin response factor (ARF) gene family in maize. *BMC Genomics*, *12*, 178.

Xu, C., Tai, H., Saleem, M., Ludwig, Y., Majer, C., Berendzen, K. W., Nagel, K. A., Wojciechowski, T., Meeley, R. B., Taramino, G., & Hochholdinger, F. (2015). Cooperative action of the paralogous maize lateral organ boundaries (LOB) domain proteins RTCS and RTCL in shoot-borne root formation. *The New Phytologist*, *207*(4), 1123–1133.

Xu, M., Zhu, L., Shou, H., & Wu, P. (2005). A PIN1 family gene, OsPIN1, involved in auxin-dependent adventitious root emergence and tillering in rice. *Plant & Cell Physiology*, *46*(10), 1674–1681.

Yamaji, N., & Ma, J. F. (2014). The node, a hub for mineral nutrient distribution in graminaceous plants. *Trends in Plant Science*, *19*(9), 556–563.

Yang, T., & Poovaiah, B. W. (2000). Molecular and biochemical evidence for the involvement of calcium/calmodulin in auxin action. *The Journal of Biological Chemistry*, *275*(5), 3137–3143.

Yue, R., Tie, S., Sun, T., Zhang, L., Yang, Y., Qi, J., Yan, S., Han, X., Wang, H., & Shen, C. (2015). Genome-wide identification and expression profiling analysis of ZmPIN, ZmPILS, ZmLAX and ZmABCB auxin transporter gene families in maize (Zea mays L.) under various abiotic stresses. *PloS One*, *10*(3), e0118751.

Yu, P., Baldauf, J. A., Lithio, A., Marcon, C., Nettleton, D., Li, C., & Hochholdinger, F. (2016). Root Type-Specific Reprogramming of Maize Pericycle Transcriptomes by Local High Nitrate Results in Disparate Lateral Root Branching Patterns. *Plant Physiology*, *170*(3), 1783–1798.

Yu, P., Eggert, K., von Wirén, N., Li, C., & Hochholdinger, F. (2015). Cell Type-Specific Gene Expression Analyses by RNA Sequencing Reveal Local High Nitrate-Triggered Lateral Root Initiation in Shoot-Borne Roots of Maize by Modulating Auxin-Related Cell Cycle Regulation. *Plant Physiology*, *169*(1), 690–704.

Zhang, Y., Paschold, A., Marcon, C., Liu, S., Tai, H., Nestler, J., Yeh, C.-T., Opitz, N., Lanz, C., Schnable, P. S., & Hochholdinger, F. (2014). The Aux/IAA gene rum1 involved in seminal and lateral root formation controls vascular patterning in maize (Zea mays L.) primary roots. *Journal of Experimental Botany*, *65*(17), 4919–4930.

Zhang, Z., Zhang, X., Lin, Z., Wang, J., Xu, M., Lai, J., Yu, J., & Lin, Z. (2018). The genetic architecture of nodal root number in maize. *The Plant Journal: For Cell and Molecular Biology*, *93*(6), 1032–1044.

Zinkgraf, M., Gerttula, S., & Groover, A. (2017). Transcript profiling of a novel plant meristem, the monocot cambium. *Journal of Integrative Plant Biology*, *59*(6), 436–449.

Chapter 2

MICROSCOPIC ANALYSIS OF AUXIN REPORTERS DURING BRACE ROOT DEVELOPMENT

2.1 Rationale

There is a limited understanding of how brace root development proceeds both at the anatomical and molecular level. In this chapter, I first establish the anatomical changes that occur over time (plant age) and space (plant nodes) during the course of brace root development in the maize inbred B73 line. I then leveraged this spatio-temporal developmental information to analyze auxin-related markers in transgenic reporter lines with the goal of uncovering the expression of auxin during brace root development.

2.2 Methods

2.2.1 Seed lines

Inbred line B73, Zea mays subsp. Mays, Newark, DE 2017, was used for all experiments not involving transgenic reporter lines.

Transgenic reporter lines (Table 3) were provided by Dr. Dave Jackson of Cold Spring Harbor Laboratory (CSHL) (TZUF12#1/B73 DR5::erRFP ev.#1, TZUF12#1/B73 DR5::erRFP ev.#2, TZUF12#1/B73 DR5::erRFP ev.#3, TZ173#1/B73 DR5::erRFP/PIN1::PIN1-YFP, TZ172#1/B73 DR5::erRFP,

TZ171/B73 DR5::erRFP, TZ170/B73 DR5::erRFP, TZ175/B73 PIN1::PIN1-YFP, TZ176/B73 PIN1::PIN1-YFP, TZ177/B73 PIN1-YFP) and from Dr. Carolyn Rasmussen of University of California Riverside (UCR-FP001-DII DEGRON-YFP event, UCR-FP002- mDII DEGRON-YFP event).

Table 3. Seeds lines used for transgenic reporter line experiments.

Seed line	Source
172#1/B73 DR5::erRFP ev. #3	Dave Jackson - CSHL
171#1/B73 DR5::erRFP ev. #2	Dave Jackson - CSHL
170#1/B73 DR5::erRFP ev. #1	Dave Jackson - CSHL
TZ173#1/B73 DR5::erRFP/PIN1::YFP	Dave Jackson - CSHL
TZ172#1/B73 DR5::erRFP	Dave Jackson - CSHL
TZ171/B73 DR5::erRFP	Dave Jackson - CSHL
TZ170#1/B73 DR5::erRFP	Dave Jackson - CSHL
TZ175/B73 PIN1::YFP	Dave Jackson - CSHL
TZ176/B73 PIN1::YFP	Dave Jackson - CSHL
TZ177/B73 PIN1::YFP	Dave Jackson - CSHL
UCR-FP001 - DII DEGRON::YFP event	Carolyn Rasmussen- UCR
UCR-FP002 - mDII DEGRON::YFP event	Carolyn Rasmussen-UCR

2.2.2 Spatio-temporal anatomical analysis

B73 plants were grown to four vegetative stages (V4, V6, V8, V10; Table 4) under greenhouse conditions in the University of Delaware Fisher Greenhouse Zone #4 in 3-gallon pots. Plants were grown and maintained by M.S. student Nathan Harlan.

Plants were staged using the drooping leaf method, which counts the number of leaves that have emerged and started to bend outward (Figure 1).

Table 4. Number of plants used at each vegetative stage for anatomical analysis.

Vegetative Stage	Number of Plants
V4	12
V6	6
V8	6
V10	6

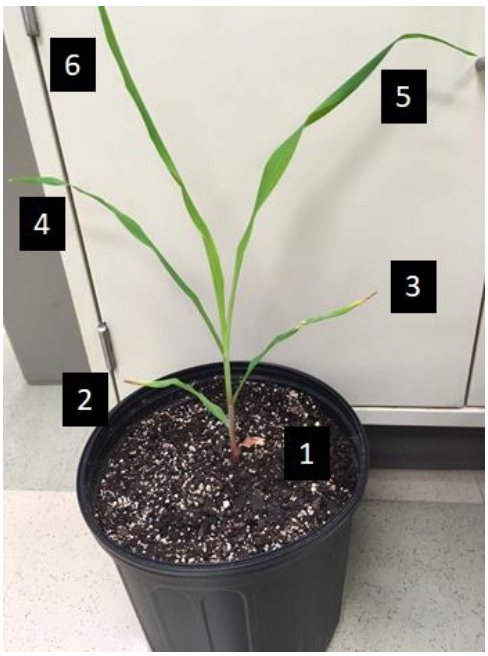

Figure 1. Maize plant (inbred B73) at vegetative leaf stage 6. Each number corresponds with a leaf. Numbering begins at the base of the plant with the thumb leaf and moves upward.

At each stage, plants were transported to the lab for sectioning and staining. Leaves were removed to expose stem nodes, and the bottom three aboveground nodes of each plant were used for analysis. Nodes were numbered starting from the base of the plant (node 1) and sequentially upward to node 3. Each node was hand sectioned using a kitchen knife and sections were placed in 24-, 12-, or 6-well plates in sequential order from bottom to top of the node. Sections were fixed overnight at 4°C in 4% PFA in 1X PBS. The following day, PFA was removed and sections were washed 2 times with 1X PBS. Sections were stained with 0.2% fuchsin in Clearsee (Kurihara et al., 2015; Ursache et al., 2018) and left overnight at room temperature. ClearSee was prepared as follows: 250 grams urea, 150 grams sodium deoxycholate, 100 grams xylitol, and distilled water was added up to 1 liter. The next day the stain was removed, and sections were rinsed once with Clearsee, then washed with Clearsee and incubated for 30 minutes with agitation, washed once more, and then left in Clearsee for 1 hour-to-overnight. Sections were imaged on a Zeiss Axiozoom microscope using a 2X magnification lens and metal halide lamp excitation with an mRFP filter cube (EX BP 572/25, BS FT 590, EM BP 629/62), housed in the DBI Bio-Imaging Center. The number of primordia were counted for each node and averaged for each node at each stage. The length of each primordia at each stage was measured using ImageJ. Node 1 had 13 primordia used for measurements, node 2 had 32 primordia, and node 3 had 2 primordia. P values were calculated using student's t-test in Excel.

2.2.3 Confirmation of transgene expression

Transgenic maize lines are maintained as outcrossed to non-transgenic lines (e.g. B73 for the lines used here). This outcrossing is to prevent transgene silencing,

which is common in maize. Thus, all lines analyzed are segregating 1:1 for the presence of the transgene. To confirm the presence and expression of the transgene in individual plants, I designed three different confirmation approaches: 1. Microscopic analysis for expression in lateral roots, 2. BASTA painting of leaves, 3. qRT-PCR for transcript expression.

2.2.3.1 Microscopic Analysis: For confocal analysis of lateral roots, transgenic seeds were placed in a 50 ml conical tube with 40 ml of 35% 1N H_2O_2 and incubated on an orbital shaker at 80RPM for 20 minutes to sterilize. H_2O_2 was decanted and the seeds washed 5x with sterile water. Seeds were submerged in sterile water overnight at room temperature. The next day the sterilization and washing process was repeated, and then the seeds were placed on moistened germination paper, rolled up, and placed in a beaker of sterile water at 28°C for a week or until lateral roots appeared. Lateral roots emerging from the primary root were visualized on a Zeiss Axiozoom microscope for their respective fluorescent protein - RFP, YFP, or Venus (Figure 2). Plants with positive (or negative for control) lateral root expression were transplanted in cone-tainers in the University of Delaware's Fisher Greenhouse Zone #4, and then transplanted into 3-gallon pots at approximately the V3 stage. The greenhouse was kept at an average temperature of 24.5°C, average humidity was 57.2%, and supplemental lighting in the form of 400 Watt High Pressure Sodium and 400 Watt Metal Halide bulbs was provided from 7 AM - 9 PM when outside light radiation levels were below 600 W/m^2 (watts per square meter). Plants were watered twice a week, once a week supplemented with nutrient solution, and soil (PROMIX BK55) was prepared with approximately 30 grams of slow release 19-6-9 osmocote pellets.

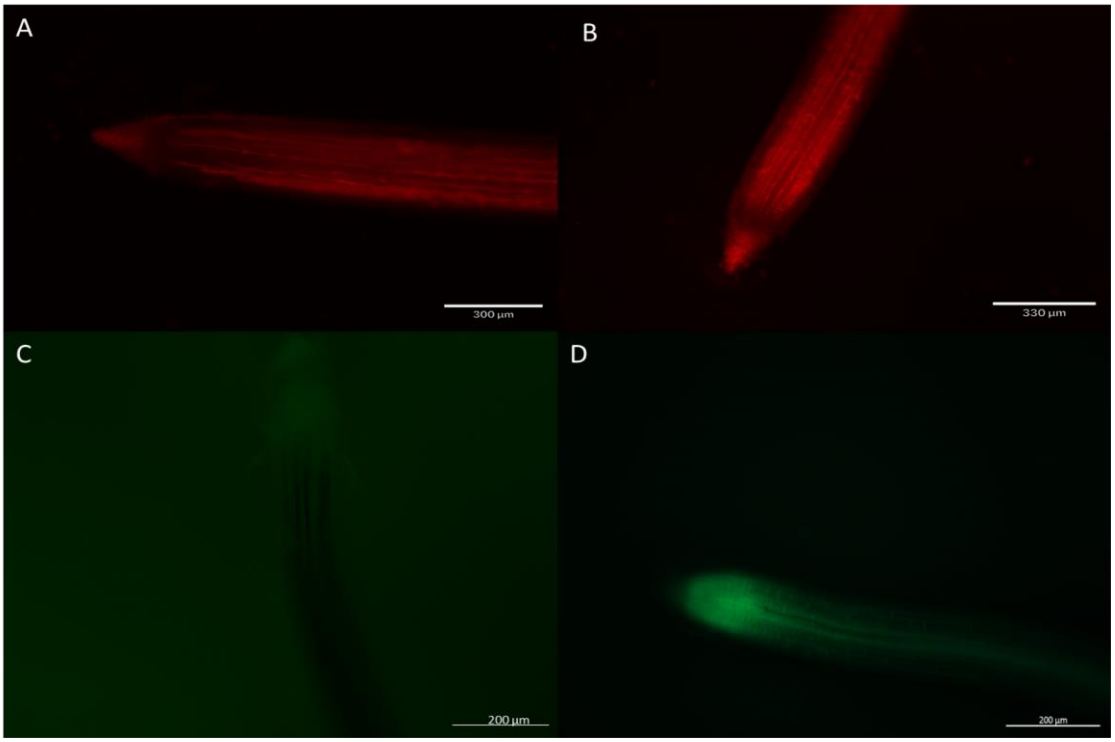

Figure 2. Fluorescent imaging of lateral roots to identify positive transgenic plants. A) A lateral root that was scored negative in the DR5::erRFP line. Scale bar= 300 µm. B) A lateral root that was scored positive in the DR5::erRFP line. Scale bar= 330 µm. C) A lateral root that was scored negative for the PIN1::PIN1-YFP line. Scale bar= 200 µm. D) A lateral root that was scored positive for the PIN1::PIN1-YFP line. Scale bar=200 µm. Paired images were obtained using the same gain and exposure settings.

2.2.3.2 BASTA Painting: The second approach to identify transgene-positive plants relies on the presence of an herbicide resistance cassette within the transgene. If the transgene is expressed, then a BASTA-resistance is also imparted. Thus, transgene-positive plants will not die in the presence of herbicide. Transgenic lines were grown

as described above. A solution of Finale (11.33% glufosinate) was diluted 1:10 in water and applied to either the tip or the middle of the leaf at approximately the V2-V3 stage. 3-5 days later the plants were scored for cell death, indicating the presence/absence of the transgene (Figure 3). Finale application to the middle of the leaf provided the most reliable quantification of transgene expression.

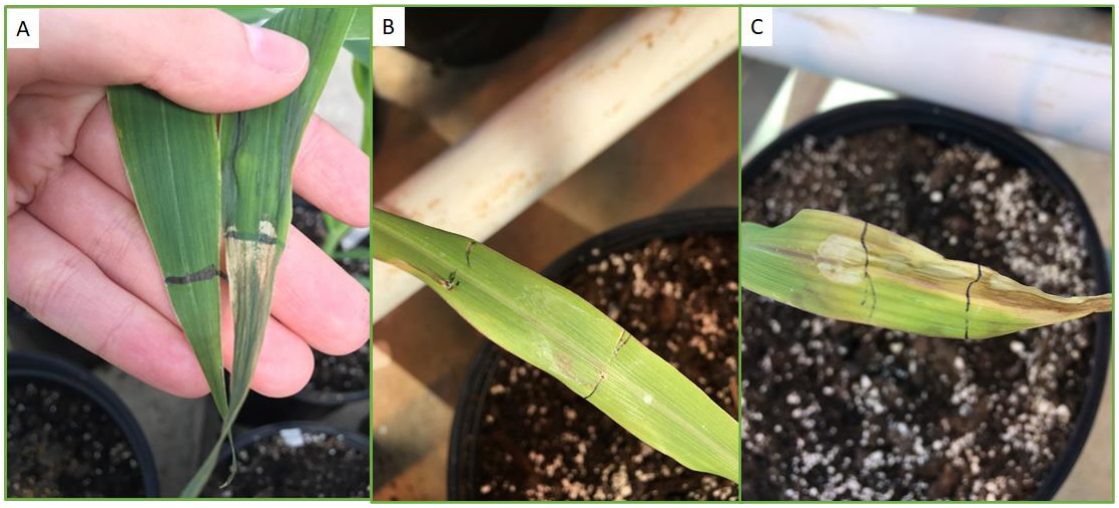

Figure 3. Basta painting of transgenic reporter lines. A) A Sharpie was used to mark the tips of the leaves and the herbicide was painted on this area with a cotton applicator. The left leaf shows a plant that displayed no cell death and was scored positive for the transgene. The right leaf shows a plant that displayed necrosis and was scored negative for the transgene. B-C) A Sharpie was used to draw a section across the middle of the leaf. B) A plant that was scored positive for the transgene. C) A plant that was scored negative for the transgene.

2.2.3.3 qRT-PCR Expression: Lastly, I designed a strategy to quantify the amount of transgene RNA present in the plants. This involves running a qRT-PCR using primers designed for the fluorophore sequence. Plants were grown under greenhouse conditions as described above. All instruments used were sterilized prior to use with

RNAse zap. At the V6 stage, a leaf was cut off and placed in a mortar pre-chilled with liquid nitrogen. A pestle, also pre-chilled, was used to grind the leaf tissue into a powder. The grounded leaf tissue was placed into an RNAse free microcentrifuge tube and stored at -80°C. Primers were designed with Primer3Plus to detect the expression of the transgene (Table 5), but not tested. Ultimately, this approach was not implemented to determine transgene expression, but may be useful for future studies.

Table 5. Primers for qRT-PCR analysis for the presence of RFP in transgenic lines. Primers were designed around the RFP sequence (SP1 and SP2).

Name	Forward sequence	Reverse sequence	Product Size (bp)	Temperature (°C)
SP1	CGAGGACGTC ATCAAGGAGT	CTTGGCCATGT AGGTGGTCT	541	60.3 (forward) 60 (reverse)
SP2	GAGTTCATGC GCTTCAAGGT	GTCCAGCTTGA TGTCGGTCT	573	60.4 (forward), 60.3(reverse)

2.2.4 Microscopic analysis of transgene expression during brace root development

Plants that were positive (experimental) and negative (control) for the transgene were further analyzed. Plants were harvested at the V6 stage (Figure 1), the first three aboveground nodes were hand-sectioned with a razor blade and placed in ClearSee. ClearSee was prepared as above. Sections were imaged on a Zeiss Axiozoom microscope.

For confocal analyses, hand excised nodes were embedded in tissue freezing medium (O.C.T.) and immediately flash frozen in liquid nitrogen. The first three

aboveground nodes were cryosectioned on a Leica 3050S Cryostat with CryoJane tape transfer. Slides were stored at -80°C before imaging and analysis.

PIN1::PIN1-YFP node sections were imaged on a LSM710 confocal microscope in the DBI Bio-Imaging Center. YFP was excited at 514 nm, and emission data collected across a broad spectrum. The YFP protein emitted at a specific peak of 554 nm. The RFP signal was excited at 594 nm, and emission data collected across a broad spectrum. RFP emitted at a specific peak of 676.5 nm. To differentiate emission from fluorescent proteins and autofluorescence (cell walls or chlorophyll), spectral imaging with linear unmixing was used to compare the emission spectra from B73 tissue (control) to DR5::erRFP tissue.

2.3 Results

2.3.1 A spatiotemporal analysis of brace root development

The first step in elucidating the mechanisms of brace root development was to ascertain the stage of plant and node at which brace roots were first initiating. The node closest to the ground was designated node 1, and the next highest node was designated node 2, etc. Nodes from plants at four stages (V4, V6, V8, and V10) were analyzed.

Analysis of these sections highlight a unique anatomical feature of grass nodes. First noted in the early 1900s (Arber 1930; Evans 1928; Hitch & Sharman 1971; Sharman 1942), monocot stem nodes contain horizontal vascular strands distinct from the vasculature found in internodes (Figure 4A-B). These strands have been called by many different names including anastomosis, nodal plexus, or vascular plexus (see

introduction). These strands are distinct by running horizontally as well as displaying a unique pattern vertically across the node. At the bottom of the node, the strands form a dense network throughout the entire cross section (Figure 4B). At the top of the node, the anastomosis gradually recedes to form a ring around the periphery of the cross section (Figure 4C-D). It is at this particular part of the node that brace root primordia initiate (Figure 4D). The formation of anastomosis in a ring-like structure serves as a landmark for identifying where brace root primordia will initiate.

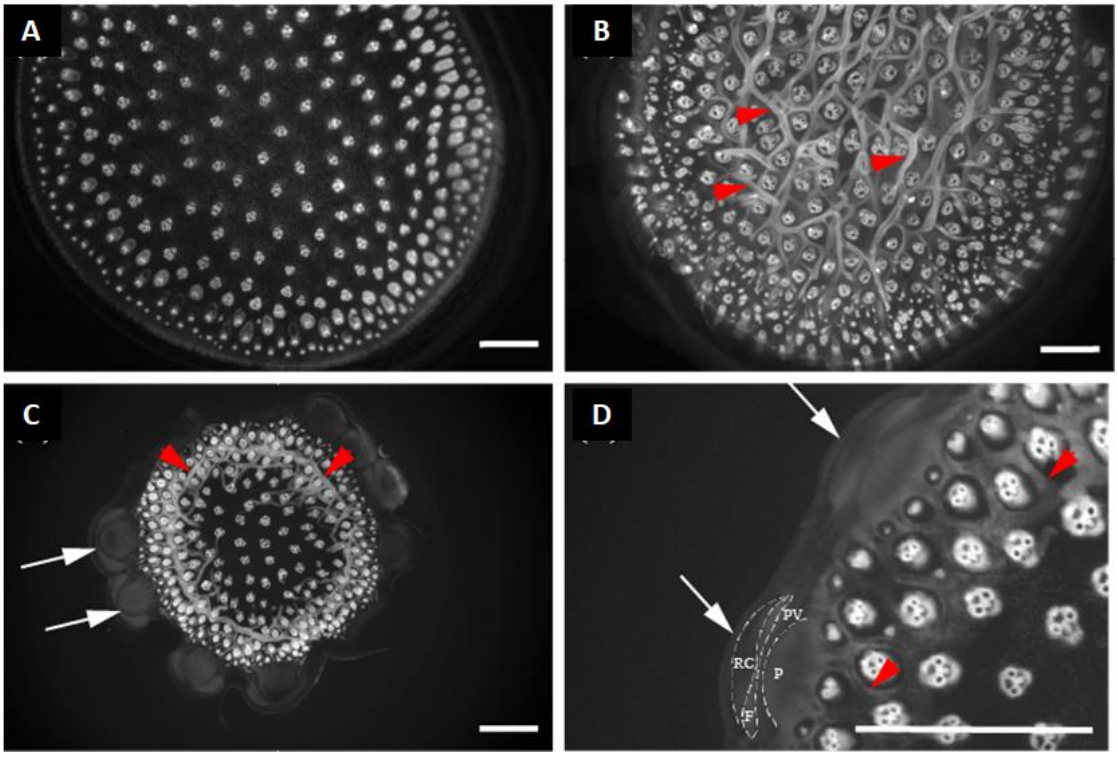

Figure 4. Maize Stem Anatomy. A) Typical anatomy of a maize internode section. White indicates lignin-positive vascular bundles. B) The base of the maize node is characterized by the presence of an extensive horizontal vascular plexus. C) The upper portion of the maize node is characterized by a peripheral vascular plexus and the presence of nodal root primordia. D) A higher magnification of the nodal root primordia. Note the flattened root cap (RC) morphology characteristic of the brace root primordia. Dashed lines indicate different tissues: RC - root cap; F - flanking; PV – pro-vascular; P - pith. Aboveground nodal sections from B73 plants at V10 that are stained with fuchsin (lignin). Red arrowheads indicate vascular plexus. White arrows indicate nodal root primordia. Images acquired on a Zeiss Axiozoom microscope. Scale bars = 2,000 µm. Figure adapted from Blizard & Sparks, 2020

Since brace root development proceeds across both space and time, I analyzed node sections across space (the first three aboveground nodes) and time (stages V4, V6, V8, and V10). The primordia found in node 1 of a plant are usually more mature

than primordia found in any higher nodes (Figure 5). In early stages (V4-V8), node 1 usually contains more primordia than the other nodes (Figure 6) In later stages (V10), nodes 2 and 3 can contain similar numbers of primordia as node 1 (Figure 6). At the V4 stage, primordia are initiating in node 1, are in the induction phase at node 2, and no development is visible at node 3. At the V6 stage, brace roots are emerging from node 1, primordia are initiating at node 2, and node 3 is at the induction phase. At the V8 stage, brace roots are fully emerged from node 1, and primordia are initiating at nodes 2 and 3. At the V10 stage, brace roots are fully emerged from nodes 1 and 2, but primordia are initiating at node 3 (Figure 5).

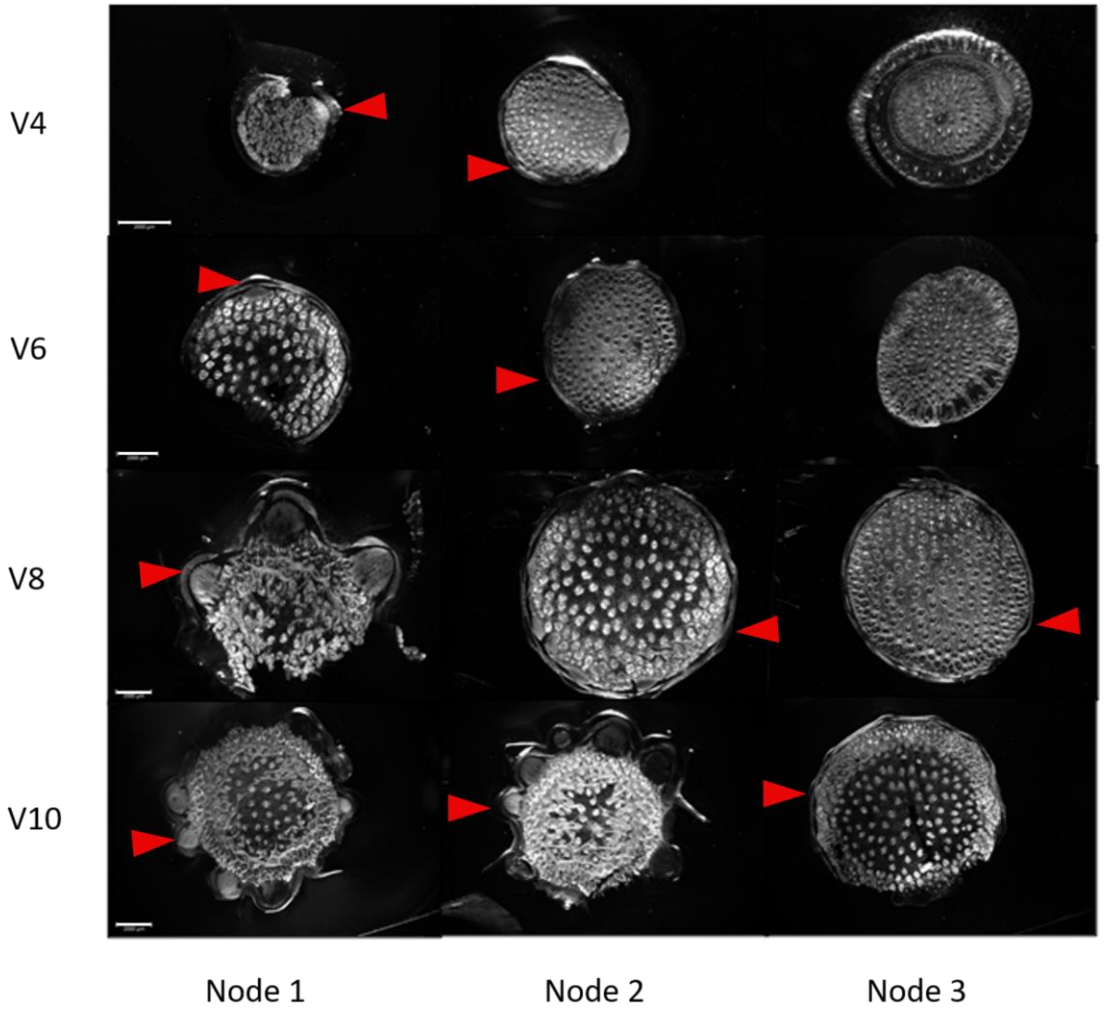

Figure 5. Cross sections of maize B73 stem across vegetative stages and nodes. Sections were stained with fuchsin and imaged on a Zeiss Axiozoom microscope. Scale bar=2,000 µm. Red arrowheads indicate a representative primordium or emerged brace root in each section.

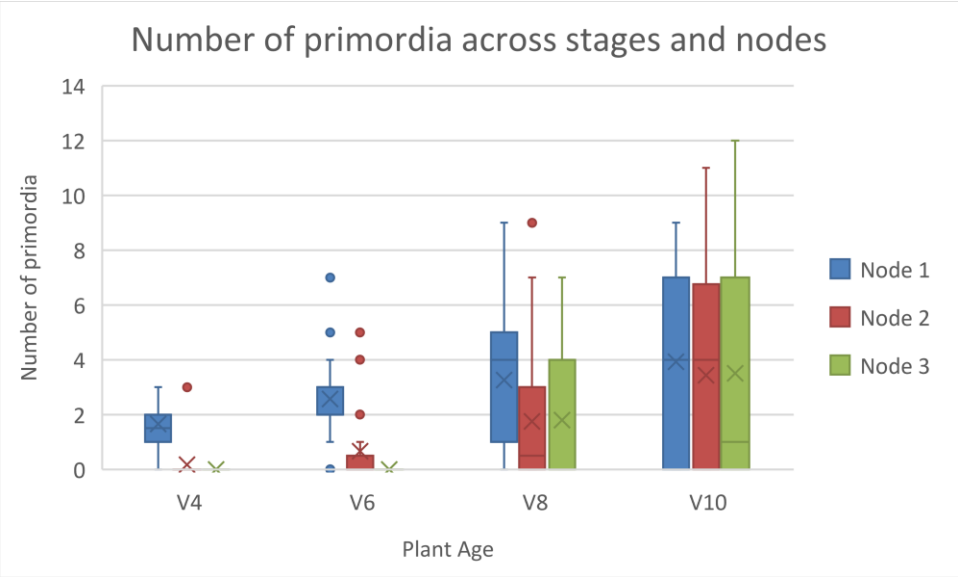

Figure 6. Number of primordia across stages and nodes. The number of primordia in each section was counted for nodes 1-3 at each stage: V4 (n=12), V6 (n=6), V8 (n=6), and V10 (n=6). Standard deviation=2.693.

The three nodes of a V6 plant encapsulate the three stages of root development: induction (node 3- no primordia), initiation (node 2- primordia within the stem) and emergence (node 1- primordia beginning to emerge from the stem) (Figure 7). I also measured the length of primordia at each node of a V6 plant (Figure 8). While there was a statistically significant difference between the lengths of primordia at node 1 and node 2 (p=0.000782), it was not significant between node 3 and node 2, likely because there are a lower number of primordia in node 3 (n=2) due to the rarity of observing primordia in node 3 at the V6 stage. Because there was a range in the length and number of primordia at each node of a V6 plant, and all three stages of development are represented across the three nodes, I determined that V6 was ideal for capturing the spectrum of brace root development.

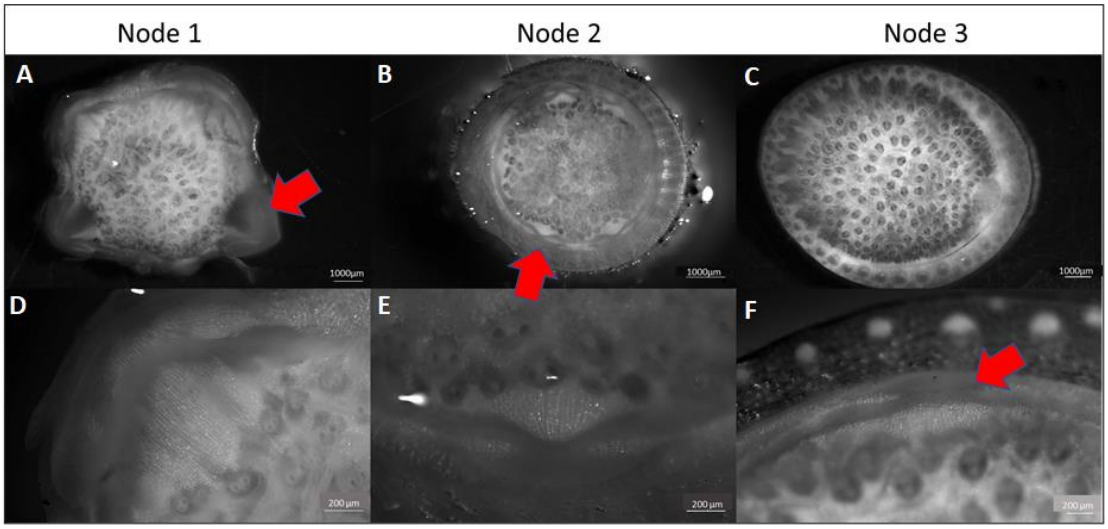

Figure 7. B73 Maize stem anatomy at vegetative stage 6. A) Brightfield image of B73 maize node 1 cross section. B) Brightfield image of node 2 cross section. C) Brightfield image of node 3 cross section. D) A higher magnification of a brace root primordia at node 1. E) A higher magnification of a brace root primordia at node 2. F) A higher magnification of a brace root primordia at node 3. Top row scale bars= 1,000 µm, bottom row scale bars= 200 µm.

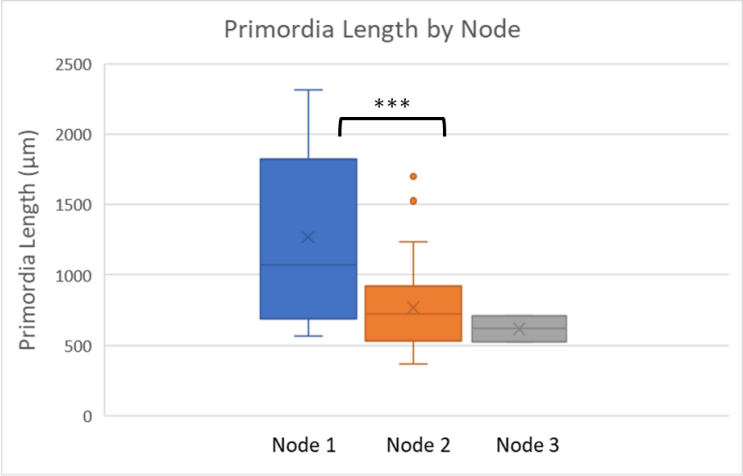

Figure 8. Primordia Length by Node at V6. There was a statistically significant difference in primordia length between nodes 1 and 2 (p=0.000782). Primordia length was not significantly different between node 2 and node 3 (p=0.506537) or between node 1 and node 3 (p=0.179775).

2.3.2 Analysis of auxin reporters during brace root development

Reporter lines DR5::erRFP and PIN1::PIN1-YFP were grown to the V6 stage and their first three above ground nodes sectioned and imaged. Initial results from images acquired on an Zeiss AxioZoom microscope suggested that auxin was not involved in brace root development, as the DR5::erRFP line did not show auxin was transcriptionally active in the primordia, although it appeared active in the vasculature (Figure 9). PIN1 also appeared in the vasculature, but not in the primordia. However, comparison of sections from transgene-positive and transgene-negative plants showed that the fluorescence observed was due to autofluorescence from the secondary cell walls found in mature tissue, indicating that a new approach to visualize these reporter lines was warranted.

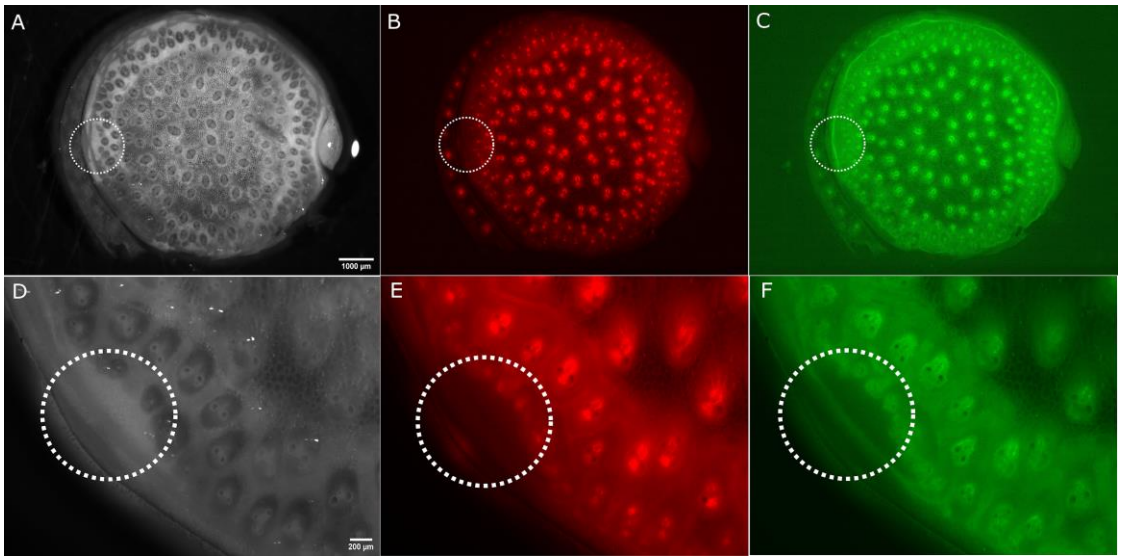

Figure 9. Sections of V6 maize double transgenic DR5::erRFP/PIN1::PIN1-YFP at node 3. A) Brightfield image of a whole section at node 3. B) DR5::erRFP is seen in the vasculature, but not in the primordia. C) PIN1-YFP, also mostly seen in the vasculature, not in the primordia itself. D) Higher magnification of A showing a brace root primordium. E) Higher magnification of RFP channel. F) Whole section of C. White dotted circles surrounds the same primordia in all images. Scale bar top row: 200 µm. Scale bar bottom row: 1,000 µm.

I worked with Dr. Jeff Caplan and Tim Chaya of the UD Bio-imaging Core to test alternative imaging strategies to separate autofluorescence from fluorescent proteins. We used laser scanning confocal microscopy coupled with a spectral imaging detector to gather fluorophores and then linearly unmix and assign pseudo colors to clearly delineate the autofluorescence from the fluorescent protein signal. When this approach was applied for the erRFP signal it was still impossible to distinguish RFP signal from chlorophyll autofluorescence (Figure 10), thus it is not possible to image the DR5::erRFP line in mature tissues given our current constraints.

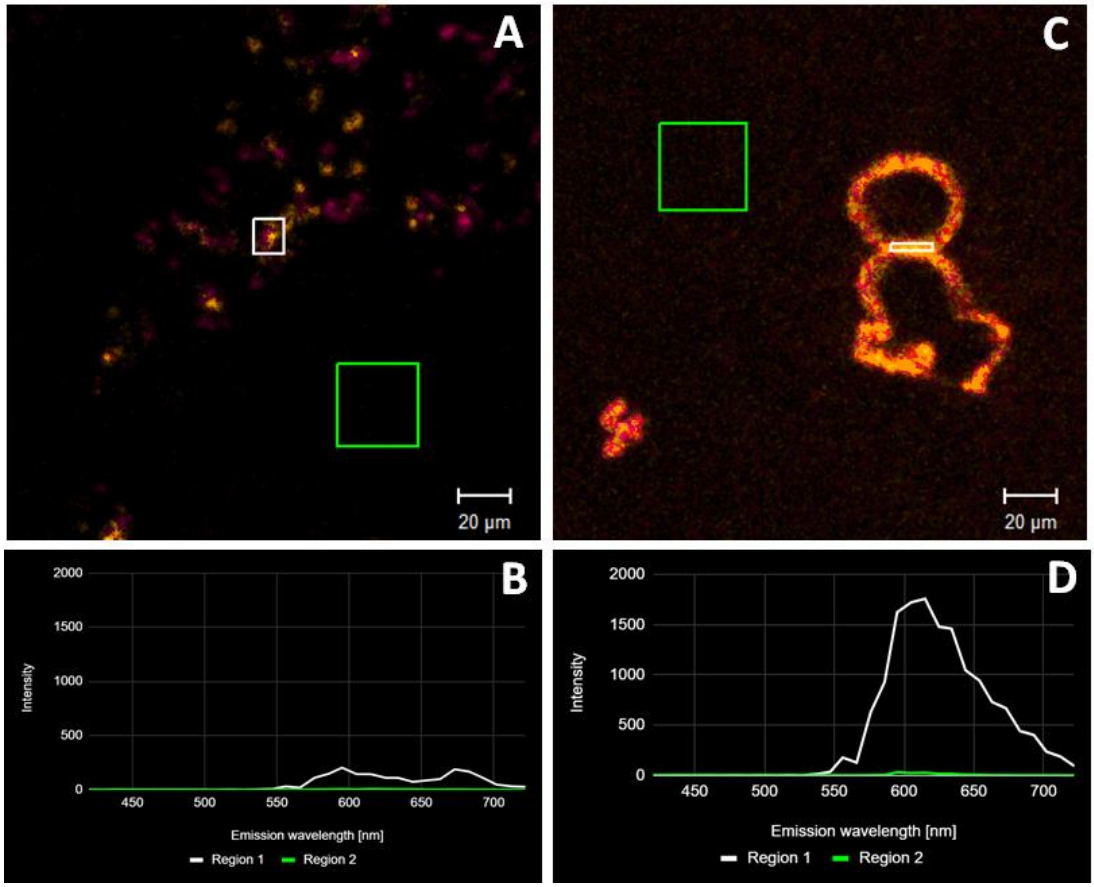

Figure 10. Spectral analysis for DR5::erRFP and B73 cryosections of node 2 of a V6 stage plant. A) B73 section at 5x. The green box outlines an area of background signal (region 1) and the white box outlines region 2; an area of autofluorescence. B) Graph of spectral unmixing data from A. The Y axis shows intensity, and the x axis shows emission wavelength. C) DR5::erRFP section at 5x. The white box outlines an area of RFP signal and the green box outlines an area of background fluorescence. D) Graph of spectral unmixing of DR5::erRFP section. While the intensity of the peak is greater in the DR5::erRFP section, the overlap of this peak with peaks from autofluorescence prevents the real signal from being separated and analyzed independently. Scale bars= 20 µm.

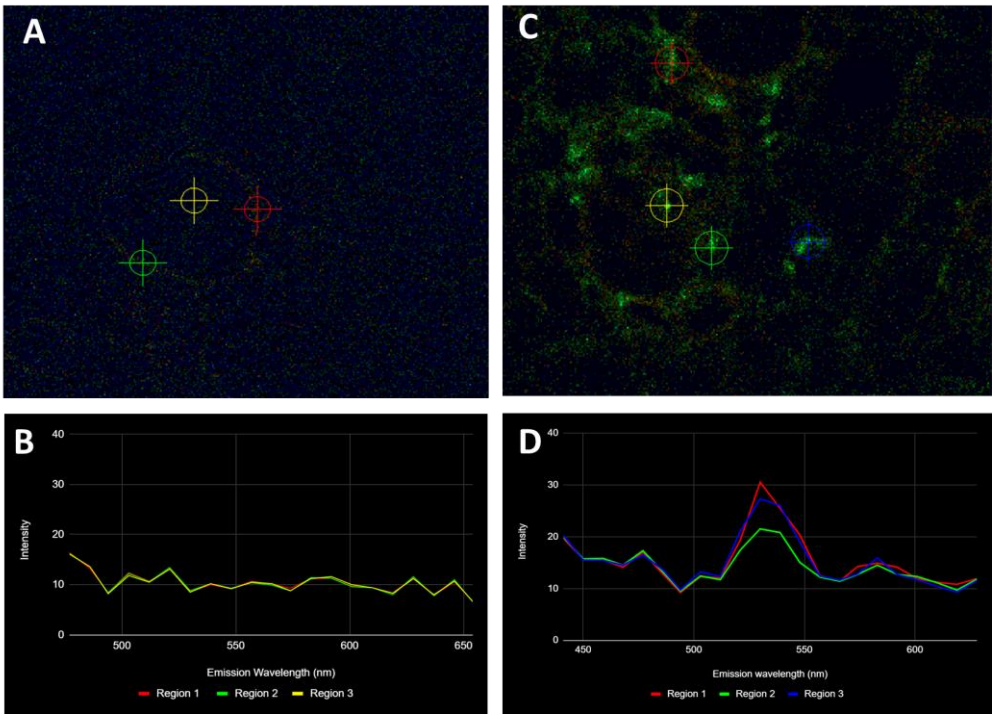

Figure 11. Spectral analysis for PIN1::YFP and B73 cryosections of node 3 of a V6 stage plant. A) B73 section at 10x. The colored cross hairs correspond to region 1-3 in B. B) Graph of spectral unmixing data from A. The Y axis shows intensity, and the x axis shows emission wavelength. C) PIN1::YFP section at 10x. The cross hairs correspond to regions 1-3 in D. D) Graph of spectral unmixing of PIN1::YFP section, revealing an emission peak around 530 nm.

Analysis of the PIN1::PIN1-YFP by confocal and spectral imaging was more successful at differentiating between autofluorescence and fluorescent protein than the DR5::erRFP, showing a clear emission peak around 530 nm (Figure 11). Preliminary analysis of node 2 of a V6 plant, demonstrates that PIN1-YFP localizes to an unknown cell type interior to the hypodermis, in a ring of cells around the periphery of the section (Figure 12). Within the brace root primordia, PIN1-YFP signal could be found within the pro-vascular tissue and it outlined the root cap (Figure 11A-inset). These

preliminary results suggest that spectral imaging can be used to fully explore the expression of PIN1-YFP during brace root development.

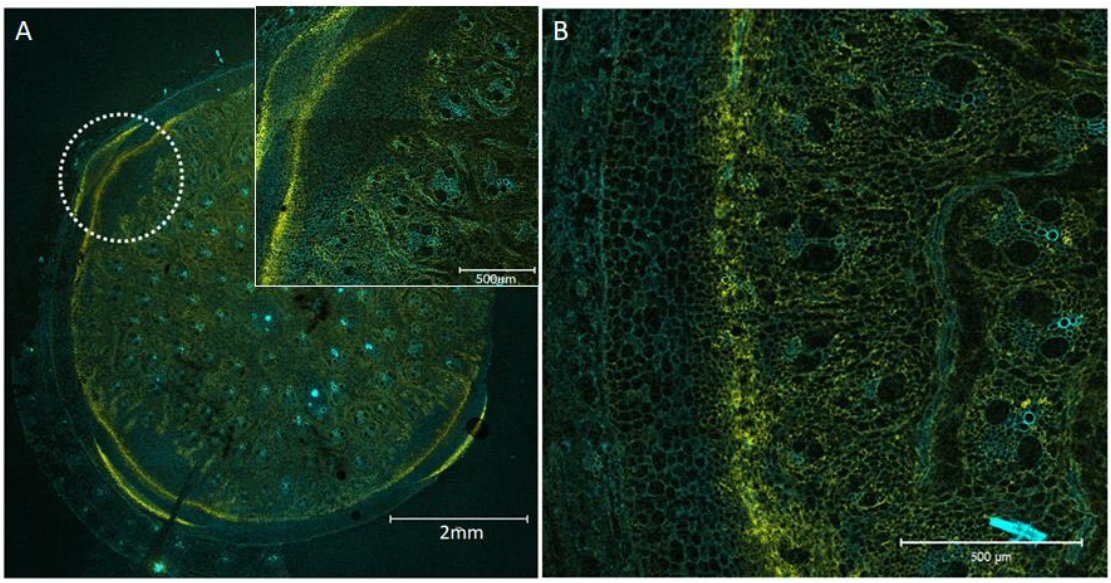

Figure 12. Tile scan of DR5::erRFP/PIN1::PIN1-YFP node 2 of a V6 cryosection. Yellow pseudo color has been assigned to the PIN1-YFP signal and the teal blue color was assigned to autofluorescence. A) Whole cryosection of V6 node 2, taken at 5x magnification. Dotted line outlines a brace root primordium. Inset shows a higher magnification of the outlined primordia. Scale bar: 2 mm. Inset scale bar: 500 µm. B) Periphery of the section showing the PIN1 localized to an unknown cell type. Scale bar: 500 µm.

2.4 Conclusions & Future Directions

My sectioning of stem nodes revealed the pattern of brace root development across both space and time. Nodes closest to the ground mature first, followed by each progressively higher node. In the V6 stage, all three stages of root development are observed, making this an ideal stage for analyzing brace root development in B73.

This analysis of development across nodes and stages builds upon past work that had described brace root development but did not look at nodes from different aged plants (Hoppe et al., 1986). It remains unclear if the timing of development is variable across different inbred lines.

A major conclusion from Hoppe et al. (1986) was that the first indication of brace root primordia forming was the reduction of calcofluor white staining in the cortex. My results show that this may be a specific subtype of cortex cell that is defined by the expression of PIN1. While additional spatiotemporal analysis of the PIN1::PIN1-YFP reporter is required, future studies could leverage this expression to define the transcriptional identity of this cortex subtype. This could be achieved through laser capture microdissection (LCM) or fluorescence activated cell sorting (FACS) to isolate cells containing the PIN1-YFP signal from other cells of the node. Transcriptome profiling of these cell populations can then be used to determine the expression patterns of sub-identities of cells. Methods optimizing LCM for RNAseq in maize have already been established (Dembinsky et al., 2007; Yu et al., 2016; Nakazono et al., 2003), as well as optimization of protoplasting and FACS (Gao et al., 2019; Ortiz-Ramírez et al., 2018; Sun He et al., 2013). I have additionally performed some preliminary baseline experiments to establish LCM on these tissues (See Appendix).

An analysis of auxin reporter lines was used to assess the role auxin might play in brace root development. These lines had previously been analyzed in maize seedlings (Bosco et al., 2012; Jansen et al., 2012), and inflorescences (Gallavotti et al., 2008), but, to the best of our knowledge, have not been analyzed in mature tissues. I have established that the DR5::erRFP line cannot be analyzed by spectral imaging in

my tissue due to the weak RFP fluorophore, and strong autofluorescence. The autofluorescence shows emission in the range from approximately 560 nm to 700nm (Figure 10A-B), and chlorophyll autofluorescence has a peak at 685 nm (Krause & Weis, 1991). The RFP signal emits at 607 nm, so it overlaps with the shoulder of chlorophyll autofluorescence, making it difficult to distinguish the two (Figure 10C-D). Future studies with fluorescence lifetime imaging (FLIM) may help resolve these two signals, and a FLIM laser was recently acquired by UD. Alternatively, the DR5 reporter could be re-constructed with a different fluorophore whose emission spectra would not overlap with autofluorescence.

While the DR5::erRFP lines were unable to be analyzed, I was able to visualize the PIN1::PIN1-YFP reporter line in a cryosection of node 2 at the V6 stage. I observed localized PIN1-YFP expression within the pro-vascular tissue of the brace root primordia (Figure 12A-inset). This expression indicates that auxin is being transported into the primordia, possibly to help establish the quiescent center, where auxin forms a maxima (Jiang et al., 2003). The role of PIN1for auxin transport has been established in the Arabidopsis root (Feraru & Friml, 2008), where it transports auxin down the stele to the auxin maxima at the quiescent center of the root tip. It is possible that the expression I observe in my brace root primordia is the beginnings of this same pattern. However, the preparation of the sample resulted in freeze fracturing, which prevents the analysis of specific cell wall localization. Future sample preparation could include sucrose acclimation to better preserve tissue integrity.

PIN1-YFP expression was also observed in a ring of cells around the periphery of the same cross section (Figure 12B). The signal is seen in cortex cells, just interior to the hypodermis. Since the expression is not consistent across the entire cortex, it is

possible that PIN1-YFP is localizing to an unknown sub-identity of cortex cells that functions in a similar manner to a cambium layer in dicots and some monocots. In woody species, in between each vascular bundle of xylem and phloem, there exists a layer of meristematic cells called the cambium that can divide to form secondary xylem and phloem, leading to radial growth (Spicer & Groover, 2010). In most monocots, vascular bundles are surrounded by terminally differentiated sclerenchyma cells, making it impossible to form secondary xylem or phloem. While a cambium layer is known to exist in some monocot species (Zinkgraf et al., 2017), it has never been shown to exist in maize. Future studies aimed at identifying this unknown cell type will provide important insights into the competence of maize stem nodes to initiate brace roots.

Other reporter lines for auxin could also be used, including the DII::Venus and its counterpart mDII::Venus (Mir et al., 2017). Since DII is the auxin-interacting domain of Aux/IAA proteins, it will degrade in the presence of auxin. The mDII line has been mutated so that it does not degrade in the presence of auxin. These lines would yield a different result from the DR5 reporter lines since DR5 represents the output of the auxin response pathway, while DII levels directly relate to auxin concentration. I have obtained seeds of these lines and am crossing them to B73 inbred lines to bulk seeds. The same approaches outlined above to determine the presence of the transgene could be utilized for these lines, as well as the spectral imaging techniques to distinguish fluorophore from autofluorescence.

In summary, I have shown that much work remains to refine the use of reporter lines in my mature tissue, but preliminary results suggest that auxin could be involved in maize brace root development.

REFERENCES

Arber, Agnes. 1930. "Studies in the Gramineae. IX. 1. The Nodal Plexus. 2. Amphivasal Bundles." *Annals of Botany* 44 (175): 593–620.

Blizard S. & Sparks E.E. 2020. Maize Nodal Roots. *Annual Plant Reviews Online* 3, 281-304.

Bosco, C.D., Dovzhenko, A., Liu, X., Woerner, N., Rensch, T., Eismann, M., Eimer, S., et al. 2012. "The Endoplasmic Reticulum Localized PIN8 Is a Pollen-Specific Auxin Carrier Involved in Intracellular Auxin Homeostasis." *The Plant Journal: For Cell and Molecular Biology* 71 (5): 860–70.

Dembinsky, D., Woll, K., Saleem, M., Liu, Y., Fu, Y., Borsuk, L.A., Lamkemeyer, T., et al. 2007. "Transcriptomic and Proteomic Analyses of Pericycle Cells of the Maize Primary Root." *Plant Physiology* 145 (3): 575–88.

Evans, A.T. 1928. "Vascularization of the Node in Zea Mays." *Botanical Gazette* 85 (1): 97–103.

Feraru, E., and Friml, J.. 2008. "PIN Polar Targeting." *Plant Physiology* 147 (4): 1553–59.

Gallavotti, A., Yang, Y., Schmidt, R.J., and Jackson, D. 2008. "The Relationship between Auxin Transport and Maize Branching." *Plant Physiology* 147 (4): 1913–23.

Gao, L., Guojing Shen, Lingdan Zhang, Jinfeng Qi, Cuiping Zhang, Canrong Ma, Jing Li, Lei Wang, Saif Ul Malook, and Jianqiang Wu. 2019. "An Efficient System Composed of Maize Protoplast Transfection and HPLC-MS for Studying the Biosynthesis and Regulation of Maize Benzoxazinoids." *Plant Methods* 15 (November): 144.

Hitch, P. A., and Sharman, B.C. 1971. "The Vascular Pattern of Festucoid Grass Axes, with Particular Reference to Nodal Plexi." *Botanical Gazette* 132 (1): 38–56.

Hoppe, D. C., M. E. McCully, and C. L. Wenzel. 1986. "The Nodal Roots of Zea: Their Development in Relation to Structural Features of the Stem." *Canadian Journal of Botany*. 64: 2524-2537.

Jansen, L., Roberts I., Riet De Rycke, and Beeckman, T.. 2012. “Phloem-Associated Auxin Response Maxima Determine Radial Positioning of Lateral Roots in Maize.” *Philosophical Transactions of the Royal Society of London. Series B, Biological Sciences* 367 (1595): 1525–33.

Jiang, K., Meng, Y.L., and Feldman, L.J. 2003. “Quiescent Center Formation in Maize Roots Is Associated with an Auxin-Regulated Oxidizing Environment.” *Development* 130 (7): 1429–38.

Krause, G. H., and Weis, E. 1991. “Chlorophyll Fluorescence and Photosynthesis: The Basics.” *Annual Review of Plant Physiology and Plant Molecular Biology* 42 (1): 313–49.

Kurihara, D., Mizuta, Y., Sato, Y., and Higashiyama, T. 2015. “ClearSee: A Rapid Optical Clearing Reagent for Whole-Plant Fluorescence Imaging.” *Development* 142 (23): 4168–79.

Mir, R., Aranda L.Z., Biaocchi, T., Luo A., Sylvester, A.W., and Rasmussen, C.G. 2017. “A DII Domain-Based Auxin Reporter Uncovers Low Auxin Signaling during Telophase and Early G1.” *Plant Physiology* 173 (1): 863–71.

Nakazono, M., Qiu F., Borsuk, L.A., and Schnable, P.S. 2003. “Laser-Capture Microdissection, a Tool for the Global Analysis of Gene Expression in Specific Plant Cell Types: Identification of Genes Expressed Differentially in Epidermal Cells or Vascular Tissues of Maize.” *The Plant Cell* 15 (3): 583–96.

Ortiz-Ramírez, C., Arevalo, E.D., Xu, X., Jackson, D.P., and Birnbaum, K.D. 2018. “An Efficient Cell Sorting Protocol for Maize Protoplasts.” *Current Protocols in Plant Biology* 3 (3): e20072.

Sharman, B. C. 1942. “Developmental Anatomy of the Shoot of Zea Mays L.” *Annals of Botany* 6 (22): 245–82.

Spicer, R., and Groover, A. 2010. “Evolution of Development of Vascular Cambia and Secondary Growth: Tansley Review.” *The New Phytologist* 186 (3): 577–92.

Sun He, Lang Zhihong, Zhu Li, and Huang Dafang. 2013. “Optimized condition for protoplast isolation from maize, wheat and rice leaves.” *Sheng wu gong cheng xue bao = Chinese journal of biotechnology* 29 (2): 224–34.

Ursache, R., Andersen, T.G., Marhavý, P., and Geldner, N. 2018. “A Protocol for Combining Fluorescent Proteins with Histological Stains for Diverse Cell Wall Components.” *The Plant Journal: For Cell and Molecular Biology* 93 (2): 399–412.

Yu, P., Baldauf, J.A., Lithio, A., Marcon, C., Nettleton, D., Li, C., and Hochholdinger, F. 2016. “Root Type-Specific Reprogramming of Maize Pericycle Transcriptomes by Local High Nitrate Results in Disparate Lateral Root Branching Patterns.” *Plant Physiology* 170 (3): 1783–98.

Zinkgraf, M., Gerttula, S., and Groover, A. 2017. “Transcript Profiling of a Novel Plant Meristem, the Monocot Cambium.” *Journal of Integrative Plant Biology* 59 (6): 436–49.

Chapter 3

MOLECULAR SIGNATURES OF BRACE ROOT DEVELOPMENT

3.1 Rationale

To determine the molecular signatures that regulate brace root development, RNA-sequencing (RNA-seq) of the first three aboveground nodes was used as a hypothesis generating approach to select candidate genes for a mutant analysis. The V6 stage was chosen because it captures the three stages of post-embryonic root development (see Chapter 2). Node 1 (closest to the soil) has brace roots beginning to emerge from the stem (emergence stage), node 2 has brace root primordia within the stem (initiation phase), and node 3 rarely contains primordia (induction phase). Genes that are differentially expressed in the node 3 v. node 2 comparison are hypothesized to be involved in brace root initiation, while those differentially expressed in the node 2 v. node 1 comparison are hypothesized to be involved in brace root emergence. My work focuses on the genes that are differentially expressed during brace root initiation (node 3 v. node 2 comparison). To enable a targeted analysis of these transcriptome data, hormone-related genes were examined as up- or down-regulated.

3.2 Methods

3.2.1 Growth conditions

B73 plants were grown to the V6 stage in 3-gallon pots under greenhouse conditions in the University of Delaware Fisher Greenhouse Zone #4. During this

period, average temperature was 24.5 °C, average humidity was 57.2%, and supplemental lighting in the form of 400 Watt HPS and 400 Watt MH bulbs was provided from 7 AM - 9 PM when outside light radiation levels were below 600 W/m^2 (watts per square meter). Plants were watered twice a week, once a week supplemented with nutrient solution, and BK 55 soil was prepared with 30 grams of slow release 19-6-9 osmocote pellets.

3.2.2 Tissue collection

At the V6 stage (determined by the drooping leaf method), node tissue was collected from the first three aboveground nodes (Figure 13). Nodes were hand sectioned with a razor blade, and tissues containing peripheral anastomosis or brace root primordia (confirmed by viewing briefly on an Echo Revolve microscope) were flash frozen in liquid nitrogen, and sent to Amaryllis Nucleics for RNA extraction, library preparation, and 3’ end RNA-seq.

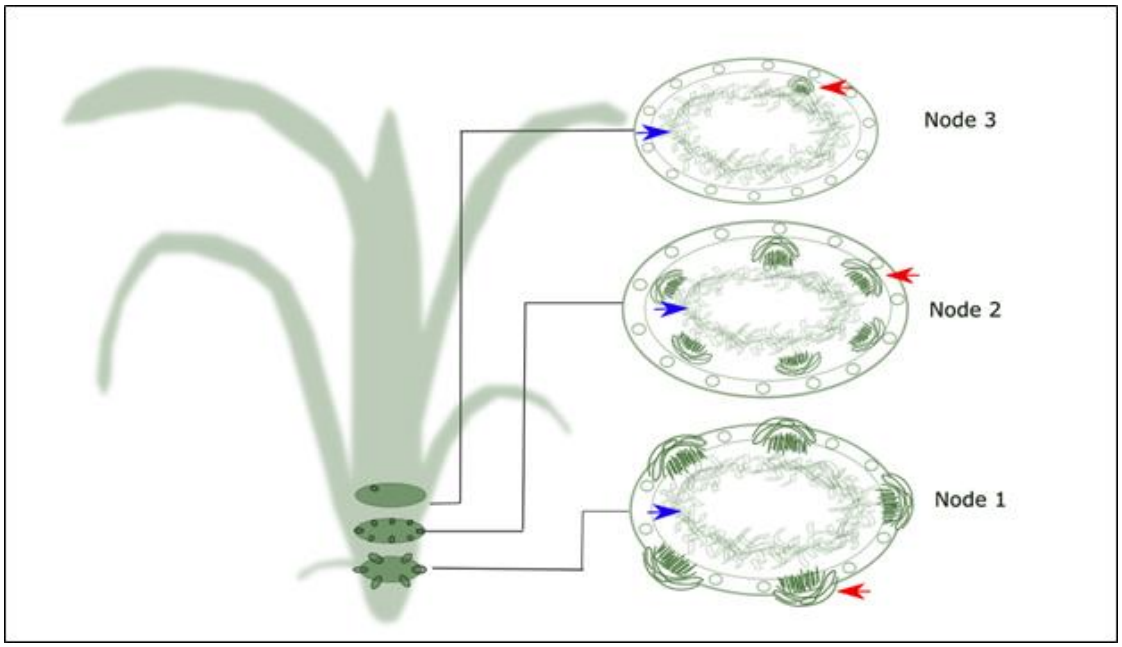

Figure 13. Maize at vegetative leaf six stage. Insets represent the anatomy of the first three aboveground nodes used for RNA-seq. In Node 1, brace root primordia (red arrowheads) are beginning to emerge from the stem. In Node 2, primordia are contained within the stem and are considered immature. In Node 3, primordia are at their earliest stage or are rarely seen at all. Horizontal vascular strands termed anastomosis (blue arrowheads) form at all monocot nodes. Since primordium initiation is correlated anatomically with these strands forming a ring around the periphery of the stem in cross section, this anatomical feature was used to identify sections for RNA-seq.

3.2.3 RNA extraction, library preparation, and sequencing

Tissue disruption, mRNA isolation, library synthesis, sequencing, and bioinformatic analysis were conducted by Amaryllis Nucleics (Oakland, CA) as follows.

Node tissue was disrupted with Zirconia/Silica beads (a mix of ~6 1.0 mm diameter beads and ~6 2.3 mm diameter beads; BioSpec Products, Inc.) for 1 minute in a MiniBeadbeater-96 (BioSpec Products, Inc.) while frozen. After adding 500 µL of

Lysis/Binding Buffer (LBB, Table 6) to each sample and vortexing until homogeneous, samples were run on the MiniBeadbeater-96 for an additional minute. Following tissue disruption samples were centrifuged at 16,000 x *g* for 10 minutes at 20 ºC. For each sample, a 50 µL aliquot of the supernatant was added to 50 µL of NEB RNA binding buffer and mRNA isolated as per the NEBNext® Poly(A) mRNA Magnetic Isolation Module manual.

RNA-seq libraries were prepared by using the Full Transcript mode YourSeq Dual (FT & 3'-DGE) RNAseq Library Kit (Amaryllis Nucleics). A Bioanalyzer 2100 (Agilent, High Sensitivity DNA Kit) was used for library quality control, to determine average library size, and together with concentration data from a Qubit 2.0 Fluorometer (Life Technologies, dsDNA High Sensitivity Assay Kit) to determine individual library molarity and pooled library molarity. A PippinHT (Sage Science) was used for size selection to get pooled libraries 250-500 bp in length. These size-selected, pooled libraries were sequenced on a NextSeq 500 (Illumina, High Output v2 75 cycle kit) to yield single-read 80 bp reads.

Table 6. Solutions used to make 50 ml of Lysis/Binding Buffer (LBB). Immediately before LBB was added to ground tissue, 5 µl/ml 2-Mercaptoethanol was added. Salt crystals were fully dissolved, and Antifoam A was fully homogenized in solution prior to use.

Amount	Solution
100 mM	Tris-HCl, pH 8
1M	LiCl
10 mM	EDTA, pH 8

1%	SDS
5 mM	DTT
1.5%	Antifoam A
Add to 50 ml	RNAse-free water

3.2.4 Mapping and differential gene analysis

FASTQ sequence files were preprocessed in two steps. A Python library (clipper.py, https://github.com/mfcovington/clipper) was used to trim off the first 8 nucleotides of each read to remove potential mismatches to the reference sequence caused by annealing of a random hexamer required for library synthesis. Trimmomatic v0.36 (http://www.usadellab.org/cms/?page=trimmomatic) was used to remove adapter sequences and trim or filter reads based on quality The parameters used for Trimmomatic were ILLUMINACLIP:TruSeq3-PE-2.fa:2:30:10 LEADING:3 TRAILING:3 SLIDINGWINDOW:4:15 MINLEN:50.

Preprocessed reads were mapped to the *Zea mays* B73 v4 genomic reference sequence (ftp://ftp.ensemblgenomes.org/pub/plants/release-42/fasta/zea_mays/dna/Zea_mays.B73_RefGen_v4.dna_sm.toplevel.fa.gz) using HISAT2 (https://ccb.jhu.edu/software/hisat2/index.shtml). Read counts for each gene in the gene annotation file (ftp://ftp.ensemblgenomes.org/pub/plants/release-42/gff3/zea_mays/Zea_mays.B73_RefGen_v4.42.gff3.gz) were calculated using htseq-count (with the -s yes parameter to enforce strand-specific alignment) from the HTSeq Python library (https://academic.oup.com/bioinformatics/article/31/2/166/2366196; http://htseq.readthedocs.io/en/master/index.html).

The R package edgeR (http://www.bioconductor.org/packages/release/bioc/html/edgeR.html) was used to identify genes differentially expressed (DE) between the three nodes of interest. Transcripts were retained for analysis if they had more than one count per million in at least three samples. After normalization factors were calculated and dispersion estimated, gene-wise negative binomial generalized linear models with quasi-likelihood tests were used to identify node effects across matched samples. Differentially expressed genes were then filtered using a false discovery rate (FDR) cutoff of 0.05. FDRs were calculated by adjusting P-values for multiple comparisons using the Benjamini–Hochberg procedure.

3.2.5 Gene Ontology analysis

A list of filtered (+/- 1 $\log_2$ fold change) gene ID's from the node 3 to node 2 comparison were placed in AgriGo's singular enrichment analysis (SEA) tool (Du et al., 2010). Test correction = Fisher, max p value = 0.05.

3.2.6 Comparison with previous RNA-sequencing data

Gene IDs from a previous study (Li et al. 2011) are no longer in existence for direct comparison. Therefore, sequence tags were BLASTed against the Maize V4 genome. Gene IDs were recorded based on BLAST results. IDs were associated with Maize V4 loci with assistance from the MaizeGDB staff. Gene lists were compared between the two datasets to identify 75 genes that were expressed and common to both datasets. The $\log_2$ fold change for these two datasets was compared as in Table 7. Fold change comparisons were graphed using ggplot2, and r-values were calculated from Pearson correlations in R.

Table 7. Comparison of previously published sequencing data (Li et al. 2011) with my node sequencing data. Comparisons were made between the $\log_2$ fold change between node 1 v. node 2, node 2 v. node 3, and node 1 v. node 3 and the fold change values from Li et al 2011. r values were calculated from Pearson's correlation in R. FC=fold change.

Comparison	r-value	P-value
Li et al 2011 FC v. N2/N1 FC	0.28	0.01417
Li et al 2011 FC v. N3/N2 FC	0.47	1.94E-05
Li et al 2011 FC v. N3/N1 FC	0.61	8.49E-09

3.3 Results

3.3.1 B73 Nodes have Distinct Transcriptional Signatures

Multidimensional scaling (MDS) plot of the top 50 differentially expressed (DE) genes in the four samples shows that one plant (plant #5) does not cluster with the other plants (Figure 14A). To understand what was different about plant #5, we did two analyses. The first was percent mapping to the B73 reference genome. Whereas plants #2, 3, and 4 have 80.3-81.2% mapping rates, plant #5 only showed 69.6% mapping. This is indicative that plant #5 may be a different genotype than B73. To further explore the possibility that plant #5 was a different genotype, SNV (single nucleotide variation) was examined between Plant #4 and #5, and clear SNV were found (Figure 15). A different genotype may have resulted from seed contamination or mis-labeling. Together these results suggest that plant #5 is a different genotype, and the decision was made to remove plant #5 from further analyses.

When plant #5 is removed from the analysis, the MDS plot shows the data clusters by node, indicating that there is differential gene expression between nodes of a V6 plant (Figure 14B). This supports my hypothesis that transcriptome analysis of nodes with different stages of development will enable the identification of genes involved in brace root initiation and emergence.

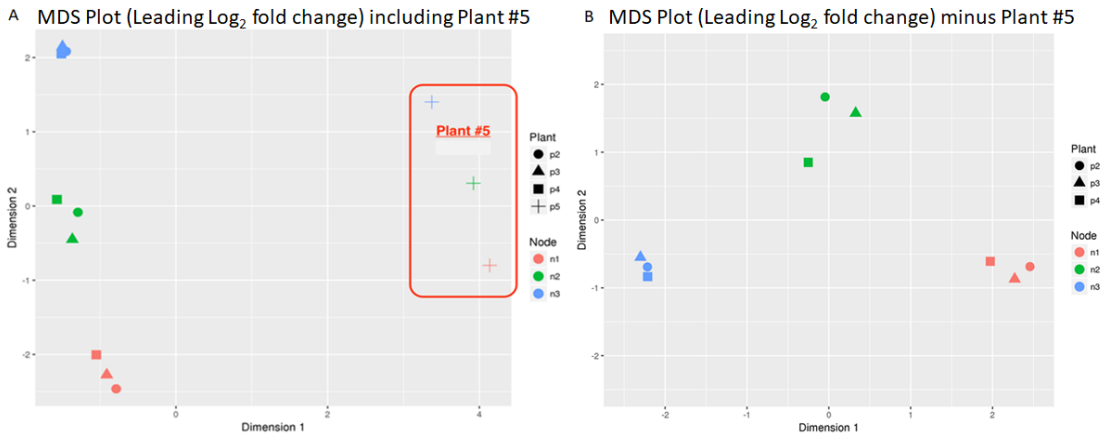

Figure 14. Multidimensional scaling plot (MDS) based on $\log_2$ fold change of the top 50 differentially expressed genes. A. Plot including plant #5. All three nodes of this plant cluster separately from the nodes of the other plants. B. MDS plot minus plant #5 shows clustering by nodes.

Figure 15. Representative view of genome browser showing SNV between plants #4 and #5. Vertical colored lines indicate the presence of a SNP that exists in plant #5 (bottom) relative to the reference genome (B73) and is not found in plant #4 (top).

There was a total of 9,290 differentially expressed (DE) genes between node 3 (no visible primordia) and node 2 (initiated primordia). After a $\log_2$ fold change filter of +/- 1 was applied, there were 2,896 genes total, with 1,847 down-regulated (63.8%) and 1,049 upregulated (36.2%) in the node 3 v node 2 comparison (Figure 16). A gene ontology (GO) search on AgriGo (Du et al., 2010) of these 2,896 genes was performed and yielded 23 significant GO terms (Figure 16). Most GO terms are related to cell cycle, cell division and transport processes, which is consistent with water and nutrients being transported within the stem, and cells actively dividing to form the brace root primordia.

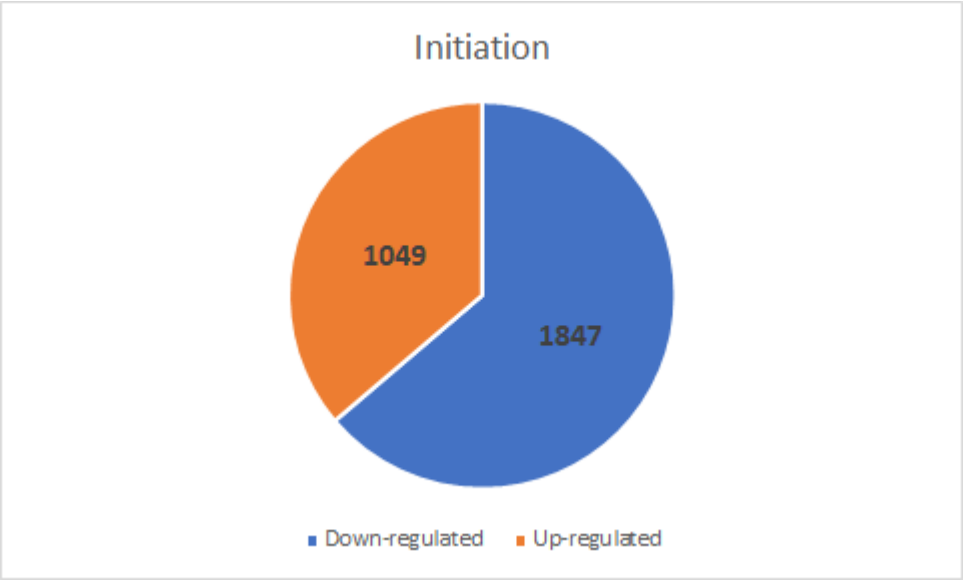

Figure 16. Number of differentially expressed genes involved in initiation from the node 2 to node 3 comparison. A $\log_2$ fold change filter of +/- 1 was applied.

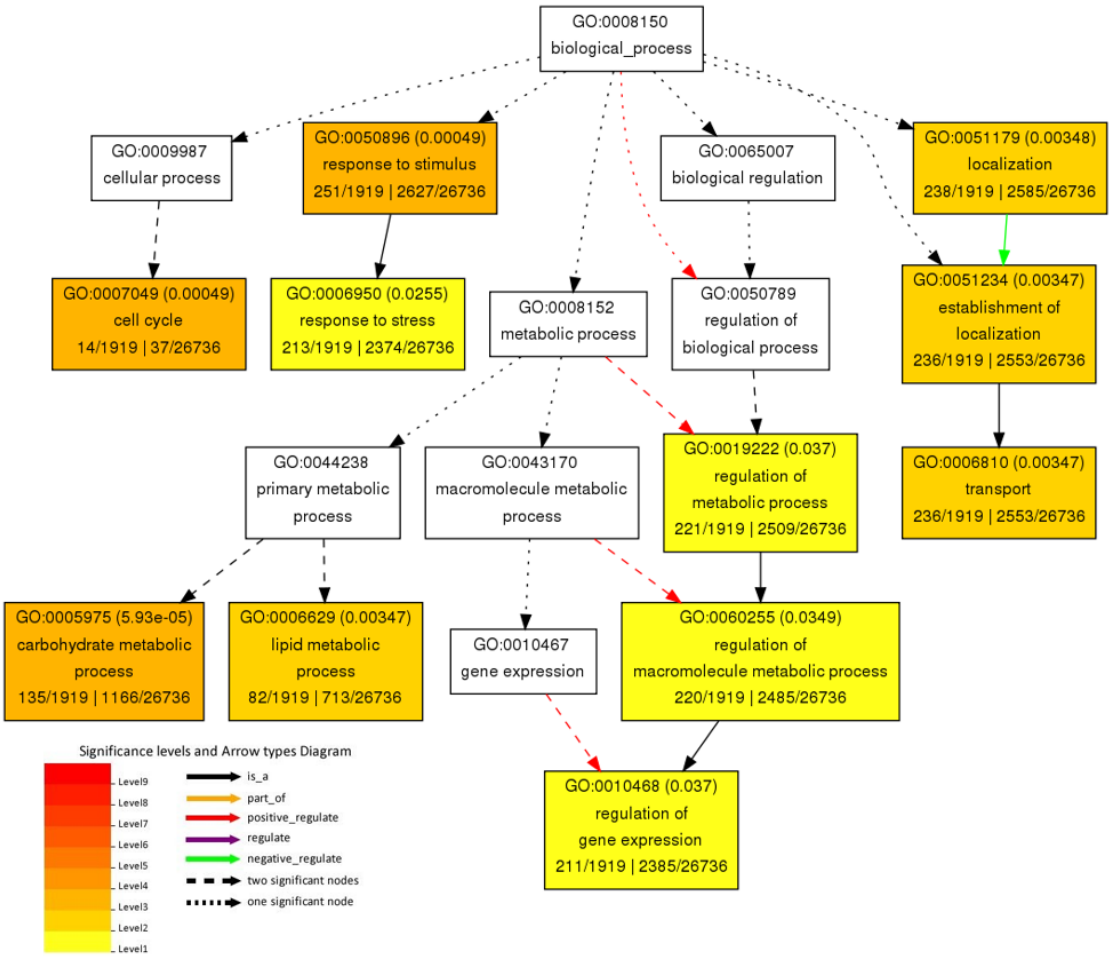

Figure 17. Gene ontology analysis from AgriGo (Du et al., 2010) given a list of 2,896 genes (log_2 fold change filter of +/- 1).

3.3.2 Comparison with previous transcriptome data

Transcript profiling of maize nodes has already been performed, however major differences in methodology exist (Li et al., 2011). Previous efforts used early Solexa sequencing technologies and a poorly annotated maize genome. Their mapping percentages were much lower than my results -- 51-55% in Li et al. 2011, and 80.3-81.2% for my data set. However, it is not clear if these differences are due to the

technology or mapping sequence from the non-reference genome -- inbred line H5468 compared to inbred B73 used in my research.

In order to analyze the molecular basis of brace root development, Li et al. (2011) compared transcripts between the first aboveground node of a V4 plant, which serves as their control tissue (N), presumably without brace roots or brace root primordia, although this was not verified anatomically. They compared this control with the first aboveground node of a V6 plant, with just-emerged brace roots (NR). The comparison between my data set and theirs is complicated by the uncertainty surrounding their staging and anatomical descriptions. The plants they used were staged using the leaf collar method, which counts the number of leaves with a fully formed leaf collar, while I used the drooping leaf method, which counts the number of leaves that have emerged and "drooped" over (See https://www.agry.purdue.edu/ext/corn/news/articles.04/VStageMethods-0515.pdf for a comparison of leaf staging methods). Based upon my anatomical studies and the comparison in staging systems, their libraries likely correspond to node 1 of V3 (N- no brace roots) and V5 (NR- just-emerged brace roots) of my data.

To determine how my data relates to that published in Li et al. (2011), a Pearson correlation analysis was performed (Table 7). When comparing my libraries to Li et al. (2011), the highest correlation occurs with my comparison of node 3 v node 1 (r=0.61), which is comparing a node with brace roots to a node without brace roots (Figure 18). Lower correlations occur when comparing to node 3 v node 2 or node 2 v node 1 data (r=0.47, and r=0.2, respectively). Thus, my analysis further expands and refines the dataset of Li et al. (2011) by refining the developmental stages and adding candidates for the initiation signal.

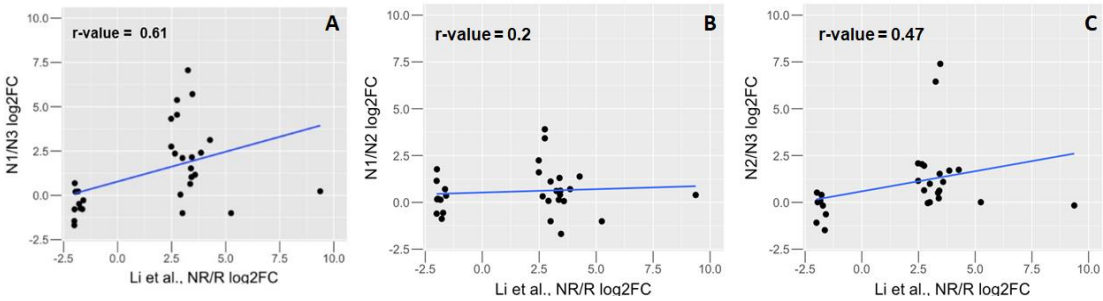

Figure 18. Comparison of node RNA-seq data to previous efforts (Li et al., 2011). Log_2 fold change values for each node comparison were graphed against the comparable data from Li et al. (2011) where their libraries consisted of nodes (N) and nodes with just emerged brace roots (NR). A. Comparison of Li et al. (2011) with node 1 v. node 3 (N3/N1) fold change. B. Comparison of Li et al. (2011) with node 1 v node 2 (N2/N1). C. Comparison of Li et al. (2011) with node 2 v node 3 (N3/N2) fold change values.

3.3.3 Hormone-related genes are differentially expressed during brace root development

Transcriptome data provides thousands of differentially expressed (DE) genes. To narrow the focus, one can take an unbiased or targeted approach. For an unbiased approach, I took the list of DE genes filtered for log_2 fold change of +/- 1 and performed a Gene Ontology (GO) analysis using AgriGo (Du et al., 2010). This result shows that many categories related to cell cycle and cell division are enriched (Figure 17). Looking at the top 12 DE genes (top 6 up-regulated and top 6 down-regulated, based on fold change), they are: 1) expressed protein, 2) SBP-domain protein1, 3) GDSL esterase/lipase, 4) sugars will eventually be exported transporter11, 5) Protein ECERIFERUM 3, 6) SBP-transcription factor 21, 7) Glycine-rich cell wall structural protein, 8) Peroxidase 42, 9) Purple acid phosphatase 3, 10) Proline-rich protein 2, and 11) MYB-transcription factor 23 and 12) S-receptor kinase1 (Table 8). Of particular note from these genes are the SBP (squamosa-promoter binding protein) transcription

factors. The *Corngrass1* mutant produces brace roots at every node, and repeated tillering at each node leads to a bush-like appearance with juvenile leaves (Chuck et al., 2007). This phenotype is due to an overexpression of microRNA miR156, which targets the SBP family of transcription factors (Rhoades et al., 2002). The fact that SBP genes are downregulated in my data set is consistent with their role in being permissive in brace root development. Analysis of a SPB5/6/7 triple mutant did not display any changes in brace root development (data from Noah Ouslander, not shown here). However, these are not the same SPB genes that are differentially expressed in my dataset. Additional SPB mutants and their combinations are being analyzed by other members of the lab.

Table 8. Top 12 differentially expressed genes in the node 3 v node 2 comparison by $\log_2$ fold change. N/A= not available.

Name	Description	Log_2 Fold Change	Gene ID (B73 v4)
N/A	Expressed protein; protein	-8.038021	Zm00001d044801
SBP-domain protein1	SBP-domain protein1	-6.390558	Zm00001d015451
N/A	GDSL esterase/lipase	-5.543421	Zm00001d033522
sugars will eventually be exported transporter11	sugars will eventually be exported transporter11	-5.350483	Zm00001d031647
N/A	Protein ECERIFERUM 3	-5.098798	Zm00001d015477

SBP-transcription factor 21	Squamosa promoter-binding protein-like (SBP domain) transcription factor family protein	-5.08232	Zm00001d026175
N/A	Glycine-rich cell wall structural protein	9.595499	Zm00001d017033
N/A	Peroxidase 42	9.132724	Zm00001d022456
N/A	Purple acid phosphatase 3	8.757841	Zm00001d053094
N/A	Proline-rich protein 2	8.752495	Zm00001d030316
MYB-transcription factor 23	Transcription factor MYB46	8.247298	Zm00001d022259
N/A	S-receptor kinase1	8.167909	Zm00001d007745

To compliment the unbiased analyses, I also took a targeted approach. Hormones are known to regulate plant development, therefore I focused on genes with known roles in hormone signaling. Genes related to hormone pathways were selected from the list of DE genes and sorted into groups: 17 auxin (Table 9, Figure 20), 15 ethylene (Table 11, Figure 21), 9 cytokinin (Table 12, Figure 22), 9 gibberellin (Table 13, Figure 23), and 8 abscisic acid (Table 14, Figure 24) related genes (Figure 19). While there are other plant hormones (i.e., strigolactone, brassinosteroids), they did not have DE genes in my data set that met the cutoff requirements. The auxin and ethylene pathways contained the greatest number of upregulated genes at 6 genes, followed by cytokinin with 3, gibberellin with 2, and abscisic acid with 1 gene. There was more down-regulated auxin-related genes than any other hormone pathway, with 12 genes down-regulated, followed by gibberellin and abscisic acid both with 7 genes, cytokinin and ethylene with 6 genes. However, the specific direction of regulation is

not indicative of the function of these genes as they may function as activators or repressors of the hormone pathway

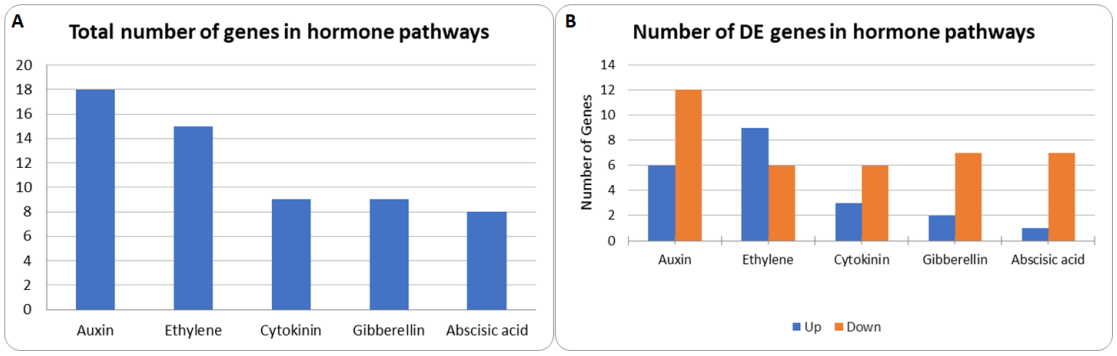

Figure 19. A. Total number of genes in each hormone-related pathway that were differentially expressed (greater than 1 or less than -1 $\log_2$ fold change) between node 3 and node 2. B. Number of up (blue) or down (orange) regulated genes in each hormone-related pathway.

Auxin-specific genes that were upregulated between node 3 and node 2 include ARF 29 (auxin responsive factor 29), ARF4 (auxin responsive factor 4), ARF26 (auxin responsive factor 26), PIN8 (Pin-formed protein 8), PIN4 (Pin-formed protein 4), and ARF13 (auxin responsive factor 13). Auxin-specific genes that were down-regulated between node 3 and node 2 include AIC2 (auxin import carrier 2), Aux/IAA9, Aux/IAA19, ARF7, Aux/IAA7, ATL1 (auxin transporter-like protein 1), ARF20 (auxin responsive factor 20), Aux/IAA20, and SAUR61 (auxin responsive protein SAUR61) (Table 9, Figure 20). A search on the maize GDB website for a list of UniformMu mutants available for this list of genes was performed (Table 10). UniformMu is a population of inbred W22 strain that has been introgressed with Mu transposable element insertions. This population is widely used for genetics research

for phenotypic comparisons as the background genetics are uniform and the Mu transposon disrupts individual genes which can then be studied for their function (McCarty et al., 2005). Mutants were unavailable for the following genes: AIC2 (Zm00001d053004), Aux/IAA19 (Zm00001d013071), and both copies of SAUR61 (Zm00001d006279, Zm00001d006282). Of the remaining genes, lines that were available have on average 21 insertions. To ensure that the insertion in the gene of interest is responsible for any phenotypes, these lines would have to be backcrossed to isolate the mutation to the specific gene. This process is beyond the timeframe of my project. Other lines have insertions outside of the coding sequence (3' or 5' untranslated region or intron), which gives less certainty that the candidate gene would be disrupted. Thus, no mutant lines were selected for further analysis.

Table 9. Auxin-related genes that were differentially expressed from node 3 to node 2. FC=fold change.

Gene ID (B73 v4)	Gene	N3 v N2 FC
Zm00001d026540	ARF-transcription factor 29	-2.56721
Zm00001d001945	ARF-transcription factor 4	-1.41638
Zm00001d012731	ARF-transcription factor 26	-1.11668
Zm00001d043660	PIN-formed protein8	-1.08621
Zm00001d052442	PIN-formed protein4	-1.07874
Zm00001d049295	ARF-transcription factor 13	-1.03641
Zm00001d053004	auxin import carrier2	1.08091
Zm00001d040541	Aux/IAA-transcription factor 9	1.09947

Zm00001d013071	Aux/IAA-transcription factor 19	1.12159
Zm00001d039267	ARF-transcription factor 7	1.17403
Zm00001d039513	Aux/IAA-transcription factor 7	1.2366
Zm00001d042809	auxin transporter-like1	1.405
Zm00001d015243	ARF-transcription factor 20	1.41927
Zm00001d013154	Aux/IAA-transcription factor 20	1.54949
Zm00001d006282	Auxin-responsive protein SAUR61	1.80017
Zm00001d006279	Auxin-responsive protein SAUR61	2.24417
Zm00001d038275	Auxin transporter-like protein 1	2.69959

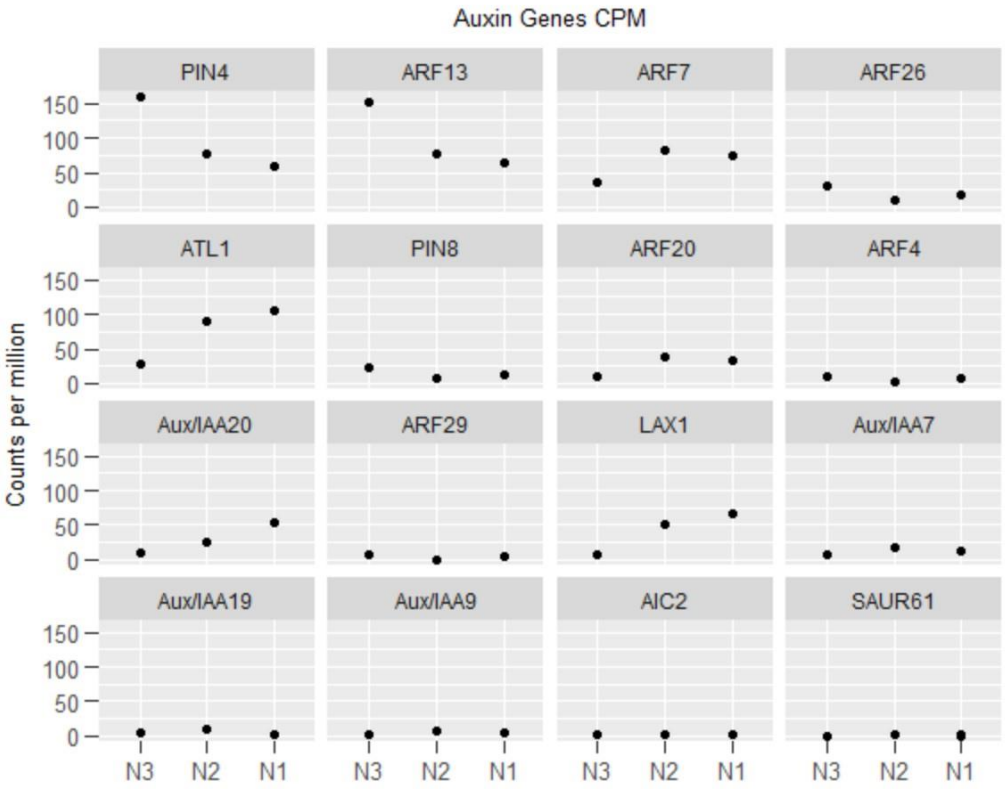

Figure 20. Auxin-related genes counts per million across nodes 1-3.

Table 10. Number of Uniform Mu lines available on MaizeGDB (maize genetics and genomics database) for the list of candidate auxin-related genes produced from RNA-seq of maize nodes. The number of insertions per line as well as the placement of these insertions (untranslated regions or introns) makes these lines impractical for a further mutant analysis. N/A= not available. UTR= untranslated region.

Gene	Uniform Mu number	Stock	Number of insertions	Insertion location
ARF29	mu1033410	N/A	N/A	N/A
	mu1083010	UFMu-10449	3	5’ UTR
	mu1004340	UFMu-07378	22	5’ UTR

		UFMu-00514	24	5’ UTR
ARF4	Mu1021266	UFMu-01723	14	Coding region
	Mu1052469	UFMu-06729	24	5’ UTR
ARF26	mu1061094	UFMu-07786	26	3’ UTR
	mu1082642	UFMu-09900	3	intron
PIN8	mu1041051	UFMu-04499	44	Coding region
PIN4	mu-illumina_127187.7	N/A	N/A	Coding region
	mu-illumina_21565.7	N/A	N/A	Coding region
	mu1053020	UFMu-06781	39	5’ UTR
	mu1100574	UFMu-02873	30	5’ UTR
	mu1019356	UFMu-00650	12	5’ UTR
	mu-illumina_15415.7	N/A	N/A	5’ UTR
ARF13	mu1045189	UFMu-05595	119	3’ UTR
	mu1045190	UFMu-05765	30	intron
	mu1014842	UFMu-01283	9	3’ UTR
	mu1086418	UFMu-10992	89	3’ UTR
	mu-illumina_116788.7	N/A	N/A	N/A
AIC2	N/A	N/A	N/A	N/A
Aux/IAA9	mu-illumina_152293.7	N/A	N/A	N/A
Aux/IAA19	N/A	N/A	N/A	N/A
ARF7	mu1094628	UFMu-11705	3	Coding region
	mu1090519	UFMu-13123	1	Coding region

	mu1052631	UFMu-06728	10	intron
	mu1017909	UFMu-01190	10	Coding region
	mu1083285	UFMu-10133	13	Coding region
	mu1076913	UFMu-08988	41	Coding region
	mu1029460	N/A	N/A	intron
	mu1070235	N/A	N/A	intron
	mu1086101	UFMu-10745	36	Coding region
	mu1080981	UFMu-09486	10	3’ UTR
	mu1076914	UFMu-09010	77	3’ UTR
	mu1069320	UFMu-08314	12	3’ UTR
	mu-illumina_16576.7	N/A	N/A	N/A
	mu-illumina_18803.7	N/A	N/A	N/A
	mu-illumina_21215.7	N/A	N/A	N/A
Aux/IAA7	mu1047926	UFMu-06162	21	intron
ATL1	mu1056152	UFMu-03658	21	intron
		UFMu-07513	43	intron
	mu1051112	UFMu-06246	9	Coding region
	mu1044946	UFMu-05422	4	3’ UTR
ARF20	mu1053629	UFMu-06542	47	3’ UTR
	mu1053630	UFMu-06542	47	3’ UTR
	mu1015422	UFMu-00899	6	3’ UTR
		UFMu-04796	10	3’ UTR

		UFMu-11169	35	3’ UTR
		UFMu-01744	4	3’ UTR
		UFMu-05080	2	3’ UTR
		UFMu-02370	10	3’ UTR
		UFMu-06554	13	3’ UTR
		UFMu-02491	6	3’ UTR
		UFMu-08414	14	3’ UTR
		UFMu-04196	6	3’ UTR
Aux/IAA20	mu1053549	UFMu-06725	7	5’ UTR
SAUR61	N/A	N/A	N/A	N/A
SAUR61	N/A	N/A	N/A	N/A
atl1	mu-illumina_170141.7	N/A	N/A	N/A
	mu-illumina_167546.7	N/A	N/A	N/A

Table 11. Ethylene-related genes that were differentially expressed from node 3 to node 2. FC=fold change.

Gene ID (B73 v4)	Gene	N3 v N2 FC
Zm00001d012585	AP2-EREBP-transcription factor 83	1.44604864
Zm00001d034204	AP2-EREBP-transcription factor 184	2.91721643
Zm00001d015759	AP2-EREBP-transcription factor 46	-4.74122851

Zm00001d009103	AP2-EREBP-transcription factor 148	1.11723616
Zm00001d037941	AP2-EREBP-transcription factor 69	1.91999459
Zm00001d007840	AP2-EREBP-transcription factor 41	2.56917405
Zm00001d018731	AP2-EREBP-transcription factor 114	1.90395203
Zm00001d048004	AP2-EREBP-transcription factor 161	2.78678893
Zm00001d002025	AP2-EREBP-transcription factor 24	1.42997435
Zm00001d035512	AP2-EREBP-transcription factor 81	-1.78208477
Zm00001d042492	AP2-EREBP-transcription factor 53	-5.42640656
Zm00001d034027	Ethylene-responsive protein	2.37053584
Zm00001d028974	ethylene insensitive-like3	-1.34336487
Zm00001d047563	ethylene insensitive-like1	-1.5061358
Zm00001d003451	EIL-transcription factor 7	-1.63369817

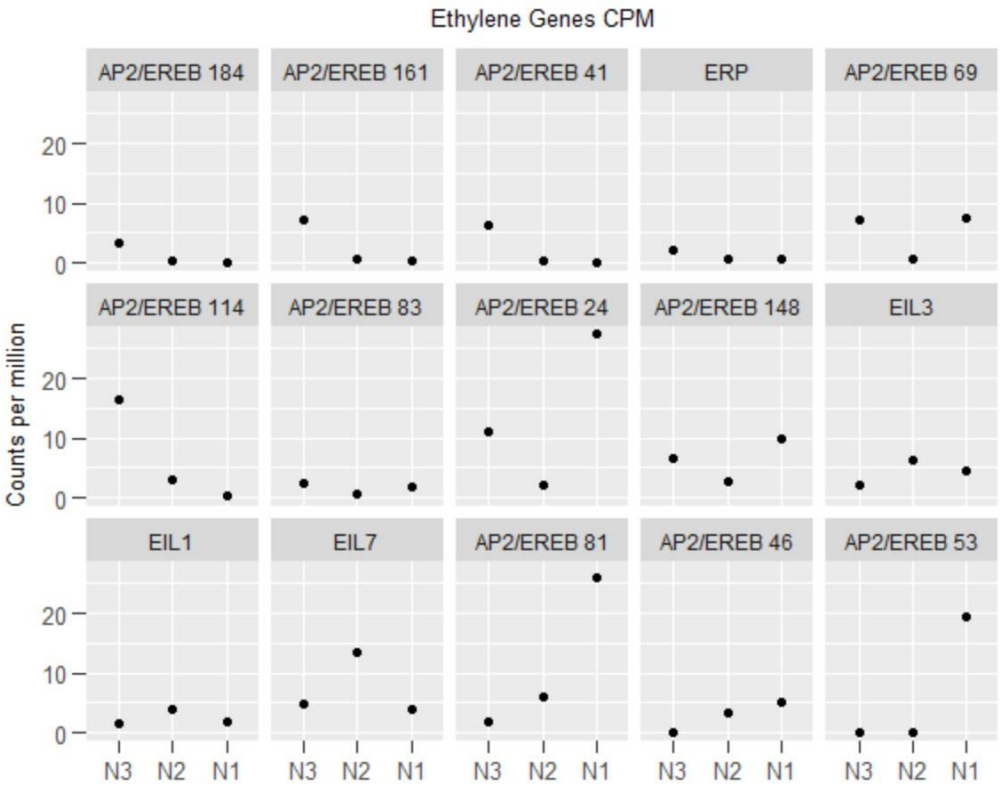

Figure 21. Ethylene- related genes counts per million across nodes 1-3.

Table 12. Cytokinin-related genes that were differentially expressed from node 3 to node 2. FC=fold change.

Gene ID (B73 v4)	Gene	N3 v N2 FC
Zm00001d043293	cytokinin oxidase 4	1.68765
Zm00001d001865	cytokinin response regulator1	-1.04119
Zm00001d011890	cytokinin oxidase 3	-3.04333
Zm00001d049282	Cytokinin-O-glucosyltransferase 1	-2.06823

Zm00001d010689	Cytokinin-O-glucosyltransferase 1	1.85721
Zm00001d003013	Cytokinin riboside 5'-monophosphate phosphoribohydrolase LOG3	-2.12709
Zm00001d032046	cytokinin oxidase10	-1.0316
Zm00001d034569	Cytokinin-O-glucosyltransferase 2	1.32587
Zm00001d021450	Cytokinin riboside 5'-monophosphate phosphoribohydrolase LOG5	-4.62792

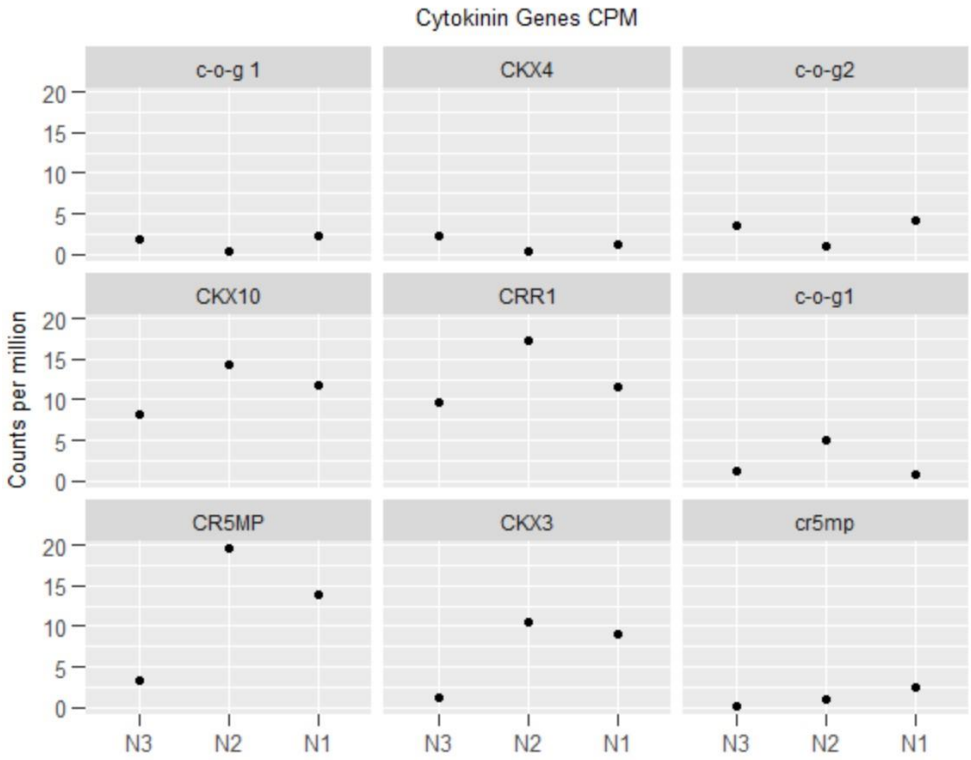

Figure 22. Cytokinin-related genes counts per million across nodes 1-3.

Table 13. Gibberellin-related genes that were differentially expressed from node 3 to node 2. FC=fold change.

Gene ID (B73 v4)	Gene	N3 v N2 FC
Zm00001d038996	gibberellin 2-oxidase8	3.56946
Zm00001d013222	Gibberellin-regulated protein 10	-1.29842
Zm00001d016895	Gibberellin receptor GID1L2	-1.18895
Zm00001d037180	Gibberellin receptor GID1L2	-1.45192
Zm00001d034898	gibberellin 20-oxidase1	-1.48511
Zm00001d042611	gibberellin 20-oxidase3	-1.0339
Zm00001d008909	gibberellin 2-oxidase9	-1.80366
Zm00001d033369	Gibberellin-regulated protein 1	1.0585
Zm00001d011225	gibberellin responsive3	-3.55189

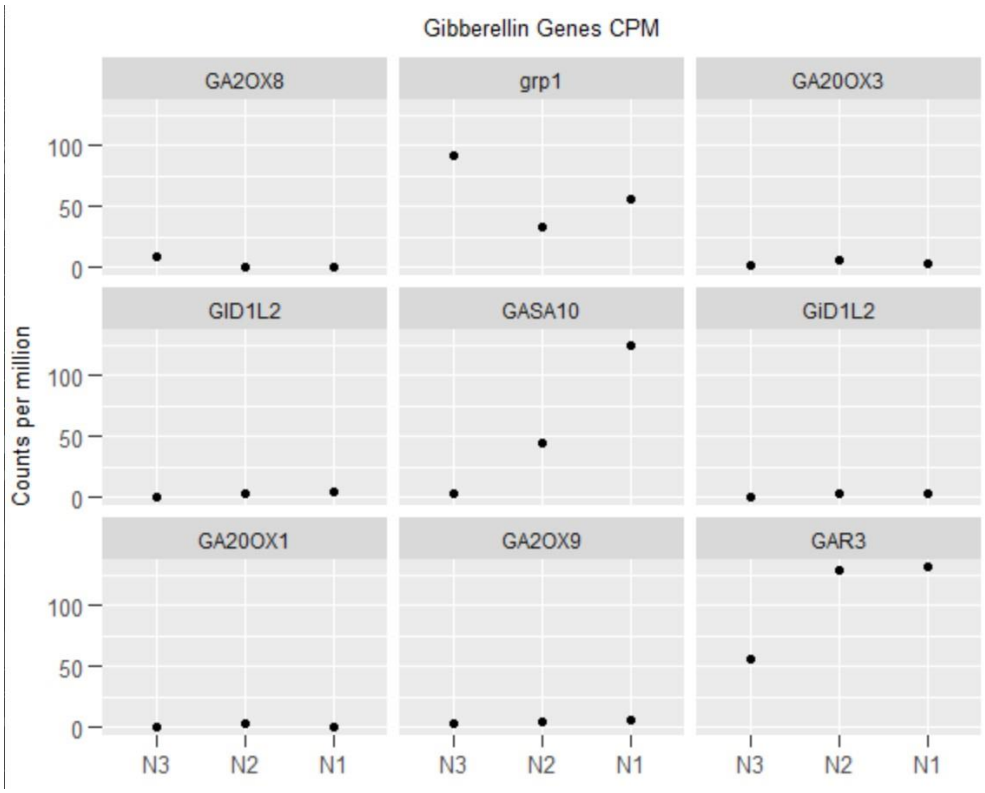

Figure 23. Gibberellin-related genes counts per million across nodes 1-3.

Table 14. Abscisic acid-related genes that were differentially expressed from node 3 to node 2. FC=fold change.

Gene ID (B73 v4)	Gene	N3 v N2 FC
Zm00001d012296	bZIP-transcription factor 75	1.21101
Zm00001d023664	ABA-responsive protein	-1.21485
Zm00001d004843	abscisic acid stress ripening2	-1.83651
Zm00001d017762	abscisic acid 8'-hydroxylase1	-1.29925
Zm00001d003712	abscisic acid stress ripening3	-5.05933
Zm00001d020717	abscisic acid 8'-hydroxylase4	-1.68364

Zm00001d023529	abscisic acid stress ripening1	-2.10011
Zm00001d025401	abscisic acid stress ripening5	-1.70398

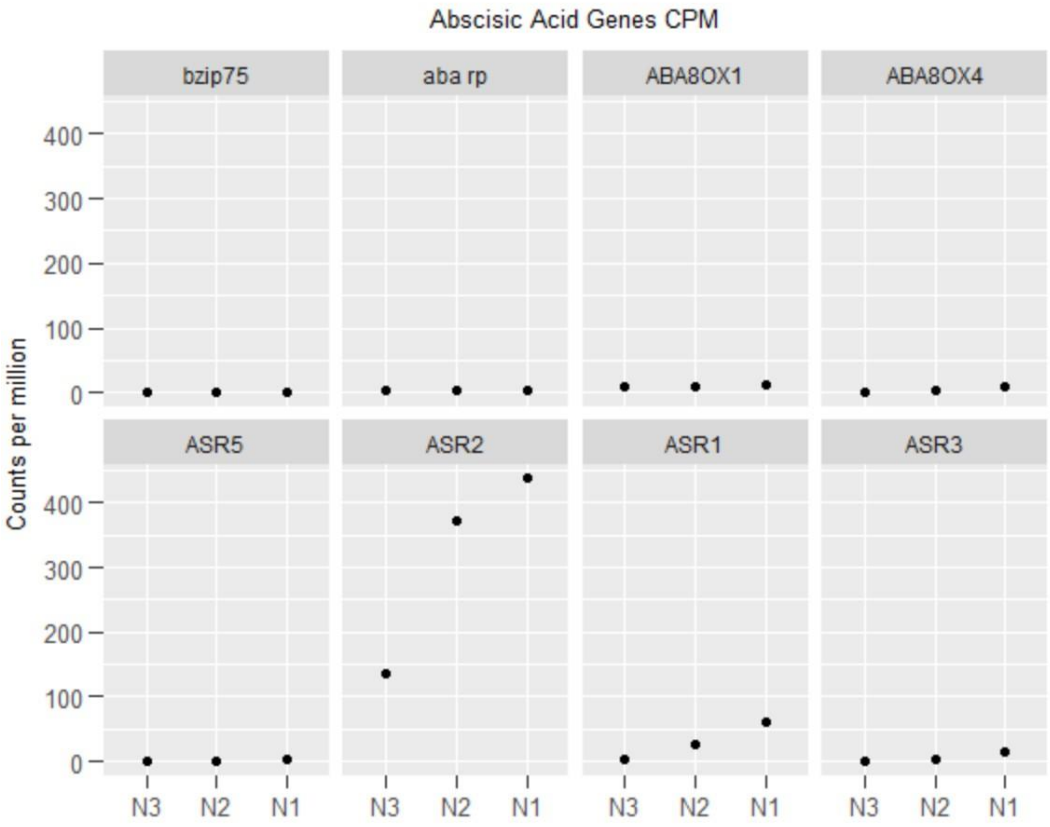

Figure 24. Abscisic acid-related genes count per million across nodes 1-3.

3.4 Conclusions & Future Directions

RNA-seq was used as a hypothesis generating approach to produce candidate genes for a mutant analysis. The first three aboveground nodes of three V6 B73 maize plants were selected for the developmental anatomy they display. The node closest to the ground was designated node 1, the next node above it was designated node 2, and

the highest from the ground designated node 3. Based on previous anatomical studies (see Chapter 2), I determined that node 1 of a V6 plant usually contains brace root primordia that are emerging from the stem, node 2 contains immature brace root primordia within the stem, and node 3 very rarely contains primordia at all, or has a few very early stage primordia. This approach proved to further refine the sequencing of developmental events, as each node displayed differential expression (Figure 14).

Filters to discover the top differentially expressed genes did not yield a clear path forward, so the choice was made to focus on hormone-related genes. A high number of auxin-related genes were differentially expressed during brace root initiation, i.e., in the node 3 to node 2 comparison. This is consistent with previous RNA-seq efforts (Li et al., 2011), which also found auxin-related genes were differentially expressed between nodes without brace roots and nodes with just-emerged brace roots. My approach further refined this data set by looking at three nodes in the course of development, not simply a node with or without brace roots. The best correlation in $\log_2$ fold change values occurred between my node 3 v. node 1 comparison and their comparison of a node and a node with just-emerged brace roots, with r=0.61. This makes sense because while (Li et al., 2011) did not show the anatomy of the tissue used, it would most closely line up with my node 3 (no brace roots) and node 1 (just-emerged brace roots). The other comparisons between my data and theirs had lower r values, at r=0.2 for the comparison with node 1 v. node 2, and r=0.47 for the comparison with node 2 v. node 3 (Figure 18).

The auxin-related genes that are differentially expressed during brace root initiation came from several different gene families. Aux/IAA's act as transcriptional repressors of auxin-related gene expression by binding to ARF's (auxin response

factors) on the auxin response element of a gene (Tiwari et al., 2001). There are 34 maize Aux/IAA's and all but one (ZmIAA23) are auxin-inducible (Ludwig et al., 2013). This family of genes has been shown to have a hierarchy of expression with expression higher in crown roots then seminal roots, primary roots, and finally lateral roots (Ludwig et al., 2013), however this study did not analyze brace roots, as the plants were too young for brace roots to emerge. It remains to be seen how Aux/IAA's are expressed during brace root development.

ARF's (auxin response factors) are transcription factors that bind to the auxin response element (AuxRE) of promoters of auxin responsive genes, either activating or repressing these genes (Guilfoyle & Hagen, 2007). There are 31 ARF genes in maize,14 of which have AuxRE in their promoters, and of which 7 have small to no response to auxin treatment (Xing et al., 2011). All maize ARF proteins contain a middle domain that confers activator or repressor functions (Liu et al., 2011; Wang et al., 2012; Xing et al., 2011). Based upon the structure of this domain, putative roles in activation or repression of auxin-regulated genes have been assigned to the maize ARF gene family (Table 15), although there is some conflicting information. Three of my differentially expressed ARF genes have putative roles as activators (ARF 4, 20, 29, (McSteen et al., 2016; Wang et al., 2012), and two have putative roles as repressors (ARF13 and ARF26, (McSteen et al., 2016 ; Xing et al., 2011). One of my ARF genes (ARF7) was reported as a putative activator in one paper (Wang et al., 2012), and as a putative repressor in another (McSteen et al., 2016). Future work to clarify ARF's roles in auxin signaling would prove useful to RNA-seq data sets such as mine.

Table 15. ARF genes that are differentially expressed in the node 3 v node 2 comparison with their putative roles in activating or repressing transcription of auxin-regulated genes.

ARF	Role	Differential expression	Reference
4	Putative activator	Downregulated	(McSteen et al., 2016; Wang et al., 2012)
7	Putative activator/repressor	Up regulated	(McSteen et al., 2016; Wang et al., 2012)
13	Putative repressor	Downregulated	(McSteen et al., 2016; Xing et al., 2011)
20	Putative activator	Up regulated	(McSteen et al., 2016)
26	Putative repressor	Downregulated	(McSteen et al., 2016)
29	Putative activator	Downregulated	(McSteen et al., 2016)

PIN proteins are named for the pin-like structure of reproductive organs first discovered in an Arabidopsis mutant (Okada et al., 1991). PIN's are plasma-membrane or endoplasmic reticulum (ER) localized proteins whose polarized location on the membrane functions to transport auxin, forming a concentration gradient that is important for many developmental processes. There are 12 maize PIN genes, 3 of which have been shown to be specific to monocots (Forestan et al., 2012). Within my node 3 v node 2 comparison, PIN8 and PIN4 were upregulated. PIN8 is one of the four shorter maize PIN proteins that localize to the ER (Forestan et al., 2012). The Arabidopsis ortholog, AtPIN8, was shown to be pollen-specific, and a loss-of-function mutant showed no phenotype (Bosco et al., 2012), while overexpression of AtPIN8 resulted in more auxin accumulation in source tissue than in sink tissue, such as roots.

The maize PIN8 was shown to be expressed globally with the exception of root tissue, and also was shown to be involved in kernel development (Forestan et al., 2012). While there is scarce research on PIN4 in maize, the tissue-specific expression of PIN proteins suggests that each member of the maize PIN gene family may have specific roles in polar auxin transport and development (Forestan et al., 2012).

The rest of the auxin-related genes that were upregulated in the node 3 v node 2 comparison have not been well described in the literature. SAUR's are small auxin up RNAs that are the largest family of early auxin response genes. There are 79 SAUR genes in the maize genome, and most have an auxin-responsive element in their promoters, only 2 have been described in maize (Chen et al., 2014; Knauss et al., 2003; Yang & Poovaiah, 2000). The rest of the auxin-related DE genes (auxin import carrier 2- Zm00001d053004, Auxin transporter-like protein 1-Zm00001d038275, auxin transporter-like1-Zm00001d042809) have not been well described in the literature.

Because the entire cross section of nodes was used in this transcriptome analysis, it is quite possible that the differentially expressed genes discussed here are involved in processes other than brace root development. Auxin is constantly flowing down the stem from source tissue (meristems, leaves) to sink tissues (roots). The auxin signaling and transport-related transcripts detected in my analysis could be involved in this process. To separate the brace root developmental processes from the natural flow of auxin down the stem, two approaches could be used. First, laser capture microdissection could narrow the area of tissue used for RNA-seq, separating cells near the periphery where brace roots are initiating from cells of the interior- where the vasculature is transporting auxin. A second approach using *in situ* hybridization would

look at where these transcripts are localized within the node. If they are indeed localized to the site of brace root initiation, we could be more confident that these genes are candidates for a mutant analysis, either using lines that are currently available, or using CRISPR-Cas9 technology to disrupt these genes and observe the effect on brace root development.

While my focus has been on the role auxin plays in brace root development, other hormones could also be involved. For example, ethylene is known to be involved in adventitious root development under flooding conditions in maize (Drew et al., 1979). Under normal conditions, application of an ethylene precursor has been shown to promote the emergence of brace roots, and plants with reduced ethylene sensitivity showed delayed emergence of brace roots (Shi et al., 2019). It would be interesting to compare hormone-related genes between the initiation and emergence steps of development, as my work indicates that auxin-related genes dominate during the initiation step, and literature supports the role of ethylene in emergence (Drew et al., 1979; Shi et al., 2019). Future work will explore the role of other phytohormones in maize brace root development.

REFERENCES

Bosco, C. D., Dovzhenko, A., Liu, X., Woerner, N., Rensch, T., Eismann, M., Eimer, S., Hegermann, J., Paponov, I. A., Ruperti, B., Heberle-Bors, E., Touraev, A., Cohen, J. D., & Palme, K. (2012). The endoplasmic reticulum localized PIN8 is a pollen-specific auxin carrier involved in intracellular auxin homeostasis. *The Plant Journal: For Cell and Molecular Biology*, *71*(5), 860–870.

Chen, Y., Hao, X., & Cao, J. (2014). Small auxin upregulated RNA (SAUR) gene family in maize: identification, evolution, and its phylogenetic comparison with Arabidopsis, rice, and sorghum. *Journal of Integrative Plant Biology*, *56*(2), 133–150.

Chuck, G., Cigan, A. M., Saeteurn, K., & Hake, S. (2007). The heterochronic maize mutant Corngrass1 results from overexpression of a tandem microRNA. *Nature Genetics*, *39*(4), 544–549.

Drew, M. C., Jackson, M. B., & Giffard, S. (1979). Ethylene-promoted adventitious rooting and development of cortical air spaces (aerenchyma) in roots may be adaptive responses to flooding in Zea mays L. *Planta*, *147*(1), 83–88.

Du, Z., Zhou, X., Ling, Y., Zhang, Z., & Su, Z. (2010). agriGO: a GO analysis toolkit for the agricultural community. *Nucleic Acids Research*, *38*(Web Server issue), W64–W70.

Forestan, C., Farinati, S., & Varotto, S. (2012). The Maize PIN Gene Family of Auxin Transporters. *Frontiers in Plant Science*, *3*, 16.

Guilfoyle, T. J., & Hagen, G. (2007). Auxin response factors. *Current Opinion in Plant Biology*, *10*(5), 453–460.

Knauss, S., Rohrmeier, T., & Lehle, L. (2003). The auxin-induced maize gene ZmSAUR2 encodes a short-lived nuclear protein expressed in elongating tissues. *The Journal of Biological Chemistry*, *278*(26), 23936–23943.

Liu, Y., Jiang, H. Y., Chen, W., Qian, Y., Ma, Q., Cheng, B., & Zhu, S. (2011). Genome-wide analysis of the auxin response factor (ARF) gene family in maize (Zea mays). *Plant Growth Regulation*, *63*, 225–234.

Li, Y.J., Fu, Y.R., Huang, J.G., Wu, C.A., & Zheng, C.C. (2011). Transcript profiling during the early development of the maize brace root via Solexa sequencing. *The FEBS Journal*, *278*(1), 156–166.

Ludwig, Y., Zhang, Y., & Hochholdinger, F. (2013). The maize (Zea mays L.) AUXIN/INDOLE-3-ACETIC ACID gene family: phylogeny, synteny, and unique root-type and tissue-specific expression patterns during development. *PloS One*, *8*(11), e78859.

McCarty, D. R., Mark Settles, A., Suzuki, M., Tan, B. C., Latshaw, S., Porch, T., Robin, K., Baier, J., Avigne, W., Lai, J., Messing, J., Koch, K. E., & Curtis Hannah, L. (2005). Steady-state transposon mutagenesis in inbred maize: Maize steady-state transposon mutagenesis. *The Plant Journal: For Cell and Molecular Biology*, *44*(1), 52–61.

McSteen et al., 2016 – *Auxin Regulatory and Expression Database for Maize.* (2016.). Retrieved May 28, 2020, from https://maizeauxre.missouri.edu/home_gene_catalog_1/

Nielsen, R. L. (2014). Determining corn leaf stages. *Corny News Network*. https://www.agry.purdue.edu/ext/corn/news/articles.04/VStageMethods-0515.pdf

Okada, K., Ueda, J., Komaki, M. K., Bell, C. J., & Shimura, Y. (1991). Requirement of the Auxin Polar Transport System in Early Stages of Arabidopsis Floral Bud Formation. *The Plant Cell*, *3*(7), 677–684.

Portwood, J. L., Woodhouse, M. R., Cannon, E. K., Gardiner, J. M., Harper, L. C., Schaeffer, M. L., Walsh, J. R., Sen, T. Z., Cho, K. T., Schott, D. A., Braun, B. L., Dietze, M., Dunfee, B., Elsik, C. G., Manchanda, N., Coe, E., Sachs, M., Stinard, P., Tolbert, J., … Andorf, C. M. (2019). MaizeGDB 2018: the maize multi-genome genetics and genomics database. *Nucleic Acids Research*, *47*(D1), D1146–D1154.

Rhoades, M. W., Reinhart, B. J., Lim, L. P., Burge, C. B., Bartel, B., & Bartel, D. P. (2002). Prediction of plant microRNA targets. *Cell*, *110*(4), 513–520.

Shi, J., Drummond, B. J., Habben, J. E., Brugire, N., Weers, B. P., Hakimi, S. M., Lafitte, H. R., Schussler, J. R., Mo, H., Beatty, M., Zastrow-Hayes, G., & O'Neill, D. (2019). Ectopic expression of ARGOS8 reveals a role for ethylene in root-lodging resistance in maize. *The Plant Journal: For Cell and Molecular Biology*, *97*(2), 378–390.

Tiwari, S. B., Wang, X. J., Hagen, G., & Guilfoyle, T. J. (2001). AUX/IAA proteins are active repressors, and their stability and activity are modulated by auxin. *The Plant Cell*, *13*(12), 2809–2822.

Wang, Y., Deng, D., Shi, Y., Miao, N., Bian, Y., & Yin, Z. (2012). Diversification, phylogeny, and evolution of auxin response factor (ARF) family: insights gained from analyzing maize ARF genes. *Molecular Biology Reports*, *39*(3), 2401–2415.

Xing, H., Pudake, R. N., Guo, G., Xing, G., Hu, Z., Zhang, Y., Sun, Q., & Ni, Z. (2011). Genome-wide identification and expression profiling of auxin response factor (ARF) gene family in maize. *BMC Genomics*, *12*, 178.

Yang, T., & Poovaiah, B. W. (2000). Molecular and biochemical evidence for the involvement of calcium/calmodulin in auxin action. *The Journal of Biological Chemistry*, *275*(5), 3137–3143.

Chapter 4

EXOGENOUS APPLICATION OF HORMONE TO MAIZE STEMS

4.1 Rationale

A common approach to determine if a phytohormone is sufficient for a developmental process is the exogenous application of that hormone and/or its inhibitor. While methodology for this has been well established in model systems such as *Arabidopsis thaliana*, the same cannot be said for maize stems. In this chapter, I establish methodology for the exogenous application of hormones to maize stems to determine if auxin is sufficient to induce developmental changes.

4.2 Methods

4.2.1 Growth conditions

Inbred B73 plants were grown in 3-gallon pots under greenhouse conditions in the University of Delaware Fisher Greenhouse Zone #4. During this period, average temperature was 24.5 °C, average humidity was 57.2%, and supplemental lighting in the form of 400 Watt HPS and 400 Watt MH bulbs was provided from 7 AM - 9 PM when outside light radiation levels were below 600 W/m^2 (watts per square meter). Plants were watered twice a week; once a week supplemented with nutrient solution and BK 55 soil was prepared with approximately 30 grams of slow release 19-6-9 osmocote pellets.

4.2.2 Exogenous application of hormones

Maize inbred B73 plants were grown as described above to the V8-V10 stage. A size 14 sewing needle was used to poke a small hole in the caps of microcentrifuge tubes. An approximately 12 inch long crochet thread was pre-soaked in water to enhance capillary action. The needle brought the pre-soaked thread through the tube (from inside to outside) and a knot was tied on the inside portion of the thread to prevent it slipping out through the hole, leaving approximately 1 inch of thread left inside the tube. The needle and thread were inserted through the stem of a plant either at the node or just below the node. The needle and thread were then used to poke a hole through another microcentrifuge tube on the other side of the stem (from outside to inside). A knot was tied on the inside portion of the thread (Figure 25), making sure to adjust the tubes to be as close to the stem as possible, to facilitate capillary action. The tubes were filled to the top with varying concentrations of hormone or water (Table 16). Approximately 3 drops of red food dye (McCormick's) were also added to the tubes to track the spread of solution in the plant. The solution-filled tubes were left on the plants for 7-10 days and refilled approximately every 2 days. Nodes above and below the site of application were hand sectioned and brightfield images were taken on an upright Echo Revolve microscope at 4x magnification.

Figure 25. Experimental set-up for exogenous application experiments. A sewing needle was used to poke holes in the tops of two microcentrifuge tubes. The needle was poked through the maize stem at the specified location and the thread knotted inside both tubes. The tubes were filled with food dye and the hormone solution. Tubes were re-filled as needed for the duration of the experiment.

4.3 Results

4.3.1 Food dye travels above and below the site of application

Initial experiments used only water and food dye to assess how far the solution traveled within the maize stem. Three plants at the V11 stage were used for initial experiments and the tracking solution was applied at the 5th node from the soil. Sectioning through nodes above and below the site of application at 3 days after application revealed that the food dye solution travels approximately two nodes above and two nodes below the site of application (Figure 26). Food dye appeared to accumulate more at nodes than internodes and appeared to travel more above the site

of application than below. These results show that my method works to deliver food dye solution to the maize stem.

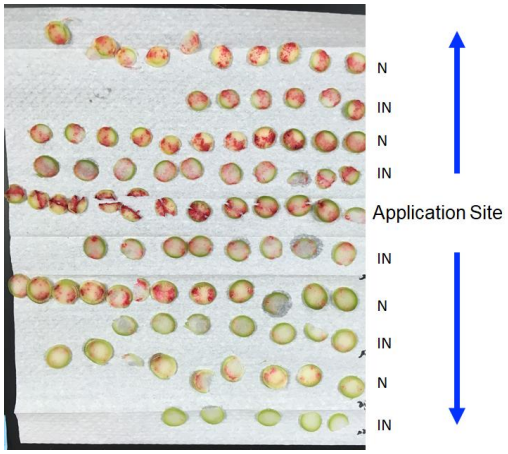

Figure 26. Results from initial experiment detailing how far the food dye travels within the maize stem. The food dye was observed two nodes above and two nodes below the application site. N=node, IN=internode.

4.3.2 Application of 2,4-D and NPA to the upper nodes of V12-V15 plants did not affect brace root initiation

Experiments #1-3 using solutions of 2,4-dichlorophenoxyacetic acid (2,4-D, a synthetic auxin) and N-1-naphthylphthalamic acid (NPA, an auxin inhibitor) at varying concentrations (100, 10, and 1µM) applied at nodes 7 and 8 of V12 and V15 plants were performed (Table 16). These stages were chosen because the nodes were clearly visible beneath the leaf sheath. Nodes 7 and 8 were chosen because they do not normally form brace roots. Solutions were re-filled every 2-3 days until the plants were harvested for sectioning 10-11 days later. Application at the node resulted in

badly damaged nodes which were difficult to view and count primordia at the application site. No apparent developmental changes were detected when 2,4-D or NPA were applied to the nodes (data not shown).

Table 16. Summary of Exogenous Application experiments.

Experiment	Duration	Concentration	Solution	Node	Stage	Notes
1	10 days	100 µM	2,4-D	N7	V12	
		100 µM	NPA	N7	V12	
		-	Water	N7	V11	
2	10 days	10 µM	2,4-D	N7	V12	
		10 µM	NPA	N7	V12	
		-	Water	N7	V12	
3	11 days	1 µM	2,4-D	N8	V15	
		1 µM	NPA	N8	V15	
		-	Water	N8	V15	
4	14 days	10 µM	NAA	below N4	V10	insect damage
		10 µM	NPA	below N4	V8	stem broke
		-	Water	below N3	V8	insect damage
5	12 days	10 µM	NAA	below N3	V8	1 tiller
		10 µM	NPA	below N4	V8	0 tillers
		-	Water	above N1	V8	5 tillers
6	9 days	10 µM	NAA	above N3	V10	2 tillers
		10 µM	NAA	below N3	V9	1 tiller
		10 µM	NPA	below N3	V10	2 tillers
		10 µM	NPA	above N3	V9	0 tillers

	8 days	-	Water	below N3	V11	2 tillers
		-	Water	below N3	V10	2 tillers
		-	Wound	above N3	V11	1 tiller
		-	Wound	above N3	V10	2 tillers
		-	Control	-	V11	2 tillers
		-	Control	-	V11	2 tillers
7	11 days	10 µM	NAA	above N3	V9	0 tillers
		10 µM	NPA	above N3	V9	0 tillers
		-	Water	above N3	V9	0 tillers
		-	Wound	above N3	V10	0 tillers

4.3.3 Application of NAA and water to V8 plants induced tiller initiation

Due to damage at the site of application, and the lack of response in initial experiments, several modifications were made to the procedure. First, 1-Naphthaleneacetic acid (NAA) was substituted for 2,4-D. 2,4-D was originally chosen from unpublished reports that maize primary roots have the greatest response to 2,4-D of all the auxin analogs (Paula McSteen, personal communication). However, 2,4-D requires active transport and thus may not be reaching the site of brace root initiation (Delbarre et al., 1996; Donaldson et al. 1973). Second, the site of application was moved from at the node to just above or below the node, since in the first round of experiments the node was destroyed by the needle. Third, the application site was moved from the upper nodes, to the nodes closer to the ground. At these nodes, brace roots will form, and the application of auxin and auxin inhibitor was used to observe a possible increase or decrease in the number of brace roots initiated.

During experiment #4, the stem of the 10 µM NPA plant snapped, and the water and 10 µM NAA plants suffered from greenhouse pests, and so these plants were not sectioned or imaged.

During experiment #5, treatments were applied to V8 plants and treatments were applied approximately 1 inch above node 1. After 5 days of treatment, nodal tillers began to form on the water treated plants. At 12 days of treatment, the plant treated with water formed 5 tillers from nodes 2-6. At the end of the experiment, the tubes in the water treatment had moved up the stem and were found at node 7 (Figure 27b).

The 10 µM NAA treatment also showed nodal tillers beginning to form at 5 days of treatment. At the end of the experiment, the NAA-treated plants only produced one tiller- at node 3, just above the site of application (Figure 27C). In contrast, the 10 µM NPA treatment did not induce any tillers (Figure 27D).

Figure 27. Results from exogenous application experiment #5 12 days after treatment began. A) Control V11 stage plant that was not used for application. B) Water control- only dH_2O and red food dye was applied above node 1. Blue arrows indicate tillers. C) The 10 µM 1-Naphthaleneacetic acid (NAA) treated plant produced one tiller below node 3 (blue arrow). D) The plant treated with 10 µM 1-N-Naphthylphthalamic acid (NPA), an auxin inhibitor, did not produce tillers. All treatments and controls produced brace root primordia in nodes 1-6.

All plants were sectioned at nodes 1-7, with some sections taken at the internode, and sections were immediately imaged on an Echo Revolve microscope, and the number of primordia counted (Figure 28). A V11 staged plant with no application was also sectioned and its primordia were counted as a control (Figure 27A). Brightfield images reveal that the food dye traveled at approximately the same rate in all plants (Figure 29-34) and could be detected in vascular bundles near the site of brace root initiation (Figures 29,30,31B-C). Large holes and necrotic tissue could also be seen near the site of application where the needle caused damage (Figure 30C).

Sections from the same node were similar across the treatments (Figures 29-34). The number of primordia proved difficult to compare across treatments because the tubes of solution were located at different nodes by the end of the experiment (Figure 28F). Assuming my initial experiments of food dye were an accurate reflection of chemical travel, the nodes affected include the two above and two below the site of application. The water treated plant had less primordia than the control (no application) from nodes 4 and higher (Figure 28B). Comparing the NPA-treated plant to control, it shows a similar pattern to the water-treated plant and has less primordia than control from nodes 3 and higher (Figure 28C). The NAA-treated plant showed a similar number of primordia to control at all nodes except node 4, which is one node higher than the site of application (Figure 28D). The two treatments can be compared to each other since by the end of the experiment, the tubes were in a similar place (node 3 for NAA and node 4 for NPA). The NPA-treated plant showed a decrease in the number of primordia compared to NAA, especially at higher nodes (Figure 28E). Finally, when all treatments are compared, the overall pattern remains unclear (Figure 28F). The water showed a difference from the control-treated plant (no application), and the auxin inhibitor NPA also showed a difference from the control plant. The auxin treatment (NAA) did not show as difference from control.

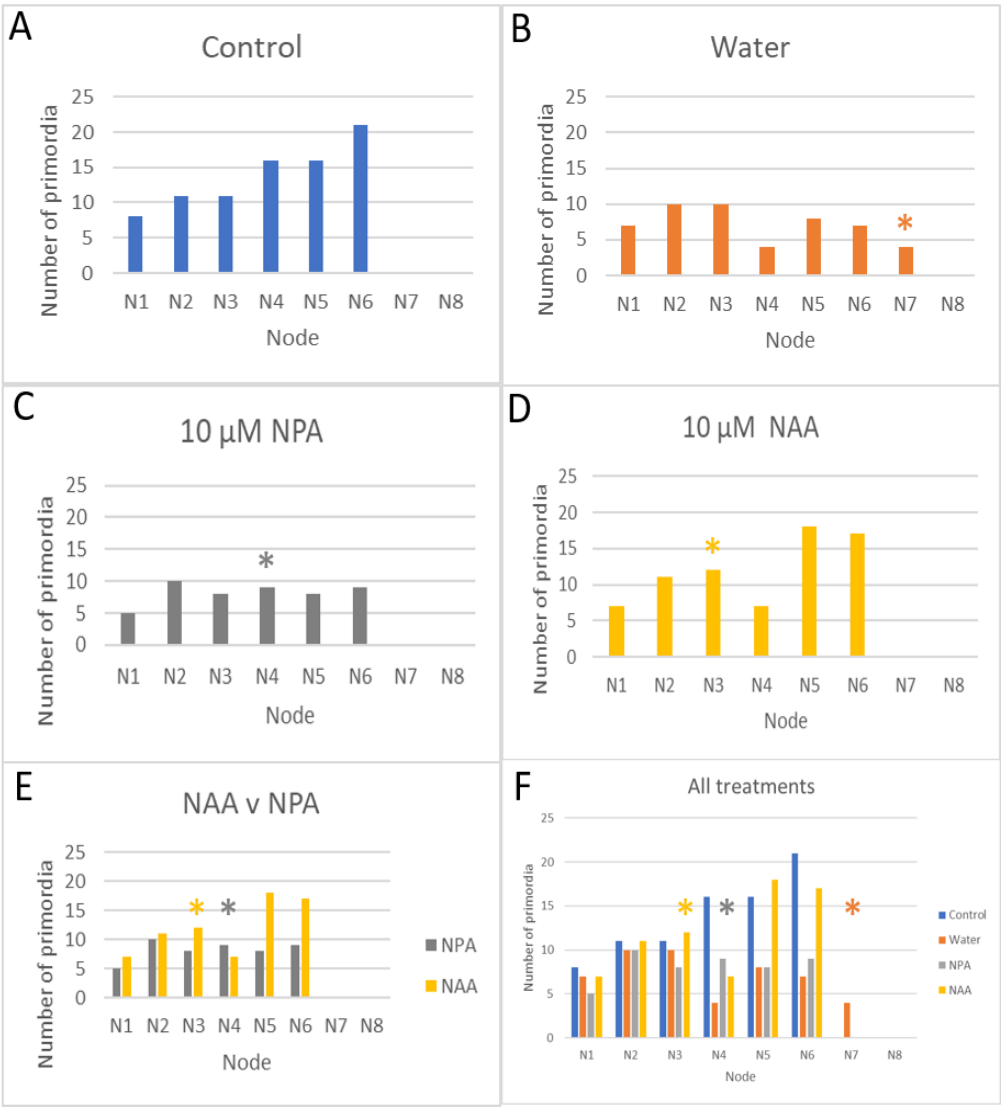

Figure 28. Results from exogenous application experiment #5. A) Number of primordia in nodes 1-8 in a V11 stage control plant. B) Number of primordia in nodes 1-8 in the water control. C) Number of primordia in nodes 1-8 in 10 µM NPA treatment. D) Number of primordia in 10 µM NAA treatment. E) Number of primordia compared between auxin (NAA) and auxin inhibitor (NPA). F) Number of primordia compared across all treatments. Asterisks indicate where the thread and tubes ended up at the end of the experiment.

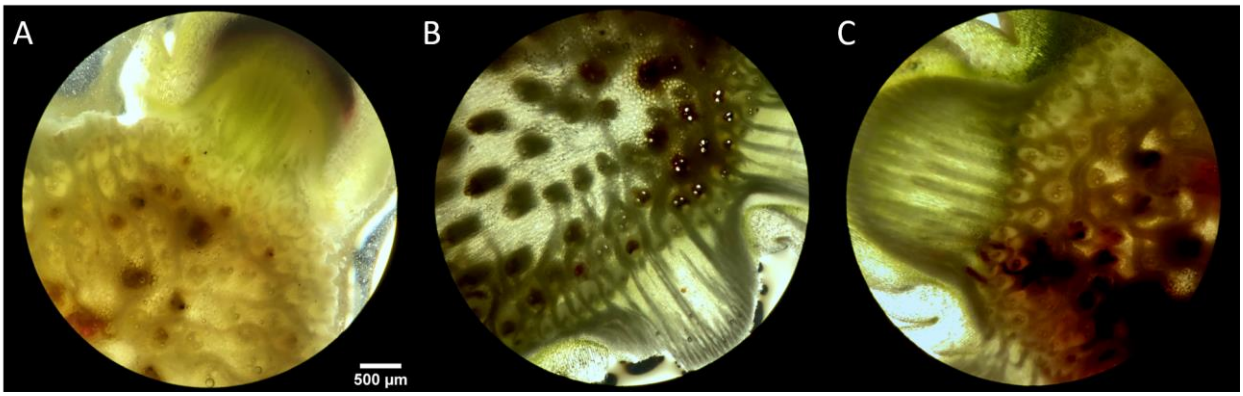

Figure 29. Exogenous application experiment #5 cross sections at node 1. A) Water. B) 10 µM NAA C) 10 µM NPA. Images acquired on an Echo Revolve microscope at 4x magnification. Scale bar= 500 µm.

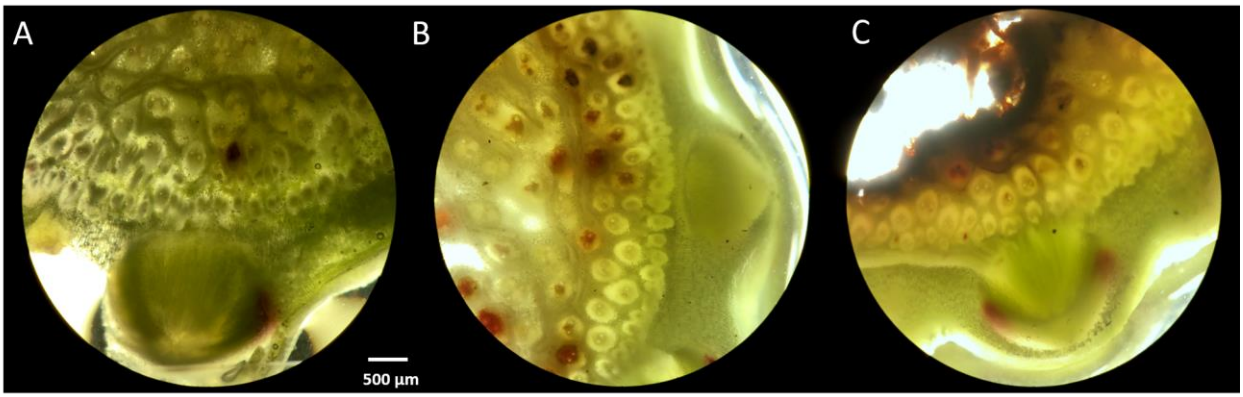

Figure 30. Exogenous application experiment #5 cross sections at node 2. A) Water. B) 10 µM NAA C) 10 µM NPA. Images acquired on an Echo Revolve microscope at 4x magnification. Scale bar= 500 µm.

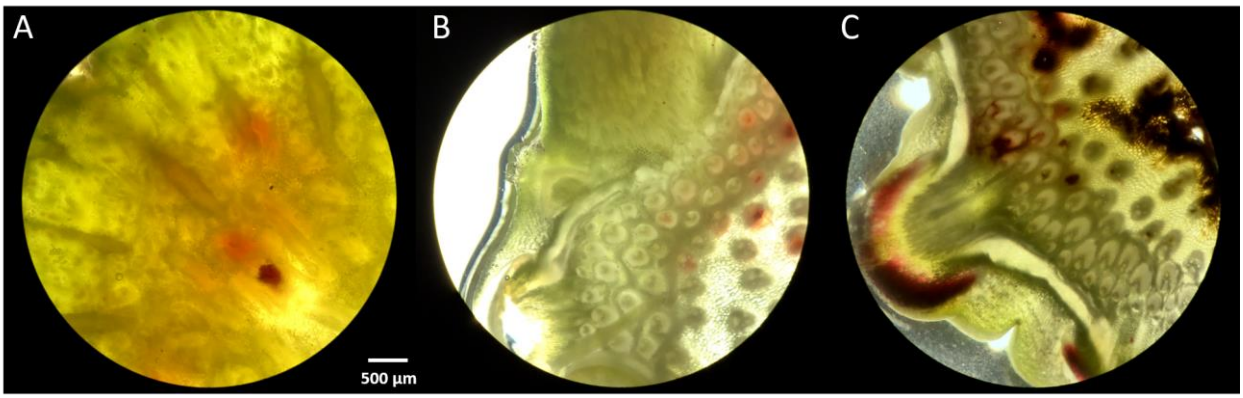

Figure 31. Exogenous application experiment #5 cross sections at node 3. A) Water. B) 10 µM NAA C) 10 µM NPA. Images acquired on an Echo Revolve microscope at 4x magnification. Scale bar= 500 µm.

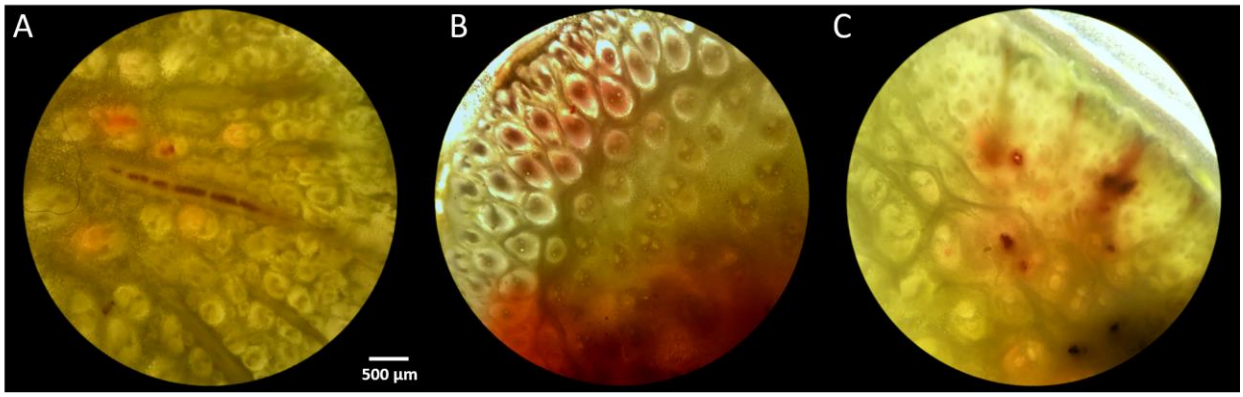

Figure 32. Exogenous application experiment #5 cross sections at node 4. A) Water. B) 10 µM NAA C) 10 µM NPA. Images acquired on an Echo Revolve microscope at 4x magnification. Scale bar= 500 µm.

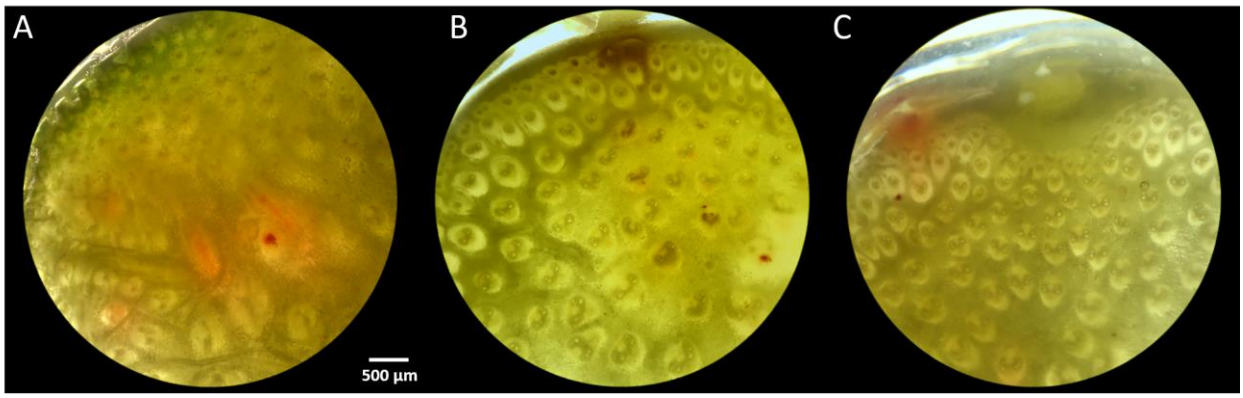

Figure 33. Exogenous application experiment #5 cross sections at node 5. A) Water. B) 10 µM NAA C) 10 µM NPA. Images acquired on an Echo Revolve microscope at 4x magnification. Scale bar= 500 µm.

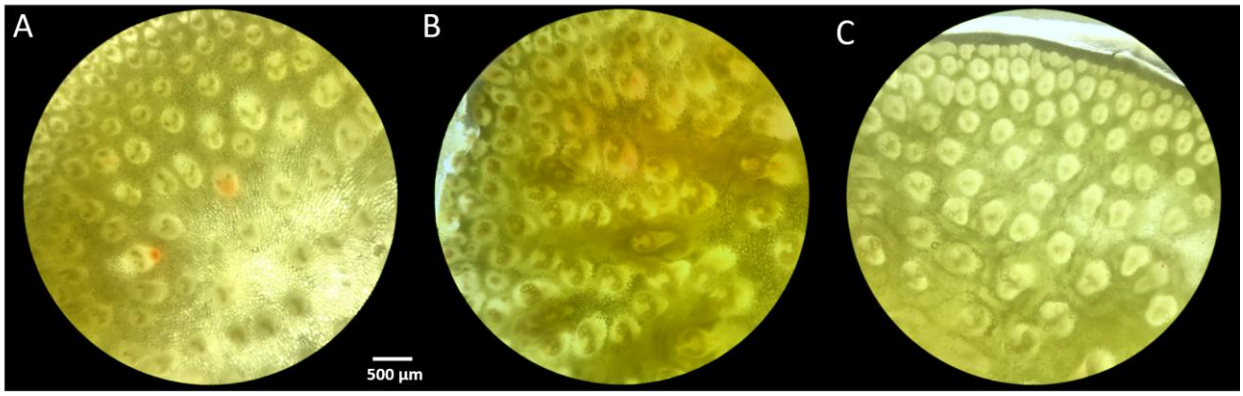

Figure 34. Exogenous application experiment #5 cross sections at node 6. A) Water. B) 10 µM NAA C) 10 µM NPA. Images acquired on an Echo Revolve microscope at 4x magnification. Scale bar= 500 µm.

4.3.4 Experimental Replication yielded mixed results on tillering

This experiment was replicated 3 more times (experiments #6-7), adding a control plant that was wounded with the needle, but had no solution added. During experiment #6, each treatment was replicated two times with the treatment applied above and below node 3, using V9-V11 stage plants. At the start of the experiment,

the two control plants had tillers already forming at their base. By the end of the experiment (8-9 days), all plants had formed tillers except one of the NPA treated plants (Table 16).

During experiment #7, plants at the V9/V10 stage were treated the same as before, with the treatment applied above node 3. No tillers were observed during the course of this experiment (Table 16).

4.3.5 No significant difference found in the number of primordia

The number of primordia formed across nodes was graphed and revealed that there is to be a higher variation in the number of primordia formed at higher nodes compared to lower nodes, but this variation is consistent across control and treated plants (Figure 35). There was no significant difference in the number of primordia across treatment ($p=0.1211$), or the interaction between treatments and nodes ($p=0.7736$), but there was a significant difference across nodes ($p<0.001$, Table 17).

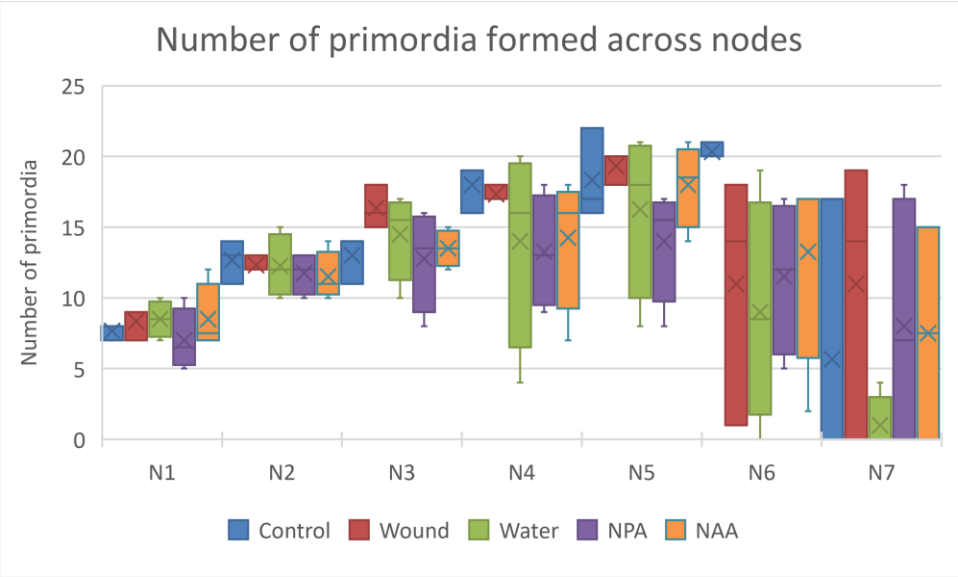

Figure 35. Number of primordia formed across nodes for experiments #5-7. For control and wound plants n=3; for water, NPA, and NAA plants n=4.

Table 17. Summary statistics for exogenous application experiments #5-7 using two way ANOVA in R.

Variable	Df	Sum Sq	Mean Sq	F value	P value
Treatment	4	176.22	44.055	1.8778	0.1211
Node Number	6	1541.08	256.847	10.948	3.77E-09***
Interaction	24	428.59	17.858	0.7612	0.7736

4.4 Conclusions & Future Directions

I have established methods for exogenously applying hormones to the maize stem and have preliminary results showing that this application method can elicit a developmental response. My experiments showed that the food dye travels both up and down the plant from the site of application. The food dye used contained FD&C

red 40 and red 3. Red 40 is also known as Allura Red AC, whose molecular weight is 496.4 g/mol and has no charge. Red 3 is also known as erythrosine and has a molecular weight of 879.9 g/mol and also has no charge. The cell permeability of these compounds is not known. In comparison with NAA, which has a molecular weight of 186.21 g/mol, and NPA, which has a molecular weight of 291.3 g/mol, has no charge, and enters the cell by passive diffusion, these dyes are heavier and therefore could be moving at a slower rate within the plant. Future work to investigate the travel of these dyes within the plant versus other compounds could help clarify how far the added auxin or auxin inhibitor has traveled within the maize stem. Another option would be to quantify the amount of auxin or auxin inhibitor that has accumulated in the maize stem. Methods for auxin quantification in plant tissues have been summarized in Porfírio et al., 2016. Auxin responses could also be visualized using reporter lines, as in Chapter 2.

In the first experiment, there was no effect on upper nodes. It is possible that this was due to the type of auxin used (2,4-D) or the fact that it was applied directly at the nodes, destroying them in the process. Another possibility is that the upper nodes do not have the competence to form brace roots, and thus the auxin or its inhibitor would have no effect.

In the next round of experiments, lower nodes on younger plants were used to ensure that the nodes had the ability to produce brace roots. For this approach, the hypothesis was that the addition of auxin would increase the number of brace roots, or speed up the initiation process, while the auxin inhibitor would do the opposite. Unexpectedly, nodal tillers were formed in the water control and the auxin-treated plant, but not in the auxin inhibitor plant during experiment #5 (Figure 27). It is

known that wounding can cause tillers to form (De Wolff, 1971). Thus, additional experiments #6 and #7 add a control that was wounded with the needle but had no hormone or dye solution applied. These experiments showed variable formation of tillers- 9 out of 10 plants formed tillers during experiment #6, while none formed during experiment #7 (Table 16). Further, the tillers that formed were tillers from the base, which are a standard developmental variation, as opposed to nodal tillers, which do not typically form in maize. The irreproducibility of nodal tiller formation across these experiments indicates that addition of hormones is not causing the nodal tillers to form. It remains unclear if the nodal tiller formation is due to the application strategy (wounding with a needle) or some unknown environmental effect.

Overall, there were no statistically significant differences between the number of primordia formed in control plants and those that were wounded, or treated with water, NPA, or NAA. The lack of a conclusive trend in the number of primordia formed indicates that this method is not sufficient to detect changes in the initiation of brace roots. Future work to assess the size of primordia, along with quantifying the number that have emerged from the stem could show that there are other ways auxin could be affecting brace root development than simply the number of primordia that form.

Additional considerations for future experiments are the method of application. Different exogenous application approaches in maize have been reported in the literature. Popular approaches include adding hormones to the growth medium, adding hormones to the nutrient solution or water, foliar sprays, applying via a lanolin paste, or scuffing. Most of these methods have been used on maize seedlings, where the tissue is at an earlier stage of development and does not have a cuticle, whereas brace

roots only start to develop around the V4 stage (see Chapter 2). While this approach outlined in this chapter was selected for the ability to apply directly to the site of brace root initiation and observe local effects, future experiments could compare methods of exogenous application of hormones and their effects on the formation of brace roots.

The type and concentration of auxin and auxin inhibitor should also be evaluated in the context of brace root development. For auxin analogs, 2,4-D has been shown to have a repressing effect on crown root formation in maize, while NAA and IBA stimulated crown root formation in a dose-dependent manner (Martínez de la Cruz et al., 2015). The decision was made to switch from 2,4-D to NAA because NAA has been shown to enter cells by passive diffusion, while 2,4-D needs an influx carrier to be transported (Delbarre et al., 1996). Both of these are synthetic auxins, and it would be interesting to compare the effects of synthetic auxins (NAA, 2,4-D) to naturally occurring auxins (IAA and IBA).

Along with comparing the effects of various auxin analogs, it would be intriguing to compare the effects of different auxin inhibitors. NPA used in this study is a phytotropin, while other synthetic inhibitors are not (Rubery, 1990). 2,3,5-triiodobenzoic acid (TIBA) and 2-(1-pyrenoyl) benzoic acid (PBA) act by interfering with the actin dynamics that allow for the vesicular trafficking of auxin efflux carriers between the plasma membrane and the endosomes (Dhonukshe et al., 2008). The differing effects of these auxin inhibitors is presumed to be due to their mode of action, but the exact mechanism or binding sites of NPA are still under investigation (Teale & Palme, 2018). Varying the concentration as well as the type of auxin inhibitor is another avenue of research to pursue.

The work highlighted in this chapter establishes the foundation for future exogenous application of hormones to maize stems. The future directions are to test different concentrations of auxin analogs and their inhibitors. However, should the preliminary result that auxin does not change brace root initiation hold across different types of concentrations of auxin, then looking at combinations of hormones would be the next step. As outlined in Chapter 2, genes in both the ethylene and cytokinin pathways are also differentially expressed during brace root initiation. As auxin is known to function cooperatively with ethylene and cytokinin in different developmental contexts (Alarcón et al., 2014; Fukaki & Tasaka, 2009; Kushwah et al., 2011; Swarup et al., 2002), future experiments could investigate combinatorial hormone treatments.

REFERENCES

Alarcón, M. V., Lloret, P. G., & Salguero, J. (2014). The Development of the Maize Root System: Role of Auxin and Ethylene. In A. Morte & A. Varma (Eds.), *Root Engineering: Basic and Applied Concepts* (pp. 75–103). Springer Berlin Heidelberg.

Delbarre, A., Muller, P., Imhoff, V., & Guern, J. (1996). Comparison of mechanisms controlling uptake and accumulation of 2,4-dichlorophenoxy acetic acid, naphthalene-1-acetic acid, and indole-3-acetic acid in suspension-cultured tobacco cells. *Planta*, *198*(4), 532–541.

De Wolff, F. (1971). Techniques for the vegetative propagation of maize (Zea mays L.). *Euphytica/ Netherlands Journal of Plant Breeding*, *20*(4), 524–526.

Dhonukshe, P., Grigoriev, I., Fischer, R., Tominaga, M., Robinson, D. G., Hasek, J., Paciorek, T., Petrásek, J., Seifertová, D., Tejos, R., Meisel, L. A., Zazímalová, E., Gadella, T. W. J., Jr, Stierhof, Y.-D., Ueda, T., Oiwa, K., Akhmanova, A., Brock, R., Spang, A., & Friml, J. (2008). Auxin transport inhibitors impair vesicle motility and actin cytoskeleton dynamics in diverse eukaryotes. *Proceedings of the National Academy of Sciences of the United States of America*, *105*(11), 4489–4494.

Doebley, J., Stec, A., & Hubbard, L. (1997). The evolution of apical dominance in maize. *Nature*, *386*(6624), 485–488.

Donaldson, D.E. Bayer, and O.A. Leonard. (1973). Absorption of 2,4-Dichlorophenoxyacetic Acid and 3-(p-Chlorophenyl)-1,1-dimethylurea (Monuron) by Barley Roots1. *Plant Physiology*, *52*, 638–645.

Fukaki, H., & Tasaka, M. (2009). Hormone interactions during lateral root formation. *Plant Molecular Biology*, *69*(4), 437–449.

Gerik, T. J., & Neely, C. L. (1987). Plant Density Effects on Main Culm and Tiller Development of Grain Sorghum 1. *Crop Science*, *27*(6), 1225–1230.

Kushwah, S., Jones, A. M., & Laxmi, A. (2011). Cytokinin interplay with ethylene, auxin, and glucose signaling controls Arabidopsis seedling root directional growth. *Plant Physiology*, *156*(4), 1851–1866.

Martínez-de la Cruz, E., García-Ramírez, E., Vázquez-Ramos, J. M., Reyes de la Cruz, H., & López-Bucio, J. (2015). Auxins differentially regulate root system architecture and cell cycle protein levels in maize seedlings. *Journal of Plant Physiology*, *176*, 147–156.

Porfírio, S., Gomes da Silva, M. D. R., Peixe, A., Cabrita, M. J., & Azadi, P. (2016). Current analytical methods for plant auxin quantification--A review. *Analytica Chimica Acta*, *902*, 8–21.

Rubery, P. H. (1990). Phytotropins: receptors and endogenous ligands. *Symposia of the Society for Experimental Biology.*, *44*, 119–146.

Swarup, R., Parry, G., Graham, N., Allen, T., & Bennett, M. (2002). Auxin cross-talk: integration of signaling pathways to control plant development. *Plant Molecular Biology*, *49*(3-4), 411–426.

Teale, W., & Palme, K. (2018). Naphthylphthalamic acid and the mechanism of polar auxin transport. *Journal of Experimental Botany*, *69*(2), 303–312.

DISCUSSION

In this thesis, I set out to discover the morphological and molecular mechanisms of maize brace root development. Since plant hormones are main regulators of development, and auxin is involved in most aspects of development, I focused my research on the role of auxin in brace root development. I hypothesized that auxin is necessary and sufficient for maize brace root development. I tested this hypothesis with three aims. If auxin is necessary for brace root development, auxin could be 1) visualized in developing brace roots using reporter lines and 2) detected by molecular changes through RNA-seq. If auxin is sufficient for brace root development, 3) exogenous application of auxin will induce brace root development. My research has established the foundation to define the role of auxin in brace root development and has raised additional questions.

In my first aim, I successfully defined the spatio-temporal development of brace roots in maize. Examination of auxin reporter lines proved difficult to analyze due to interference from the autofluorescence of mature tissues. In collaboration with the DBI Bio-Imaging Center, I have developed spectral imaging approaches to resolve fluorescent proteins from autofluorescence. From initial PIN1::PIN1-YFP results, I found that PIN1-YFP localized to a previously undefined layer of cortex cells in the area where brace roots initiate. Future work to characterize this cell type and develop approaches for the analysis of other reporter lines in mature tissue has been outlined in chapter 2.

In my second aim, a molecular approach is utilized to understand if auxin is necessary for brace root development. RNA-seq of nodes throughout brace root

development was used as a means of generating candidates for a mutant analysis. Since the top differentially expressed genes did not yield compelling candidates, a targeted approach focused on phytohormones was used. Mutants of these genes were not immediately available, so work to produce these mutants is a future direction of my research. Because the tissue used for RNA-seq included the entire node section, future work could utilize laser capture microdissection (LCM), or fluorescence activated cell sorting (FACS) to isolate tissue where brace roots initiate. This would refine the list of differentially expressed genes and lead to more confidence that these transcripts are indeed involved in brace root development, and not other processes at the node. It would also be interesting to use *in situ* hybridization to correlate the localization of these transcripts with the site of brace root initiation.

In my final aim, I tested whether auxin is sufficient to induce brace root development. I approached this question by using exogenous hormone applications. I established the methodology for exogenously applying auxin and auxin inhibitor locally to the maize stem. Preliminary results elicited a developmental response-unexpectedly in the form of nodal tillers, not brace roots. No significant differences were found between the number of primordia found in control plants versus those that were wounded, treated with water, a synthetic auxin (NAA) or a synthetic auxin inhibitor (NPA). Varying concentrations and combining hormonal treatments will further refine and verify these results.

In summary, many open questions remain regarding maize brace root development. These include: what is the cell type that PIN1-YFP localizes to and is this the cell type that brace roots initiate from? Does auxin form a maxima at the site of brace root initiation in the same way it does in other developmental contexts

(Gallavotti et al., 2008; Jansen et al., 2012)? What is the connection between the vascular plexus and brace root primordia? Do brace root primordia develop in an established pattern (phyllotaxy)? My work has laid the groundwork for these questions to be answered in the future.

REFERENCES

Gallavotti, A., Yang, Y., Schmidt, R. J., & Jackson, D. (2008). The Relationship between auxin transport and maize branching. *Plant Physiology*, *147*(4), 1913–1923.

Jansen, L., Roberts, I., De Rycke, R., & Beeckman, T. (2012). Phloem-associated auxin response maxima determine radial positioning of lateral roots in maize. *Philosophical Transactions of the Royal Society of London. Series B, Biological Sciences*, *367*(1595), 1525–1533.

Appendix

ESTABLISHING METHODS FOR LASER CAPTURE MICRODISSECTION OF MAIZE STEM CRYOSECTIONS

A.1 Rationale

To use cryosections of maize stems for laser capture microdissection (LCM) and for downstream RNA-seq, I established methods for LCM and evaluated the quality of RNA captured from cryosections. For LCM, slides will need to be exposed to room temperature for a certain amount of time while the laser is cutting. I prepared a series of slides that were left at room temperature to determine what time frame the LCM needs to be performed before the RNA quality of the tissue is unusable for RNA-seq.

A.2 Methods

A.2.1 Growth conditions

Inbred B73 plants were grown in 3-gallon pots under greenhouse conditions in the University of Delaware Fisher Greenhouse Zone #4. During this period, average temperature was 24.5 °C, average humidity was 57.2%, and supplemental lighting in the form of 400 Watt HPS and 400 Watt MH bulbs was provided from 7 AM - 9 PM when outside light radiation levels were below 600 W/m^2 (watts per square meter).

Plants were watered twice a week, once a week supplemented with nutrient solution, and BK 55 soil was prepared with approximately 30 grams of slow release 19-6-9 osmocote pellets.

A.2.2 Cryosectioning

Plants were grown to the V6 stage and the first three aboveground nodes were harvested and immediately flash frozen in intermediate size plastic molds filled with tissue freezing medium O.C.T. Nodes were sectioned using a Leica 3050S Cryostat with cryojane tape transfer that was sterilized with 90% ethanol prior to use. Sections were stored at -80°C.

A.2.3 Time series and fragment analysis

Slides were left for varying amounts of time at room temperature before RNA isolation (Table 18). Tissue was scraped off the slides using a laboratory spatula sterilized with RNaseZap. RNA was isolated using a Qiagen RNeasy Plant mini kit. RNA was diluted to 0.5-5 ng/µL (checked on a Nanodrop) before submission to the University of Delaware's DNA Sequencing & Genotyping Core for fragment analysis.

A.3 Results

Fragment analysis provides an RNA Quality Number (RQN) of total RNA, assigned on a scale of 1-10, where 1 represents completely degraded RNA, and 10 represents intact RNA. RQN is based off of the major ribosomal RNA peaks. Scores ranged from 3.1 to 6.3, with no clear pattern of increased degradation based on time left at room temperature.

Table 18. RNA quality numbers (RQN) for cryosections left at room temperature for increasing amounts of time.

Sample ID	Time	RQN
1a	5 minutes	5.5
1b	5 minutes	6.2
2a	15 minutes	4.6
2b	15 minutes	5.3
3a	30 minutes	3.1
3b	30 minutes	5.3
4a	1 hour	5.2
4b	1 hour	3.9
5a	1.5 hours	6.1
5b	1.5 hours	6.3

A.4 Conclusions

RNA is easily degraded by endogenous or exogenous RNases. In my experiment, time did not affect the RNA quality of cryosections. It is likely that other factors could help preserve RNA quality, such as using sucrose as a cryoprotectant (Anjam et al., 2016), storing slides in a moisture-free environment, and overall improving the experimental procedures by working fast, keeping reagents on ice, and ensuring instruments and materials are prepared with RNaseZap before use. Other

ways to improve results include using fixed tissue, dehydrating slides with ethanol after cryosectioning, and removing the tissue freezing medium by dipping in ice cold RNase-free water (Nakazono et al., 2003). Future work will incorporate these methods into the LCM protocol to preserve RNA quality for downstream RNA-seq.

REFERENCES

Anjam, M. S., Ludwig, Y., Hochholdinger, F., Miyaura, C., Inada, M., Siddique, S., & Grundler, F. M. W. (2016). An improved procedure for isolation of high-quality RNA from nematode-infected Arabidopsis roots through laser capture microdissection. *Plant Methods*, *12*, 25.

Nakazono, M., Qiu, F., Borsuk, L. A., & Schnable, P. S. (2003). Laser-capture microdissection, a tool for the global analysis of gene expression in specific plant cell types: identification of genes expressed differentially in epidermal cells or vascular tissues of maize. *The Plant Cell*, *15*(3), 583–596.